1985

An experimental study of the in-plane characteristics of waffle slab panels, 1985.

Xuerun Ji

Ti Huang

Le-Wu Lu

Sheng-Jin Chen

Diaphragm Behavior of Floor Systems and Its Effect

on Seismic Building Respons

AN EXPERIMENTAL STUDY OF THE IN-PLANE CHARARCTERISTICS OF WAFFLE SLAB PANELS

Sponsored by National Science Foundation CEE-8120589

by
Xuerun Ji
Ti Huang
Le-Wu Lu
Sheng-Jin Chen

August 1985

Fritz Engineering Laboratory Report 481.3

Table of Contents

Chapter 1

Introduction

The primary function of floor systems in a building structure is to carry vertical loads by their out-of-plane bending action and to transmit these loads to the supporting members such as walls or columns. They also combine with these supporting members to form vertical frames which resist the lateral load, again ultilizing the out-of-plane bending action of the floor systems. Both of these actions are taken into consideration in the traditional design of the building structures. Recently, structural engineers have recognized another important function of the floor system. Under lateral loads, the floor systems must act as diaphragms between parallel vertical systems, transmitting and distributing these horizontal loads. Here the performance of the floor system is controlled by its in-plane stiffness and strength. Furthermore as the lateral loads on building structures are usually dynamic in nature (wind or seismic), the dynamic properties of the slab systems also exert very significant influence.

The in-plane characteristics of two common reinforced concrete floor systems had been studied in detail at the Fritz Engineering Laboratory of Lehigh University from 1977 to 1981. The systems studied were the flat plate and the slab-on-edge-beams. Results of these studies have been presented in several reports.(5,6,7,8,9,10)

In this report is described the experimental investigation of waffle slab floor system, and additional studies on the flat plate system. The work was carried out under a NSF grant entitled "Disphragm Behavior of Floor Systems and Its Effect on Seismic Building Response." (Grant no. CEE-8120589) The experimental work was conducted at Lehigh University from July, 1982 to February, 1983.

The waffle slab floor system has important economical advantage over the flat plate, flat slab, or slab-on-edge-beam systems. The standardized dome forming and the reduced weight make this system particularly suitable for structures intended for moderate floor load. In addition, the waffle slab system also represents an extreme condition with regard to the presence of intermediate beams. Therefore, combined with the flate plate and the slab-on-edge-beam floor systems, the three systems studied covered the entire range of rib-stiffening of slabs.

The basic test specimen chosen for the experimental study represented an interior panel of a prototype building. Two specimens, each containing three consecutive slab panels, were fabricated. Testing was done on each slab panel separately. Fig. 1.1 shows the dimensions and supproting condition of specimens as well as the testing setup. All of these characteristics were common to the tests of the three systems.

Chapter 2

Design and Fabrication of the Specimens

The prototype floor slab for this study was taken to be a part of a rectangular multi-story, multi-bay reinforced concrete building structure of medium- to high-rise. Resistance to lateral loading was taken to be provided primarily by shear walls. General dimensions of the structure were identical to those used previously in the study of other concrete floor systems. The columns were 24 in. (610 mm) square, and spaced 24ft (7.32m) center to center in both directions. The floor height was 12 ft (3.66m) center to center of slabs. The service live gravity load was 80 psf (3.83 kPa). Following the previous study, a scale ratio of 4.5 to 1 was used for the specimens, resulting in a panel size of 64 in. (1.63m), and a column size of 5.33in. (135mm)

In order to be compatible with the gravity load distribution system developed previously, the dome module for the waffle specimen was chosen to be one-sixth of the panel dimension, or 10.67in. (271mm). This corresponded to a prototype dome module of 48 in. (1.22m), which was larger than the most common commercial sizes of 24 or 36 inches (0.61 or 0.91 m).

Design of the test specimens were made by the direct design method of the ACI Building Code, 1977 (1). The design was based on gravity load consideration using a

concrete strength of 4,000 psi(27.6MPa), and a steel yield strength of 60,000 psi (414MPa). Dimensions were intially determined for the prototype structure, then reduced to the specimen by applying the 4.5 to 1 scale factor. This procedure resulted in a specimen top plate thickness of 2/3 in. (17mm), and rib stem size of $1\frac{2}{3}$in. x $2\frac{2}{3}$in. (42mm x 68mm). These dimensions correspond to prototype values of 3in., 7.5in., and 12in. (76mm, 191mm, and 305 mm), respectively. Figures 2.1 and 2.2 shows the detailed dimensions of the waffle slab specimen.

The reinforcement arrangements were determined for the specimens directly, with no attempt to model the prototype structure reinforcing bars. This was necessary on account of the very limited choice of available small-sized reinforcing elements. Reinforcement in the specimen was chosen to satisfy the required tensile force at the various critical sections. Table 2.1a lists the critical design moments, the required amounts of reinforcement, and the provided reinforcements.

As stated earlier, two specimens were fabricated and tested. Each contained three consecutive square panels. They were supported on two interior shear walls and four columns. Quarter-panel extensions were provided all around beyond the column lines, in order to provide continuity and anchorage for reinforcing bars.

The middle panel of one specimen (designated as WS-2) was a flat plate panel similar to the specimen tested previously. Its thickness was 2.22 in. (56mm), same as the previous specimen. However, the reinforcement arrangement was changed. Cutoff points for negative reinforcement were extended from 1/4 panel to 1/3 panel distance. This was done to examine the effect of reinforcing bar details on the behavior of the flat plat

panel. Table 2.1b lists the reinforcement used in this panel, as well as a comparison with the previous design. Figure 2.3 shows the arrangement of reinforcement for the waffle slab as well as the flat plate panels.

The two specimens were fabricated simultaneously in the Fritz Engineering Laboratory of Lehigh University. To form the waffle domes in the specimens, special plastic molds were used. These box forms were made of 0.1 inch (2.5mm) thick material, heat-formed to the desired shape with the ribs having tapered sides at a gradient of 1:8 (same as the commercial dome molds). These molds provided to be very successful in forming the waffle panels, as can be seen from several photographs (Figs. 4.2, 4.4). Fig.2.4 shows the details of the formwork.

Chapter 3

Mechancial Properties of Materials

3.1. Reinforcing Bars

Special small-sized deformed wires (D1, D2, D2.5) and standard No. 3 deformed bars were used for reinforcement in the specimens. The D2.5 wires and one lot of D2 wires showed no clearcut yield plateau when initially received. These were annealed in order to achieve a clearcut yield point. The D1 wires and an older suply of D2 wires (designated $D^0 2$) behaved satisfactorily in a typical elastic-yield fashion, and were used without further treatment. The No. 3 deformed bars were used only in shear walls and columns.

The mechanical properties of these wires and bars were determined by standard tension tests. Table 3.1 lists the average results from three tests. Fig. 3.1 shows the typical stress-strain curves of the annealed deformed wires, D2 and D2.5, used in the waffle slab specimens.

3.2. Concrete

The concrete mix was designed for a 28 days compressive strength of 4,000 psi (27.6 MPa). The maximum size of aggregate was limited to 1/4 in. (6.4mm) in order to maintain the approximately 3:1 ratio of slab thickness to size of aggregate. Table 3.2 lists the detail of concrete mix and table 3.3 lists the gradation of the coarse aggregate. Plasticizer was used to facilitate the concrete placement in the narrow ribs.

Two batches of concrete were used in each floor slab specimen. Eighteen 6in. x 12in. (152mm x 305mm) standard cylinders and twenty 3in. x 6in. (76mm x 152mm) smaller cylinders were made from each batch. These were cured together with the respective specimens under moist burlap at room temperature for 28 days. Nine of the smaller cylinders for each batch were tested for compressive strength at the age of seven days. Nine more small cylinders and twelve larger ones were tested at 28 days for modulus of elasticity, Poisson's ratio, compressive strength and split tensile strength. The remaining cylinders were tested for compressive strength, modulus of elasticity and the Poisson's ratio after the completion of the corresponding specimen test. Tabel 3.4 lists the mechanical properties of concrete. Fig.3.2 shows a typical stress-strain curve of the concrete cylinder. Fig.3.3 shows the typical stress-Poisson's ratio relationship.

Chapter 4

Testing Facilities

4.1. Loading systems

The same test setup used in the previous study was used for this research. The floor system specimen was supported on four reinforced concrete pedestals which were tightly anchored to the laboratory test floor (Figs.1.1 and 4.1). During the test, the columns were supported against vertical movement only, and were allowed to rotate and slide freely. The shear wall was either fixed to the pedestal, or allowed to slide freely, according to the desired boundary conditions. Details of the flexibility of the supporting conditions were given in several previous reports. (5,8,9,10) (Figs.4.2 to 4.4)

The in-plane load was applied by a double-acting mechanical jack. To simulate the desired uniformly distributed shear force, two horizontal steel frames and five embedded studs were used. The frames and studs were carefully designed so that each stud would transmit approximately one-fifth of the total horizontal load to the center plane of slab. The total applied horizontal load was measured by a loadcell located between the jack and the frames (Fig.4.5).

During the stiffness tests, in-plane loads were applied at two points simultaneously. As only one mechanical jack was available, the second load was provided with a

turnbuckle, which was capable of delivering only a tensile force. In these stiffness tests, loads were applied to the middle studs only, not distributed as in the strength tests. (Fig. 5.1)

The uniform out-of-plane (vertical) loading was simulated by a series of concentrated loads acting at the centers of each ninth portion of the slab panel. As pointed out earlier, the size of the specimen waffle dome was seleted so that these point loads would occur at the intersections of ribs. This was necessary to assure firm anchorage of the metal insert loading devices. All loads within one panel width, including those in the quarter panel extensions, were controlled by a single hydraulic jack. A series of statically determinate levers was used to distribute the jack load equally among the fifteen load points. The other end of the hydraulic jack was connected to a gravity load simulator which permitted substantial horizontal displacement of the specimen without affecting either the direction or the magnitude of the applied vertical load (Figs.4.6 and 4.7).

For the quarter panels at the extreme ends of the three-panel specimen, the out-of-plane loading was supplied by heavy metal cylinders. Again, a series of levers was used to deliver equal loads to the five load points in this strip (Figs.4.6 and 4.8).

4.2. Instrumentation and recording of data

Loads, displacements and strains were measured and recorded throughout the tests.

All loads (in-plane load and vertical load) applied to the specimens were monitored by calibrated loadcells mounted at (or near) the source of loading (Figs. 4.5a, 4.7 and 4.8).

In-plane displacements of the slab panel under test were measured by Linear Variable Differential Transformers (LVDT's), with minimum reading of 0.0001 in.(0.0025mm). The vertical deflection at various locations were measured by dial gages having minimum graduations of 0.0001 in.(0.0025mm). All dial gages were attached to a triangular frame, with three legs resting on the top of two columns and the middle point of the shear wall. Thus the dial gage readings were not affected by any movement of the column and wall supports (Fig. 4.9).

Strains in concrete and reinforcing bars were measured by electrical strain gages and rosettes. The deformed wires were filed to a smooth surface for the attachment of the strain gages during fabrication.

Fig.4.10 shows the typical arrangement of strain gages, rosette gages, LVDT's and dial gages for the strength test of an end panel. The instrumentation plans for specific panels are given in the Appendix.

All LVDT's and strain gages were connected to a B&F data-aquisition unit, which produced a printed record as well as a punched paper tape for each load step. The LVDT L3 (Fig. 4.10) measuring the main displacement at the "free" edge of the test panel, was also connected to an X-Y plotter, as was the loadcell measuring the in-plane load. A continuous and complete record was thus obtained for the load-displacement relationship. Such a continuous record was very useful during the cyclic load tests.

A uniform sign convention for all loads and displacements was adopted. The positive transverse (X) and longitudinal (Y) directions are indicated in Fig. 2.1.

Chapter 5

Testing of Specimens

5.1. Testing sequence

A number of tests were carried out on each of the two floor slab specimens. The sequence of the tests in each case was carefully designed to maxmize information that could be obtained, and minimize the time and effort required to rearrange the supporting and loading devices. Figs.5.1 and 5.2 show schematically the tests in each series and the sequence of testing. Each test was identified by a five character alphanumerical designation. Table 5.1 gives a complete description of these designations.

Before each test, the specimen was preloaded to about 10 percent of the estimated ultimate load, and then unloaded. The purpose for this operation was to ensure that all instruments worked properly and to stabilize the loading systems.

Application of loading was carried out in multiple steps. Before the cracking of concrete, the specimen showed essentially linear behavior, and the loading steps were controlled by preselected loading increments. After cracking, and particularly after the first yielding of reinforcing bars, the specimen deformed much more rapidly, and the loading was controlled by specified increments of the main displacement (LVDT 3). A limit of 0.1 in. (2.5mm) main displacement per loading step was imposed in all tests.

Such a loading scheme permitted accurate determination of both the ultimate resistance and the maximum deflection of the test panel. These information are very important for the evaluation of ductility.

5.2. Stiffness test

Specimen WS-1 containing three waffle slab panels was initially tested for its overall stiffness under symmetrical and anti-symmetrical in-plane loads (Fig.5.1). For these tests, only four of the 24 anchor bolts for each shear wall were tightened on the pedestal (Fig.5.3). Under this condition, each shear wall was essentially free to rotate about its central vertical axis. All columns were supported in the free-to-slide condition. Each of the applied in-plane loads was limited to 2.5 kips (11.1 kN), corresponding to approximately one eighth of the estimated ultimate strength of the structure. This low load limit was chosen to maintain linear elastic structural response. The in-plane stiffness characteristics of the slab system were determined from displacements and rotations measured by LVDT's arranged as shown in Fig. 5.3.

5.3. Strength test

In the strength tests, one of the shear walls was firmly attached to the pedestal with 24 anchor bolts (Fig. 4.2) and two pairs of strong braces, while the other shear wall and all columns were supported in the free-to-slide condition. In this manner, the specimen was structurally separated at the fixed shear wall, and each panel was tested separately.

The in-plane load was applied along the column line parallel to the shear wall and through the horizontal load distribution frame. In monotonic loading tests, the in-plane

load was increased continuously until the ultimate resistance of the test panel was reached. At the begining of each test, loading was increased in 2-kip (8.9kN) steps. This was continued until the increment in main displacement (LVDT 3) during one loading step reached 0.1 in. (2.5 mm). Afterwards loading was controlled by main displacement increments of 0.1 in. (2.5mm) for each step. After reaching the ultimate resistance, the specimen was unloaded and then reloaded in the opposite direction until the ultimate resistance was again reached. The load was released again, and the test was completed.

In cyclic loading tests, the in-plane load was varied according to a predetermined loading spectrum. The load was applied in complete cycles with gradually increasing load or displacement amplitudes. Three complete loading cycles were applied at each amplitude. Initially, the loading cycles were controlled by load, with amplitude increments of 4 kips (17.8kN). At later stages, loading was controlled by displacement at the column line (LVDT 3) (Fig. 4.10). Figs. 5.4a and 5.4b show the loading spectrum applied to the test WH2CY and WV1CY respectively.

For the tests including out-of-plane loading, the specimen was first loaded vertically to simulate full service dead and live loading condition, before the application of the in-plane load. It was noted that the weight of the specimen and the vertical loading system was 26.7 psf (1.28kPa) which was far less than the weight of the prototype structure. Therefore, the applied vertical loading included a compensatory dead load of 57.7 psf (2.76 kPa) in addition to the service live load of 80 psf (3.83 kPa). The load required at each insert point was 435 lbs (1.94 kN). The required total load for an interior panel (15 loading points) was 6530 lbs. (29.0 kN) and that for the end extension (5 loading points) was 2180 lbs (9.7 kN). The load actually achieved were slightly higher, being 6550 lbs (29.1kN) and 2200 lbs (9.8kN), respectively.

For both specimens, the middle panels (panel 3) were tested under in-plane monotonical load with a moment-shear ratio (M/Q) of 128 in. (3.25m). This was accomplished by fixing the shear wall between panels 3 and 1, and loading along the column line in panel 2, as shown in Fig. 5.1.5 and 5.2.7. The role of panel 2 here was merely to transmit the shear and moment to the middle panel. The characteristics of panel 3, which were the goals of this test, would not be affected by the behavior of panel 2. It was therefore immaterial that a severely damaged panel 2, having been tested to failure previously, was being used. It was only necessary to ensure that the strength of panel 3 could be reached. Four steel plates were glued on the top surface of the damaged panel 2 across the major cracked region. (Fig.5.5) Such a crude repair obviously did not restore the strength, nor the stiffness, of panel 2. However, as long as a failure of panel 3 was achieved, there was no distoration on the response of panel 3 to the applied in-plane load.

Each of the strength tests was conducted according to the following procedure:

1. The boundary conditions and instrumentation were checked. All channels in the B&F data-acquisition unit were balanced. The LVDT's were checked to ensure their proper orientation and positive directions.

2. Zero readings were taken from all measuring devices. These included all loadcells, strain gages, LVDTs, and for the tests with vertical loading, the dial gages.

3. The test panel was preloaded by a 2-kip (8.9 kN) in-plane load and, where needed, a 35 psf (1.68 kPa) vertical load. All instrumentation were checked during the preloading to ensure their proper working conditions. The specimen was then returned to the unloaded condition.

4. Initial zero readings were again taken from all instruments.

5. When needed, the vertical load was applied gradually in eight equal increments. Details of the vertical loading sequence are shown in Table 5.3.

After fully applied to represent the service live and dead load, the vertical load was maintained constant throughout the remaining steps of the strength test.

6. The in-plane load was applied according to the preselected pattern, either monotonically or cyclically. The load was increased quasi-statically and held at frequent load or displacement steps for strain and displacement measurements.

7. At each loading step, the specimen was visually examined for the formation and extension of cracks.

8. The loading was terminated when the resistance dropped significantly below the ultimated strength with increased displacement, when it became impossible to maintain the required vertical load, or when concrete crushed in compression, which was usually accompanied by a sudden loss of resistance.

9. In monotonic load tests, the in-plane load was then removed and applied in the negative direction. Test continued as in steps 6, 7, and 8 until the ultimate strength was again reached. The specimen was then unloaded.

10. At the end of each strength test, after complete unloading, a set of final zero loadings was taken from all measuring devices.

11. Condition of the failed specimen was recorded by photographs as well as manual sketching of the crack patterns.

12. The thickness of slab panel at the major crack was precisely determined by a micrometer.

5.4. In-Plane Vibration Tests

The in-plane vibration tests were done before and after the strength test for each side panel. The panel was supported as in the strength test. A vibration sensor, a frequency filter and an oscilloscope were used to measure and record the vibration of the panel caused by a hammer impact. As shown in Fig. 5.6, vibration in the X- and Y-directions were studied separately by changing the direction of the hammer impact and the sensor. Each impact incited vibrations of many modes, in different directions and at different frequencies. Tests were repeated several times with the frequency filter set at

different ranges, until the dominant fundamental free vibration frequency was established. Each frequency was measured at least three times.

Chapter 6

Test Results

6.1. Stiffness Tests

The stiffness tests were made on the specimen WS-1 only. The displacements at the load points and the rotation of shear walls were determined from readings of nine LVDT's, arranged as shown in Fig.5.3. Figs. 6.1 and 6.2 show the measured displacements under 2-kip symmetrical and anti-symmetrical loading, respectively. The movements at the supports (L2 and L4), were more than originally expected, reflecting some motion of the supporting pedestals themselves. The average displacement of the loaded points (L1 and L5), relative to the displaced location of the support line (L2 and L4) was calculated to reflect the structural response of the specimen, as demonstrated in Figs. 6.1 and 6.2. Nevertheless, the rather large support movements reduced the accuracy of the calculated results, particularly for the anti-symmetrical case. Table 6.1 shows the calculated initial flexibility, as the deflection under unit load.

During the strength tests, the initial flexibility of each panel was also monitored, results are also listed in Table 6.1. It should be pointed out that because of the different support conditions, the flexibilities from the three-panel stiffness tests and the single panel strength tests were different structural quantities and should not be compared directly. Under full service vertical load, there were several cracks in panels

WV1CY and WV2MN before the application of in-plane loading. As a consequence, the initial flexibilities of these panels were higher than the coresponding panels without gravity load.

6.2. Behavior Under Gravity Load

Panels 1 and 2 of specimen WS-2 were tested for their behavior under gravity load up to the service load level prior to in-plane strength testing. As pointed out in Section 5.3, gravity load was applied in eight increments, eventually reaching the level representing the full service live and dead loads. The first crack due to vertical load was observed at approximate 60% full service load. Under full vertical load, a long line of crack due to negative bending was observed along the slab-shear wall junction on the top surface while several small cracks were found at the bottom near the middle of span. Figs. 6.3 to 6.5 show the measured vertical deflections, residual deflections and calculated results due to vertical loading for panel 1. Behavior of panel 2 was similar. Under full service vertical load, the maximum vertical deflection at the center of the panel (D_3) was 0.14 in.(3.55mm), which was 1/450 of the span length.

Figs. 6.6 to 6.7 show the typical relationship between vertical load and measured strain (stress) in rib reinforcement at mid-span. The relationship were nearly linear. Under full service vertical load, the largest measured steel stress was 22,550 psi (155.4MPa) in the middle strip and 21,260 psi (146.5 MPa) in the column strip. It should be pointed out that these stress values have been adjusted for the effect of the specimen self-weight as indicated in Figs.6.6 and 6.7. These stress values were 50 to 60% of the yield strength of steel wire, very reasonable for service loading condition.

6.3. Results of Strength Tests--- General Description

Primary interest in the strength tests was given to the displacement at the unsupported edge of the panel under test (LVDT L3 in Fig. 4.10). This LVDT was continuously monitored during the test, and plotted against the applied in-plane load by an XY-plotter. Figs.6.8 to 6.15 show these plots for the six strength tests. These plots show clearly the general in-plane behavior of each test panel, including the minor decreases in loads caused by intermittent support movements, cracking of concrete and fracturing of reinforcing bars.

The displacements recorded by LVDT 3 included the effect of movements of the "fixed" edge of the test panel. In order to study the actual structural behavior of the panel, the readings from several other LVDT's were used to eliminate the effects of any rigid body motion associated with support movements. The results of these calculations were also plotted in these figures, in dashed lines. For the sake of distinction, the measurements of LVDT L3 are refered to as the principal "displacements", while the calculated values are designated principal "deflections". Calculation of principal deflections could not be performed continuously during test, but only at pre-selected load levels. Consequently, the dashed lines in these figures consisted of short straight line segments.

Several fine cracks were obsered at the slab-shear wall junction at very early stages of the tests. (In several cases, these were observed even before testing.) Shrinkage and abrupt change of stiffness were believed to be responsible for these cracks. It was felt that these cracks would have a relatively significant effect on the principal displacements under low in-plane loads, but negligible effect under high loads. Accordingly, two values

were calculated for the principal deflections, using the center line of shear wall and the edge of the test panel, respectively, as the reference line (Fig. 6.16). These are designated Δ_1 and Δ_2, respectively.

Estimation of the initial stiffness (and flexibility) of the panel was based on Δ_2, in order to remove the effect of the opening of the minute cracks at the face of shear wall. The results are assembled in Table 6.1, in comparision with corresponding values obtained from analytical methods.

The overall behavior of the test panels, shown in Figs. 6.8 to 6.15, are based on Δ_1. It was reasoned that under high in-plane load, the relative movement between the edge of slab and the shear wall should be more appropritely considered as a part of the structural response. Table 6.2 summarizes the various critical test results from the strength test. Figs. 6.17 to 6.28 show the crack patterns of the panels at the end of the strength tests. Numerals near the cracks represent the load values for test WH1MN (Figs.6.17 and 6.18), and the load step numbers for other tests, when the crack was first obsered.

6.4. Results of Individual Strength Tests.

6.4.1. WH1MN (Figs. 6.8, 6.17, 6.18)

The load-deflection relationship was essentially linear up to a load of 10 kips (44.5kN). The first flexural crack was observed about 15 in. (380mm) from the shear wall at a load of 13.77 kips (61.2kN). The first shear crack was found in the middle part of the panel near shear wall at a load of 15 kips (66.7kN). Although the flexural crack was obsered first, the shear cracks developed faster once started. Most of shear

cracks started in the middle part of the panel, and extended from both ends at an angle of about 45 degree with the in-plane load. The widest openings of the shear cracks were mostly located in the middle part of the panel. At a load of 15.96 kips (71.0kN), a strain gage reading indicated that yield strain had been reached in a rib reinforcing bar. This load was designated as the first yield load. At a load of 20.5 kips (91.2kN), many new shear cracks were observed, while the cracks started earlier were seen to enlarge. The stiffness of the panel had decreased significantly. At 21 kips (93.4 kN), several cracks developed rapidly and merged into one major transverse crack extending from the tensile edge to the compressional region. The maximum load reached was 22.12 kips (98.4 kN). At this load, several reinforcing bars broke, and both stiffness and resistance droped significantly. The largest principal displacement, as measured by LVDT L3, was 0.73 in (18.6mm), which occured when resistance had dropped down to 21.17 kips (94.2 kN). After unloading, the residual displacement was 0.563 in (14.3 mm). Examination of the readings from the other LVDT's revealed that significant support movement was included in these displacements. The corresponding deflection value, (Δ_1), were 0.317in. (8.1mm) and 0.218in. (5.53 mm), respectively. These principal deflection values are shown in Fig. 6.8.

During negative (push) loading, the ultimate load attained was 22.04 kips (98.0 kN). At this point several reinforcing bars broke and several pieces of concrete fell off. At the same time, the resistance was reduced greatly and the major cracks from opposite edges became connected. This final major crack was located at 21 inches (533mm) from the shear wall. This location coincided with the cut-off point of the short top reinforcing bars in the column strips (Fig. 2.3). The largest deflection Δ_1 reached under negative loading was 0.497 in. (12.6mm). The residual deflection upon unloading was approximately 0.35 in. (8.9mm).

6.4.2. WH2CY (Figs. 6.9, 6.10, 6.19, 6.20)

For the three lowest amplitudes, with peak loads of 4. 8 and 12 kips (17.8, 35.6 and 5.4 kN), the behavior of the panel was essentially elastic. There was no change in the principal displacement in successive cycles under the same load, no noticeable residual deformation. Starting from the loading cycles at 16 kips (71.2 kN) load, (cycles no. 10, 11 and 12) the residual displacement became significant, and progressive deterioration was evident from the three hysteretic loops in each group. Peak displacement increased in each successive cycle to the same load, and in the later stages when loading was controlled by displacement, the resistance of the panel decreased in successive cycles. In general, there was less difference between the last two cycles than between the first two cycles of each group. The opening and development of most cracks were first observed during the initial cycle of a group, with few additional cracks starting during the second and third cycles. Such a cracking behavior is compatible with the observation of relatively little deterioration between the second and third cycles. It was reasonable to expect only minor change in the hysteretic loops under additional cycles of loading. The maxmium load, for both positive and negative directions, was reached during the first cycles at the seventh amplitude (cycle no. 19), with a peak displacement of 0.4 inch (10.2 mm). The load values were 21.05 kips (93.6 kN) and 19.76 kips (87.9 kN), respectively. The more stable third-cycle loads were highest at 19.36 kips (86.1 kN) in the sixth amplitude (cycle no. 18, 0.3 inch or 7.6 mm) and -18.0 kips (80.1kN) in the seventh amplitude (cycle no 21, 0.4 inch or 10.2 mm). After reaching the maximum resistance, the peak load decreased appreciably in successive cycles of the same amplitude.

At the end of the cycle load test, after three cycles at the ninth amplitude (0.6 inch or 15.2 mm), several reinforcing bars had broken, the major crack had extended nearly the full width of the test panel and the resistance had dropped to approximately 65% of the maximum value observed earlier. The largest structural deflections (Δ_1) attained during the last cycle of loading were 0.716 in. (18.2 mm) and -0.664 in. (16.9mm), respectively.

Between the east and west column center line, (i.e. the panel proper), most cracks were directed at an angle of 45 (or 135) degrees with the direction of the in-plane load, signifying their being diagonal tension cracks. Outside of thesse column center lines, cracks were basically parallel to the in-plane load, being flexural in nature.

6.4.3. WH5MN (Figs. 6.11, 6.21, 6.22)

The middle panel of the first specimen (WS-1) was tested with in-plane loading applied at the outer edge of panel 2 (Fig.5.1). However, attention was completely focussed on the middle panel. Panel 2 was used only to achieve the desired large moment-shear ratio. The placement of the measuring devices was similar to Fig. 4.10. The principal displacement and principal deflection were determined at the center line of the shear wall between panels 2 and 3, and reflected the behavior of panel 3 alone.

The first crack was observed near the fixed shear wall at an in-plane load of 6 kips (26.7kN). First yielding of reinforcing steel was observed at 8 kips (35.6 kN). This was followed by yielding of several more steel bars, and the opening of diagonal tension cracks in the middle of the panel. A major crack was then formed between the second and third ribs from the fixed shear wall. The panel eventually failed at a load of 12.47

kips (55.5 kN) by crushing of concrete at the north-east corner, near the fixed shear wall and beyond the first longitudinal rib, where the compressive stress was high, the thickness of slab was only 2/3 in. (16.7 mm), and many of the cracks converged (Fig.6.21). The resistance of the panel decreased by 3 kips (13.3 kN) following the crushing of concrete (Fig.6.29).

As shown by Fig. 6.11, this panel acted like a flexural member, and demonstrated considerable ductility (significant increase of displacement with little change in resistance).

Under negative loading, the load gradually increased to 10.22 kips (45.5 kN), followed by a sudden slab concrete crushing at the major crack developed previously under positive loading. Apparently, the closing of this crack was not complete, resulting in very high local concrete compressive stresses. The largest deflection Δ_1 in both positive and negative directions was over 1 inch (25 mm).

6.4.4. WV2MN (Figs. 6.12, 6.23, 6.24)

As pointed out in section 5.3, out-of-plane loading simulating the full service gravity load was applied to panel 2 of specimen WS-2 before the application of in-plane loading, and maintained throughout the test. Thus, this panel was subjected to the combined action of full service gravity load and a varying in-plane shear load.

Under full service gravity load but no in-plane loading, there existed a long negative bending cracking along the slab-shear wall interface as wel as a number of positive bending cracks in the center region of the panel. On account of the preeminence of the top plate of the waffle slab system in initial resistance to in-plane shear loading,

the positive bending cracks had very little influence on the initial in-plane stiffness of the panel. On the other hand, to calculate the measured initial stiffness, principal deflection Δ_2 was used instead of Δ_1 (Fig. 6.16), so that the effect of the negative bending crack was removed. The first yield of reinforcing bar was detected at a negative load of 10.01 kips (44.5 kN), which was significantly lower than the case without gravity load (test WH1MN).

The ultimate load was reached at 21.36 kips (95.0kN) when the slab concrete at the compression edge crushed (Fig.6.30). As soon as the concrete crushed, the resistance of the panel decreased by 0.51 kips (2.3kN), and the principal deflection Δ_1 increased by more than 0.1 inch (2.5mm). The ultimate deflection Δ_{1u} attained was 0.566 inch (14.4mm).

During unloading, the rebar's stresses at opened cracks were decreased and the cracks were closed. However, the out-of-plane loading caused vertical displacements of the opposite side of the cracks, particularly near a vertical load point. This resulted in a vertical offset of the crack after closing, leading to highly concentrated local compression stresses. The negative ultimate load was reached at 19.02 kips (84.6 kN), nearly 10% lower than the positive ultimate load. The mode of failure was again concrete crushing, but at a closed crack about 25 in. (635mm) away from the compression edge (Fig.6.31). The negative ultimate deflection was 0.576 inch (14.6mm), a little more than the corresponding positive value.

6.4.5. WV1CY (Figs. 6.13, 6.14, 6.25, 6.26)

Similar to test WV2MN, the compensatory dead and live load was applied to panel 1 of specimen WS-2 before in-plane loading, and maintained throughout the test. A few shrinkage cracks were found on top of the slab parallel to the shearwall before loading. The cracks due to vertical load were similar to those in the test WV2MN.

The loading program for WV1CY is shown in Fig. 5.4b. For the three lowest amplitudes at peak loads of 4, 8, 12 kips (17.8, 35.6, 53.4 kN), the hysteresis loops for the three cycles at each amplitude nearly conincided with each other. Deterioration was first observed during the third cycle at 12 kips (53.4kN) load (cycle no. 9), when the principal displacement increased slightly (Fig.6.13). Starting from the fourth amplitude, peak load 16 kips (71.2 kN), the three hysteresis loops of consecutive cycles ran differently. Weakening of the panel was clearly indicated by increased displacement under the same load, or in later cycles, by decreased resistance at the same displacement.

The first yield of reinforcing steel was detected at a very low load of 7.92 kips (35.2 kN). The ultimate load was 21.21 kips (94.3 kN) during the first cycle of the sixth amplitude (cycle no.16) when several rebars broke. Afterwards, the resistance of the panel decreased cycle by cycle. The maximum deflection Δ_1 obtained was 0.557 inch (14.2 mm) under a load of 8.55 kips (38.0 kN). At the ultimate stage, the major cracks from both side had merged together into one crack extending through the entire width of the panel. Considerable damage could be attributed to the action of the out-of-plane loading. The test was terminated after one and one half cycles at the eighth amplitude when the slab concrete in compressive region was crushed.

6.4.6. FH5MN (Figs. 6.15, 6.27, 6.28)

The strength of the flat plate middle panel of specimen WS-2 was tested using a setup similar to that of test WH5MN, with the in-plane loading transmitted through the reparied panel 2 (Fig.5.5).

The first crack was observed near the fixed shear wall at a load of 7.41 kips (33.0kN). Under additional loads, several more flexural cracks develọpd. The first yield of a reinforcing bar was observed at a load of 10.8 kips (48.0 kN). At a load of 12.24 kips (54.4 kN), several cracks were seen to turn into a diagonal direction. One of these eventually became the major crack causing failure.

The ultimate load was reached at 17.18 kips (76.4 kN) followed by the breaking of several reinforcing bars and a decrease in resistance by 1.18 kips (5.25 kN). The ultimate deflection reached was 0.606 in. (15.4 mm).

Under negative loading , the ultimate load was only 12.28 kips (54.6 kN), nearly 25% lower than the positive value. Failure was due to crushing of concrete at the previous major crack, which was located about 19 in. (480mm) away from the center line of the fixed shear wall.

It should be noted that the flat plate pannel was reinforced with bent-up (trussed) bars, and the major crack developed very close to the bent-up location. The straightening of the bent bars at the crack could have contributed to the increased flexibility of the panel (Fig. 6.32).

The maximum negative load of 12.28 kips (54.6 kN) was reached with a deflection

Δ_1 of 0.203 inch (5.2mm), after which the resistance gradually decreased with increased deflection. Testing was terminated at a maximum deflection of 0.44 inch (11.2 mm), when the resistance had decreased to 7.91 kips (35.2 kN).

Chapter 7

Comparison and Discussion

7.1. Stiffness and Flexibility

Elastic in-plane stiffness (load per unit Δ_2) of each slab panel and its reciprocal, the flexibility, were calculated by finite element analysis using the standard SAP IV program. The following assumptions and idealizations were made regarding the geometry and material properties:

1. Only linear elastic deformations were considered.

2. The concrete material was taken to be isotropic and homogeneous. The effect of reinforcement was ignored.

3. The modulus of elasticity and Poisson's ratio for concrete were assigned values as obtained from standard cylinders tested after the strength test of each specimen.

4. The average slab thickness, from measurements of each specimen, was used in calculation.

5. The waffle slab was treated as a three dimensional system. The top slab of each waffle dome was represented by a plate element and the ribs were represented by beam elements. Rigid link were used to connect the rib segments to the top plate at its corners. The length of the rigid links was equal to the distance from center of top slab to the center of rib.

The method of equivalent thickness (12) was also used to calculate the elastic flexibility of single slab panels.

Table 6.1 lists the calculated flexibility, together with the initial flexibility obtained experimentally. For WH1MN and WH2CY, the FEM calculated flexibility was about 80 percent of the experimental values. The difference appears reasonalbe in view of the unavoidable microcracks in the specimen, and the lower-bound nature (for flexibilities) of the finite element analysis.

Comparing the experimental flexibility of WH1MN with that of WH2CY, it is seen that the cyclic loading has no effect on the initial flexibility.

For the symmetrical stiffness test WH6SS, the flexibility calculated by finite element analysis was very nearly the same as experimental result. In contrast, the comparison was not as good for the anti-symmetrical test WH6SA. From Fig. 6.2, considerable support movements are seen to have taken place during this test. The experimental results were therefore subjected to larger inaccuracies.

Table 6.1 also lists the results calculated by equivalent thickness method (12). The results are between experimental values and the values calculated by SAP IV.

7.2. Behavior Under Service Vertical Load

Figures 6.3, 6.4 and 6.5 show the vertical deflection of panel 1 of WS-2 under various stages of vertical loading, as well as the residual vertical deflection after removal of all supplemental loading (only specimen self-weight remaining). Also shown in these figures are the deflection under service load calculated by a SAP IV elastic analysis. The experimental deflections are seen to be nearly double the corresponding calculated values. This difference is attributed to the flexural cracking of concrete and the resulting non-

linear behavior of the specimen. From Fig. 6.5, it is seen that the SAP IV analysis yielded reasonalbe estimates of the initial stiffness regarding D_3 and D_6. The largest measured deflection D_3, under full service gravity load, was 0.13 in. (3.3 mm), or approximately 1/500 of the panel length, which was 64 in. (1630 mm). About half of this deflection was non-elastic in natural, and not recovered upon unloading.

The largest measured steel stress under full service gravity load was about 22,550 psi (155.4 MPa), or 60% of the yield stress. The largest crack width under full service gravity load was about 0.005 inch (0.13 mm). These deflection, stress and crack width values all indicate an acceptable performance under service loading.

7.3. Behavior Under In-Plane Load

7.3.1. General Description

Under in-plane load the waffle slab panel behaved like a cantilever deep beam. The ultimate strength was influenced by the nature of loading (monotonic or cyclic), the moment-to-shear (span-to-depth) ratio, and the intensity of vertical load. In all cases the ultimate strength was reached immediately before the development of a major crack which extended parallel to the shear wall at a distance of 20 in. (510 mm), about 1/3 panel length, where a number of negative reinforcing bars were terminated. After the formation of this major crack, the resistance of the panel gradually decreased with additional displacement. During this phase of testing, the overall deformation of the panel was controlled primarily by the opening and closing of the major crack, with few new crack developed. The section at the major crack acted like a plastic hinge. The opening of the major crack also caused a decrease of the compression region. In several

cases, the depth of the compressive region was as low as 7 in. (178mm), barely including the first rib. Several of the panels finally failed by crushing of concrete in the compression region.

The opening of the major crack enabled the slab panel to deflect greatly without significant change of resistance. In comparision with other floor slab systems, waffle slab is superior in ductility. Table 7.1 shows the ultimate deflection values of the waffle slab panels, as well as those of flat and beam-supported slabs. It is clear that waffle slab panels sustained much more ultimate deflection although all slab panels had the same span length and were subjected to the same service gravity load. Table 7.2 lists the comparison of the test results.

The capacity of a structure to sustain inelastic deformation without significantly losing resistance is frequently represented by the ductility ratio of the largest attainable deformation to the elastic (or yield) deformation. In Table 7.3 are listed the ductility values of the various test specimens. As depicted in the sketch accompanying Table 7.3, these values were determined at the level of the calculated ultimate strength of the specimen panel, and the base deformation at yield, Δ_y, is obtained by extending the linear portion of the load-deflection curve to the selected load level. Two ductility values were show for each specimen, one based on the largest deflection measured ($\Delta_{1,max.}$), and the other based on the deflection at the maximum resistance ($\Delta_{1,u}$). It is seen that in almost all cases, the $\Delta_{1,max.}/\Delta_y$ ratio exceeds 5.0 and $\Delta_{1,u}/\Delta_y$ exeeceds 3.0. Ductilities represented by these values appered to be quite adequate.

Figs. 7.1 and 7.2 show the growth of ductility for cyclic loading tests WH2CY and

WV1CY, respectively. For each half cycle of loading, the ductility was calculated as Δ_i/Δ_y, where Δ_i was the total deflection during the current half cycle, starting from the zero load position, and Δ_y was the deflection determined from linear extrapolation, as before. These definitions are show in the figures.

In all strength tests, the ultimate resistance under negative loading was lower than that under positive loading. This strength reduction was attributed to damages during the last stages of positive loading. At the end of the positive loading phase, many cracks had developed, and the major crack had extended almost through the entire width of the test panel. Most of reinforcing bars crossing the major crack had yielded, a few even fractured. These damages would obviously weaken the panel when loaded in the opposite direction.

Despite the anchoring of the floor system specimen to the strong pedestals, significant support movements were measured during the stiffness tests. These relatively larger support movements reduced the precision of the test results.

7.3.2. Effect of Nature of In-plane Loading

The two pairs of test panels: WH1MN vs. WH2CY, and WV2MN vs. WV1CY, were compared to determine the effect of the nature of loading (monotonic vs. cyclic).

Under cyclic loading, initial yield of steel occurred at a lower load than under monotonic loading. The ratio of the first yield loads was 0.93 (without gravity load) and 0.79 (with gravity load), respectively. In contrast, the ultimate resistance was not significantly affected by the nature of loading. As shown in Table 7.2, the ratios of corresponding maximum loads in positive and negative directions were 0.95 and 0.90 for panels without gravity load and 0.99 and 0.96 for panels with gravity load.

The deterioration of the test panels under cyclic loading was more distributed than the monotonically tested panels. There were more plastic deformation and more visible cracks in the panel, but the cracks were better distrbuted over the entire panel, and their widths were smaller. The ultimate deflections of panel WH2CY, +0.716 in. (+18 mm) and -0.665 in. (-17 mm), were much larger than those of panel WH1MN, +0.316 in. (8 mm) and -0.497 in. (12.6 mm). An approximately 70% increase in total deflection was observed. On the other hand, the pair of specimen subjected to gravity loads, WV1CY and WV2MN, developed approximately the same total ultimate deflections, 1.11 in. vs. 1.14 in. (28.2 mm vs. 29.0mm). Apparently, the effect of nature of in-plane loading in this case was overshadowed by that of the presence of out-of-plane loading.

7.3.3. Effect of Vertical Load

The effect of vertical (out-of-plane) loading was examined by comparing the results of test panels WH1MN with WV2MN, and WH2CY with WV1CY. As both the out-of-plane and in-plane loads produce tensile stress in certain reinforcing bars, the initial yield occurs at a much lower in-plane load level for panels subjected to vertical load. The ratio of initial yield loads for WV2MN and WH1MN was 0.627 (Tables 6.2 and 7.2). For panels WV1CY and WH2CY, the corresponding ratio was an even lower 0.532. Thus the presence of full service vertical load caused a 40 to 50% decrease of the first yield load.

The vertical load had almost no effect on the positive ultimate in-plane resistance. Apparently, the slab panel was sufficiently ductile that at the relative low level of out-of-plane load (about 50% of ultimate), the in-plane strength was not severely impaired.

However, the same condition was not observed for the negative loading. Some material failure (yielding and fracturing of reinforcing bars and crushing of concrete) has taken place during the positive loading test. In addition, the out-of-plane loading had caused vertical offsets of parts of the panel. As a result, the observed negative ultimate in-plane strength was lower. The ratio of negative ultimate load for WV2MN to that for WH1MN was 0.86. For the pair of panels WV1CY and WH2CY, this ratio was 0.92. Thus, the service gravity load caused the in-plane strength to decrease by approximately 10 to 15 percent. Fig.7.3 shows the resistance interrelationship of waffle slab panel under combined out-of-plane (vertical) and in-plane loading. According to the ACI strength and serviceability design concept, the full service load represents only about 50 to 60% of the required structural capacity. The circular interaction relationship shown in the figure indicated that this would only have a small effect on the in-plane resistance.

7.3.4. Effect of Shear Span

While most waffle slab panels were tested with a shear span of 64 in. (1.63 m), the middle panel test (WH5MN) used a shear span of 128 in. (3.25 m). Comparision of test results from WH5MN and WH1MN provides an indication of the effect of the shear span, or the moment-to-shear ratio.

The first yield load for WH5MN was 8 kips (35.6 kN) while that of WH1MN was 15.96 kips (71.0 kN). These loads are almost precisely in inverse proportion to the shear spans, hence reflect almost identical in-plane bending moment at the fixed edges. It may be concluded that the steel stress was primarily controlled by the bending action of the slab at this stage.

The comparison of ultimate in-plane resistance revealed a ratio of 0.56 for positive loading and 0.46 for negative loading. Both ratio are somewhat different from that of the moment arms. It is felt that the location of the major crack have an important influence on the ultimate behavior under negative loading. For both WH1MN and WH5MN, the major crack was located about 21 in. (533 mm) away from the fixed shear wall. Therefore, the moment-to-shear ratio at the major crack (or the distance to applied load) was 107 in. (2.72m) for WH5MN, and 43 in. (1.09 m) for WH1MN. These distance were approximately in inverse proportion to the negative ultimate loads. These observation on the ultimate resistance in both directions indicate that the in-plane strength of waffle slab pannels is controlled primarily by the flexural capacity at the major crack section. The effect of the in-plane shear is small indeed. Panel WH5MN with the larger moment-to-shear ratio, exhibitted considerably larger ductility than panel WH1MN (Table 7.3). This difference in ductility may be viewed as a consequence of the different crack patterns in these specimens. A comparison between Fig. 6.17 and Fig. 6.21 shows that the specimen tested under the large moment-to-shear ratio (FH5MN) developed more flexural cracks, but fewer shear cracks. As the opening of the flexural cracks and the yielding of reinforcing bars at these cracks contribute significantly to the plastic deformation of the slab panel, the observed increase of ductility with the moment-to-shear ratio is understandable.

7.3.5. Effect of Reinforcement

For every one of the strength tested panels, the major crack ran parallel to the fixed shear wall and was located about 21 in. (533 mm) from the wall (Fig. 2.3). This location nearly coincided with the third span point where many of the negative moment reinforcing bars in the column strip were terminated.

The panel FH5MN, which contained bent (or trussed) bar reinforcements, behaved less satisfactoriy under in-plane loading than the other panels, which used separate straight top ane bottom bars. As described in section 6.4.6, the bent bars tended to straighten out after cracking developed at the bent position, and accelerated the widening of the crack. It is therefore recommended that bent bars not be used in floor slabs subjected to large in-plane loading.

7.4. Frequencies of In-plane Free Vibration

The results of free vibration tests are listed in Table 7.4. It is clear that cracking of concrete due to strength testing greatly reduced the stiffness, hence the freguency of free vibration. The last column of Table 7.4 shows the natural frequencies calculated by the finite element analysis (SAP IV). The generally lower frequencies predicated by the finite element analysis are attributed to the neglect of friction resistance at the column.

General conclusions could not be drawn from the "after strength test" frequency value. It was noted that after strength test, the panels were damaged to different degree of severity, some almost becoming two separate parts. The frequency measured was more closely related to the behavior of the part being impacted, than that of the entire panel. Furthermore, the two sepaate parts were connected by reinforcing bars, the boundary

condition was completely changed. So the measured frequency would not be the real frequency of the panel.

Chapter 8

Conclusion and Recommendations

The experimental research reported herein has provided information about the in-plane behavior of waffle slab panels under various supporting and loading conditions. From these experimental information, and from comparison with results generated by various analytical methods, the following observations and conclusions are obtained:

1. Both the elastic finite element analysis and the equivalent thickness method resulted in flexibility values of the waffle slab panel approximately 15% lower than the experimental value. Microcracks and residual stress caused by shrinkage and accidental loading before testing are belived to be responsible for these discrepances.

2. Under vertical (out-of-plane) loading, the first crack was observed at about two-thirds of the service dead load and live load. Under full service load, a long negative moment crack was located along the slab-shear wall junction, and several small cracks developed on the bottom of ribs in the middle of span.

3. The waffle slab panels designed in accordence with ACI Building Code performed satisfactorily under full service (out-of-plane) loading. The largest measured steel stress was about 60% of the yield strength. The maximum deflection was about 0.2% of the panel span. And, the maximum crack width was about 0.005in. (0.13 mm).

4. The presence of service vertical load lowered the in-plane load of first yield by 40 to 50%, but had almost no effect on the ultimate in-plane resistance.

5. The lack of a rib along the extreme edges of the test panels appered to be a source of weakness.

6. Shrinkage cracks developed at the slab-shear wall connection caused a

significant decrease in initial stiffness against in-plane loading. However, the effect on ultimate load and ultimate deflection was negligible.

7. Cyclic loading led to more distributed cracking and plastic deformation. Cyclic loading did not significantly reduce the ultimate resistance of test panel and did not change the development of the major crack.

8. Except for very small loading or displacement amplitudes, the stiffness of the waffle slab panel decreased for each of the three successive cycles of the same amplitude.

9. In-plane strength of the slab panels was basically controlled by the flexural strength at the major crack. In all cases, the major crack was parallel to the fixed edge, and was located near where many of the negative reinforcing bars in the column strips were terminated. A modified reinforcement arrangement could improve the strength behavior of the slab panels.

10. The bent up (or trussed) bars in a slab panel tended to straighten after the opening of the major crack, and to accelerate the growth of the cracks.

11. The ultimate in-plane loading varies approximately inversly with the moment-to-shear ratio at the location of major crack.

12. In comparison with other floor systems, waffle slab exhibits larger ductility capacity.

Based on the above observations and conclusions, the following recommendation are proposed:

1. The initial stiffness of waffle slab for in-plane loading may be estimated by a finite element analysis or the method of equivalent thickness considering both shear and bending deformation. To consider the effect of micro-cracks due to shrinkage, the calculated results may be reduced by 10 to 20 percent.

2. The arrangement and amount of reinforcement affect significantly the strength and crack pattern of the slab panel. Reinforcement with separate straight top and bottom bars is preferred to that with bent-up continuous bars. Extending negative reinforcement into the positive bending regions and placing additional bars near the edge of slab would improve the in-plane behavior of floor slab.

3. The use of an edge beam (rib) around the external edges of waffle slab is strongly recommended.

Chapter 9

Reference

1. American Concrete Institute
   BUILDING CODE REQUIREMENTS FOR REINFORCED CONCRETE AND COMMENTARY. ACI Standard 318-71, 318-77, 318-83, Detroit.

2. American Concrete Institute
   MANUAL OF STANDARD PRACTICE FOR DETAILING REINFORCED CONCRETE STRUCTURES, ACI Standard 315-65, Detroit.

3. American Society for Testing and Materials
   ASTM STANDARDS.

4. Concrete Reinforcing Steel Institute
   CRSI HANDBOOK, CRSI, Chicago, 1972.

5. Nakashima, M.,
   SEISMIC RESISTANCE CHARACTERISTICS OF REINFORCED CONCRETE BEAM-SUPPORTED FLOOR SLABS IN BUILDING STRUCTURES, PHD DISSERTATION, Department of Civil Engineering, Lehigh university, Bethlehem, Pa., March, 1981.

6. Nakashima, M., Huang, T., and Lu, L. W.,
   EXPERIMENTAL STUDY OF BEAM SUPPORTED SLABS UNDER IN-PLANE LOADING, ACI Journal, January-February, 1982

7. Karadogan, H. F., Huang, T., Lu, L. W., and Nakashima, M.,
   BEHAVIOR OF FLAT PLAT FLOOR SYSTEMS UNDER IN-PLANE SEISMIC LOADING, Proceedings of the seventh World Conference on Earthquake Engineering, Istanbul, Turkey, September, 1980.

8. Nakashima, M., Lu, L. W., Huang, T., and Karadogan, H. F.,
   CURRENT RESEARCH AT LEHIGH UNIVERSITY ON CONCRETE FLOOR SYSTEMS UNDER IN-PLANE SEISMIC LOADING, Proceedings of the seventh World Conference on Earthquake Engineering, Istanbul, Turkey, September, 1980.

9. Karadogan, H. F., Lu, L. W., and Huang, T.,
TECHNIQUES FOR IN-PLANE VIBRATION AND SHEAR TESTING OF MODEL FLOOR SLABS, Symposium on Dynamic Modeling of Concrete Structures, ACI Publication SP-73, Detroit, Michigan, 1982.

10. Nakashima, M., Huang, T., and Lu, L. W.,
EFFECT OF DIAPHRAGM FLEXIBILITY ON SEISMIC RESPONSE OF BUILDING STRUCTURES, Proceedings of the eigth World Conference on Earthquake Engineering, Sanfrancisco, California, 1984.

11. Wu, Z., and Huang, T.,
AN ELASTIC ANALYSIS OF A CANTILEVER SLAB PANEL SUBJECTED TO AN IN-PLANE END SHEAR, Fritz Laboratory Report No. 481.1, Lehigh University, May, 1983.

12. Wu, Z., and Huang, T.,
AN EQUIVALENT THICKNESS ANALYSIS OF WAFFLE SLAB PANELS UNDER IN-PLANE SHEAR LOADING, Fritz Laboratory Report NO. 481.2, Lehigh University, May, 1983.

Table 2.1a REINFORCEMENT OF THE WAFFLE SLAB PANELS

	POSITIVE STEEL *		NEGATIVE STEEL	
	COLUMN STRIP	MIDDLE STRIP	COLUMN STRIP	MIDDLE STRIP
DESIGN BENDING MOMENT (ft-lb)	843	562	1958	652
DESIGN STEEL TENSILE FORCE (lb)	3834	2520	12600	3060
STEEL PROVIDED **	3 D 2.5 3 D 1.0	3 D 2.0	13 D 2.0 4 D 1.0	9 D 1.0
STEEL FORCE PROVIDED ***	3732	2523	12333	3150
PROVIDED STRENGTH / REQUIRED STRENGTH	0.97	1.0	0.98	1.03

* POSITIVE STEEL BARS ARE EQUALLY PLACED IN 3 RIBS IN EACH 32" STRIP.

** SEE FIG. 2.3 , REINFORCEMENT OF SPECIMEMS

*** SEE TABLE 3.1 , FOR AREAS AND YIELD STRENGTH OF THE VARIOUS REINFORCING WIRES

1 lb = 4.5 N ; 1 ft-lb = 1.372 N-M

Table 2.1b REINFORCEMENT OF THE FLAT SLAB PANEL

	POSITIVE STEEL		NEGATIVE STEEL	
	COLUMN STRIP	MIDDLE STRIP	COLUMN STRIP	MIDDLE STRIP
PREVIOUS SPECIMEN:				
REINFORCMENT PROVIDED	16 D°2.0	8 D°2.0	32 D°2.0	8 D°2.0
STEEL FORCE PROVIDED	19200 lb	9600 lb	38400 lb	9600 lb
DESIGN FOR PANEL:				
REINFORCMENT PROVIDED	16 D°2.0	8 D°2.0	32 D°2.0	10 D 2.0 *
STEEL FORCE PROVIDED	19200 lb	9600 lb	38400 lb	8950 lb
PROVIDED STRENGTH / PREVIOUS STRENGTH	1.0	1.0	1.0	0.932

* D 2.0 ___ ANNEALED

1 lb = 4.5 N

TABLE 3.1 MECHANICAL PROPERTIES OF REINFORCING BARS

Bar Size	D1.0	D2.0	D2.5	D° 2.0	# 3
Area (in²)	0.00826	0.0188	0.0249	0.0197	0.11
Yield Load (lb)	350	841	894	1153	6250
Ultimate load (lb)	471	1254	1418	1290	9370
yield strength (psi)	42400	44700	35900	60100	56800
ultimate strength (psi)	57100	66700	56900	65500	85200
Modulus of Elasticity (10^6 psi)	23.5	30.4	29.9	29.6	29.1

1 in² = 645 mm² ; 1 lb = 4.5 N ; 1 psi = 6.89 KPa

Fig. 3.1 shows E_s for D 2.0 $\approx \frac{49.7}{0.0018} \approx 28 \times 10^6$

D 2.5 $\approx \frac{35.9}{0.0012} \approx 30 \times 10^6$!

Table 3.2 THE CONCRETE MIX PROPORTIONS

Materials	per yard^3	per M^3
Portland Cement, Type 1	470 lbs	163 kg
Coarse Aggregater, Crushed Limestone	1308 lbs	455 kg
Fine Aggregater, Concrete sand	1769 lbs	615 kg
Water	277 lbs	96 kg
WRDA-19 Plastisizer	85 oz	2.4 L.
Water Cement Ratio, by weight	0.59	0.59
Slump	6 in.	152 m.m

Table 3.3 GRADATION OF COARSE AGGREGATE

Sieve Size	% Retaind on Sieve	Percentage larger
0.25"	0	0
1.85"	83.6	83.6
Pan	16.4	100.0

TABLE 3.4 MECHANICAL PROPERTIES OF CONCRETE

	Specimen 1			Specimen 2		
Concrete age	7 days	28 days	107 days*	7 days	28 days	180 days*
Compressive Strength (psi)	4262	4515	5336	4188	4132	5037
Splitting tensive strength (psi)	-	403	-	-	361	-
Modulus of elasticity (psi)		3.26×10^6	3.47×10^6	-	3.06×10^6	3.46×10^6
Poisson's Ratio	-	0.18	0.18	-	0.20	0.18

*After completion of slab specimen test

1 psi = 6.89 kPa

Table 5.1 Designation of Test Programs
(Five character alphanumeric)

1	2	3	4	5

1. Type of floor system
   - W Waffle slab
   - F Flat slab
2. Presence of vertical load
   - H Horizontal (in-plane) loading only (Without supplemental out-of-plane loading)
   - V Vertical (out-of-plane) load indicated (With the equivalent of full service dead and live load.)
3. Panel or Panels being tested
   - 1 or 2 The side panels (see Fig 5.1)
   - 3 The middle panel tested alone
   - 4 Panels 1 and 3 together
   - 5 Panels 2 and 3 together
   - 6 All panels together (Stiffness test)

4 and 5. Type of test
   - SS Stiffness test, Symmetrical loading
   - SA Stiffness test, Anti-Symmetrical loading
   - MN MoNotonic loading
   - CY CYclic loading

Example:

WV1CY
- Waffle slab floor system
- Vertical loading first, then in-plane loading
- Panel 1 is tested
- Strength test with CYclic loading

Table 5.2 THE VERTICAL LOAD OF SPECIMENS

Prototype dead load	84.4	psf
Specimen dead load	18.7	psf
Weight of distribution system	7.9	psf
Compensatory dead load needed	57.7	psf
Service Live load	80.0	psf
Total vertical load needed	137.7	psf
Applied point load	435.	lb

1 psf = 47.9 Pa ; 1 lb = 4.5 N

Table 5 3

THE VERTICAL LOADING SEQUENCE

LOAD NO.	LOAD ON SLAB (psf)	EQUIVALENT CONCENTRATED LOAD AT EACH LOADING POINT (lb)	NOTE	
0	26.7 *	84.3	31.6% DL	16.2%
1	43.9	138.6	52.0% DL	26.7%
2	61.1	193.0	72.4% DL	37.2%
3	78.3	247.4	92.8% DL	47.6%
4	95.5	301.8	DL + 13.9% LL	58.1%
5	112.7	356.2	DL + 35.4% LL	68.6%
6	129.9	410.6	DL + 56.9% LL	78.9%
7	147.2	465.0	DL + 78.5% LL	89.5%
8	164.4	519.4	DL + LL	100%
9	26.7	84.3	31.6% DL	16.2%

* The self weight of specimen and distribution devices.

1 PSf = 47.9 Pa 1 lb = 4.5 N

Table 6.1 THE INITIAL FLEXIBILITY (10^{-3} INCH / KIP)

TEST	EXPERIMENT	SAP IV	THE EQUIVALENT THICKNESS METHOD
WH6SS	1.27	1.35	–
WH6SA	2.05	2.45	–
WH1MN	1.13	0.88	0.94
WV2MN	1.47 *	–	–
WH2CY	1.13	0.88	0.94
WV1CY	2.39 *	–	–
WH5MN	5.26	1.71	1.35
FH5MN	2.68	0.77	0.60

* under full service vertical load, there were several cracks in the panel which greatly reduced the stiffness of panel.

Table 6.2 SUMMARY OF THE TEST RESULTS

NO.	TEST	WH1MN	WH2CY	WH5MN	WV2MN	FH5MN	WV1CY
1	Moment-shear ratio (inch)	64	64	128	64	128	64
2	initial flexibility (10^{-3} inch/KIP)	1.13	1.13	5.26	1.47	2.68	2.39
3	Vertical crack load (PSF)	-	-	-	129.7	-	112.7
4	In-plane crack load (KIPS)	11.9	-8.03	6.00	-	7.41	-
5	first yield load (KIPS)	15.96	14.90	8.00	10.01	10.80	7.92
6	Δ'_y (10^{-3} inch)	59.00	39.00	85.50	45.60	78.10	56.80
7	ultimate load, positive (KIPS)	22.12	21.09	12.67	21.36	17.18	21.21
8	negative (KIPS)	22.04	19.89	10.22	19.02	12.28	18.30
9	Δ_1 of ult. load, Positive (10^{-3} inch)	288.2	352.4	895.4	442.7	474.8	308.4
10	negative (10^{-3} inch)	446.6	404.8	1007.4	576.0	202.7	367.0
11	ultimate deflection, positive (10^{-3} inch)	316.5	716.5	1022.7	565.2	605.9	554.6
10	negative (10^{-3} inch)	496.6	664.4	1062.4	576.0	440.2	555.6

1 inch = 25.4 mm ; 1 KIP = 4.448 KN ; 1 PSf = 47.9 Pa

Table. 7.1 COMPARISON OF ULTIMATE DEFLECTIONS

TEST	ULTIMATE DEFLECTION (INCH)		
	POSITIVE	NEGATIVE	TOTAL DEFLECTION
BH2MN	0.333	0.293	0.626
WH1MN	0.316	0.497	0.812
BH1CY	0.329	0.326	0.655
WH2CY	0.716	0.665	1.381
BH3MN	0.288	0.243	0.531
WH5MN	1.023	1.062	2.085
BV1MN	0.363	0.363	0.726
WV2MN	0.566	0.576	1.142
BV2CY	0.265	0.276	0.541
WV1CY	0.557	0.554	1.111
FH5MN	0.606	0.440	1.046
WH5MN	1.023	1.062	2.085

B____ —— Beam-supported slab ; W____ —— Waffle slab ; F____ —— Flat slab

1 inch = 25.4 mm.

Table 7.2 COMPARISON OF THE TEST RESULTS

NO.	COMPARISON ITEM	WV2MN / WH1MN	WH2CY / WH1MN	WV1CY / WH1MN	WV1CY / WV2MN	WV1CY / WH2CY	WH2CY / WV2MN	WH5MN / WH1MN	WH5MN / FH5MN
1	yield load	0.627	0.93	0.50	0.79	0.53	1.49	0.50	0.74
2	Δ'_y	0.77	0.66	0.96	1.25	1.45	0.86	1.45	1.10
3	$+P_u$	0.97	0.95	0.96	0.99	1.01	0.99	0.56	0.73
4	$-P_u$	0.86	0.90	0.83	0.96	0.92	1.05	0.46	0.83
5	ΣP_u	0.91	0.93	0.90	0.98	0.96	1.02	0.51	0.77
6	$+\Delta_{1max}$	1.79	2.76	1.76	0.99	0.78	1.27	3.23	1.69
7	$-\Delta_{1max}$	1.16	1.34	1.12	0.96	0.83	1.15	2.14	2.41
8	$\Sigma\Delta_{1max}$	1.40	1.70	1.34	0.97	0.81	1.21	2.56	2.00

Table 7.3 SUMMARY OF DUCTILITY CALCULATION

TEST	WH1MN	WV2MN	WH2CY	WV1CY	WH5MN	TH5MN
first yield Load P'_y (KIPS)*	15.96	10.01	14.9	7.92	8.00	10.8
Δ'_y (INCH)*	0.0590	0.0456	0.0590	0.0339	0.0858	0.0781
calculated capacity P^c_u (KIPS)	21.15	21.15	21.15	21.15	10.58	15.90
Calculated Δ_y (INCH)	0.0782	0.0962	0.0554	0.0904	0.1135	0.1149
$\Delta_{1\,max}$ (INCH)	0.3165	0.5652	0.7165	0.5546	1.0227	0.6059
$\Delta_{1\,min}$ (INCH)	0.4966	0.5760	0.6644	0.5541	1.0625	0.4402
Δ_{1max} / Δ_y	4.05	5.87	12.94	6.16	9.011	5.27
Δ_{1min} / Δ_y	6.35	5.99	12.00	6.13	9.361	3.83
$\Delta_{1,u}$ (INCH)	0.2882	0.4427	0.3524	0.3084	0.8954	0.4748
$\Delta_{1,-u}$ (INCH)	0.4966	0.5760	0.4047	0.3070	1.0075	0.2027
$\Delta_{1,u} / \Delta_y$	3.69	4.60	6.36	3.41	7.889	4.13
$\Delta_{1,-u} / \Delta_y$	6.35	5.99	7.31	3.40	8.877	1.76

* 1 KIPS = 4.448 KN ; 1 inch = 25.4 mm

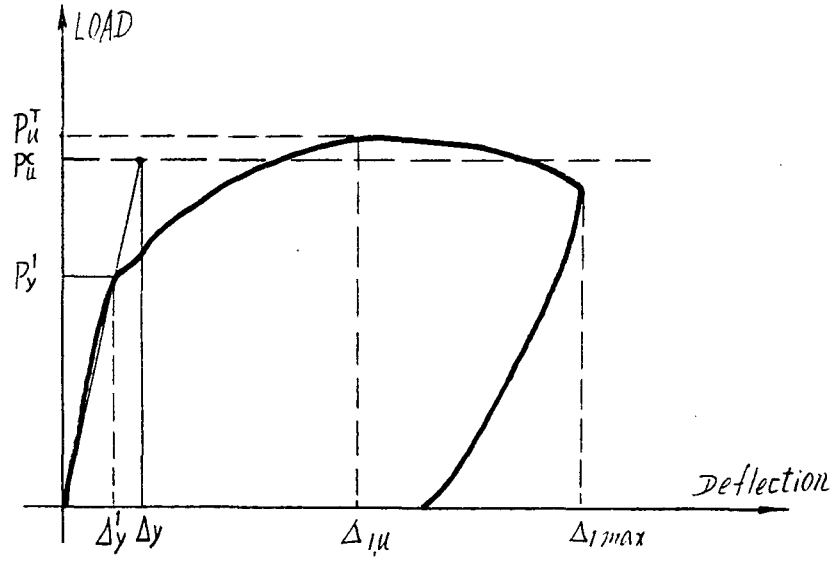

table 7.4 FREQUENCY OF IN-PLANE FREE VIBRATION OF PANELS

Direction	testing time	Measured Frequency				Frequency caculated by SAP IV
		panel 1 of WS-1	panel 2 of WS-1	panel 1 of WS-2	panel 2 of WS-2	
Y	before strength test	100	92	75.5 *	90.3	75
	after strength test	20.4	15.3	–	75.3 △	–
X	before strength test	115	109	87.9 *	180.7	127
	after strength test	16.8	35.3	–	106.4 △	–

* there were some shrinkage cracks on the panel 1 of WS-2

△ After strength test with virtical load, the panel was damaged so much that the panel was almost torn up to two parts connected by reinforcement only. On the hand, the "mass" of vibration part was completely changed.

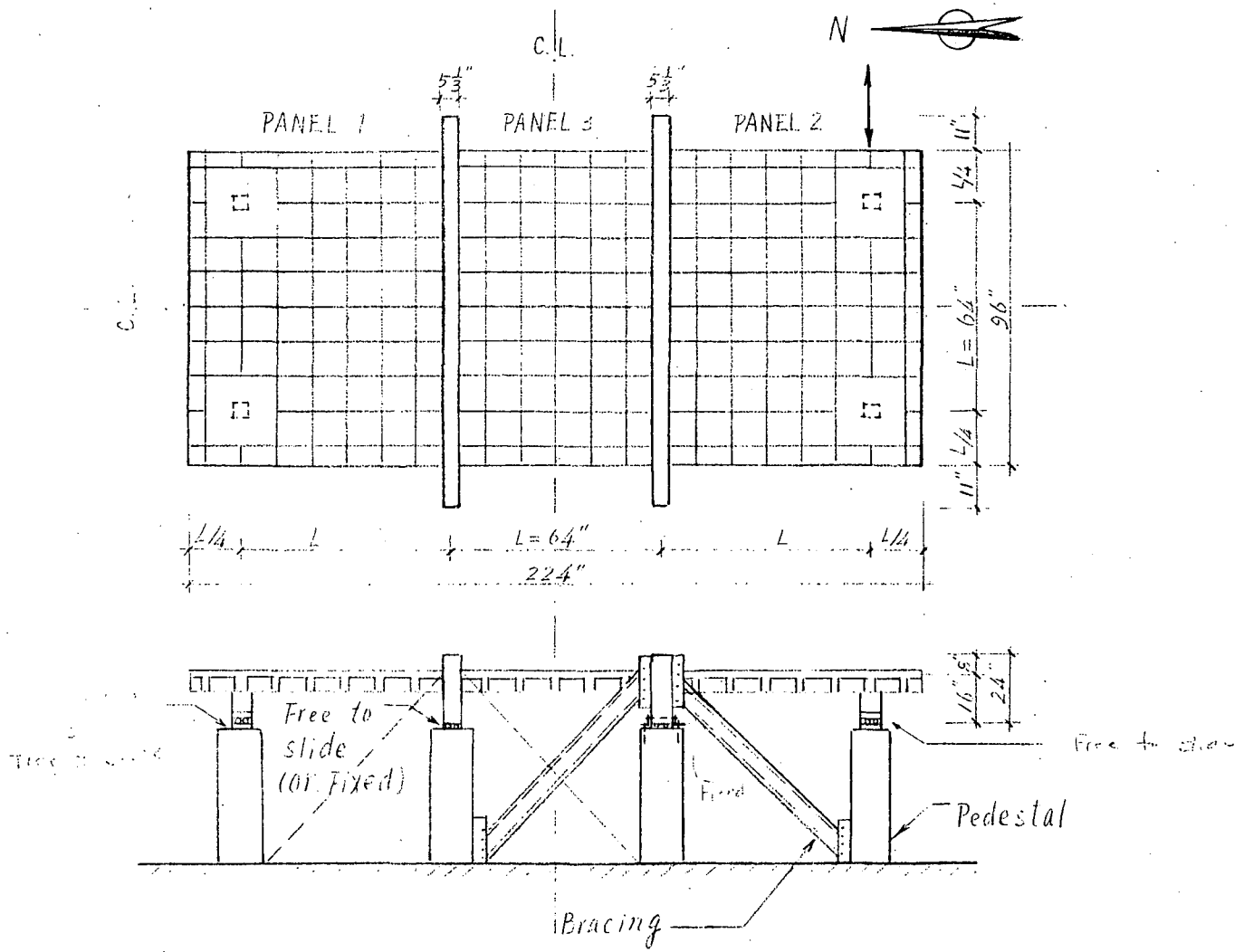

Fig. 1.1a General Dimension and Test Setup of the Specimen
View from west (1" = 25.4 m.m)

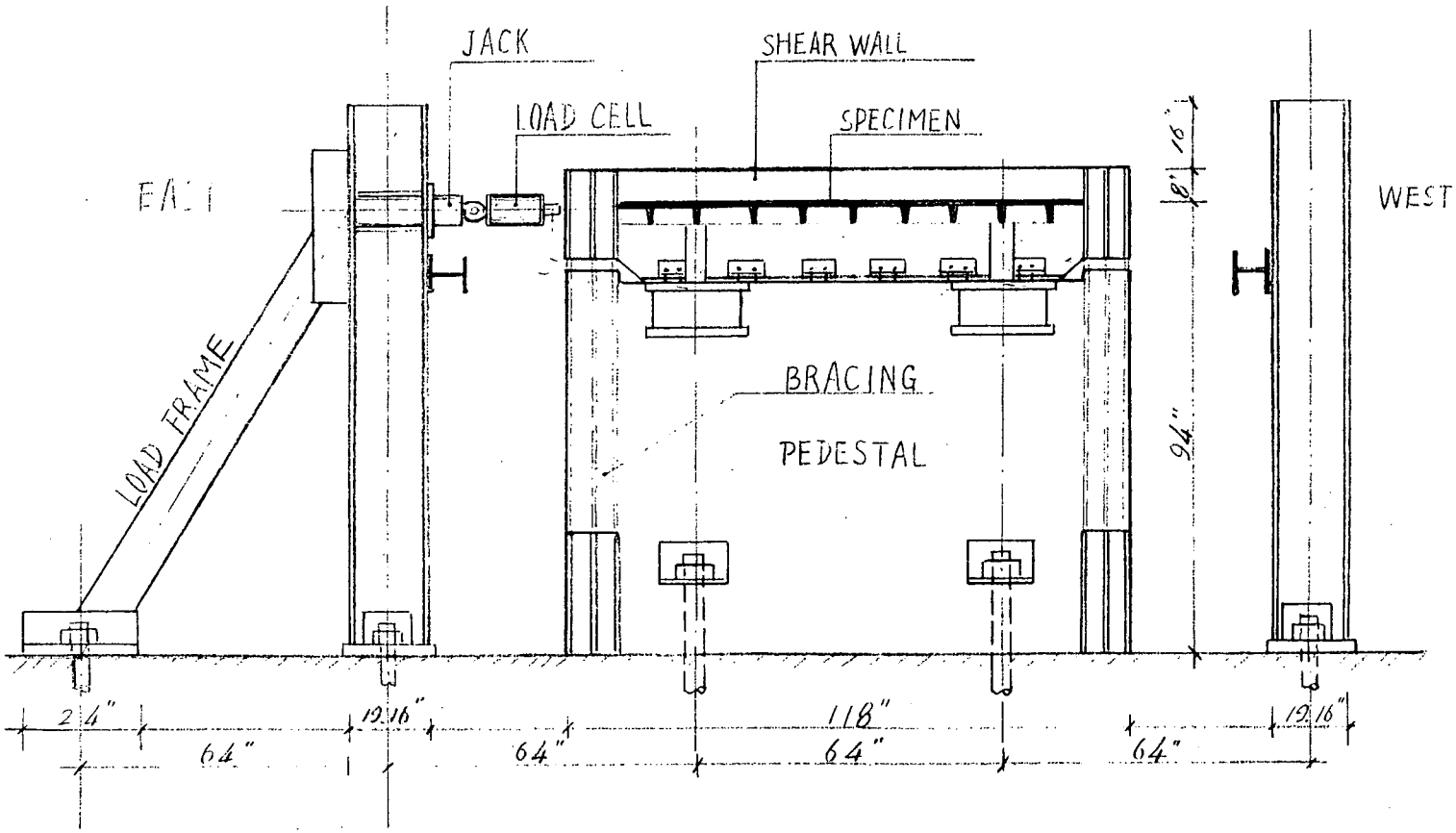

Fig 1.1b General Dimensions and Test Setup of the Specimen
View from North (1" = 25.4 mm)

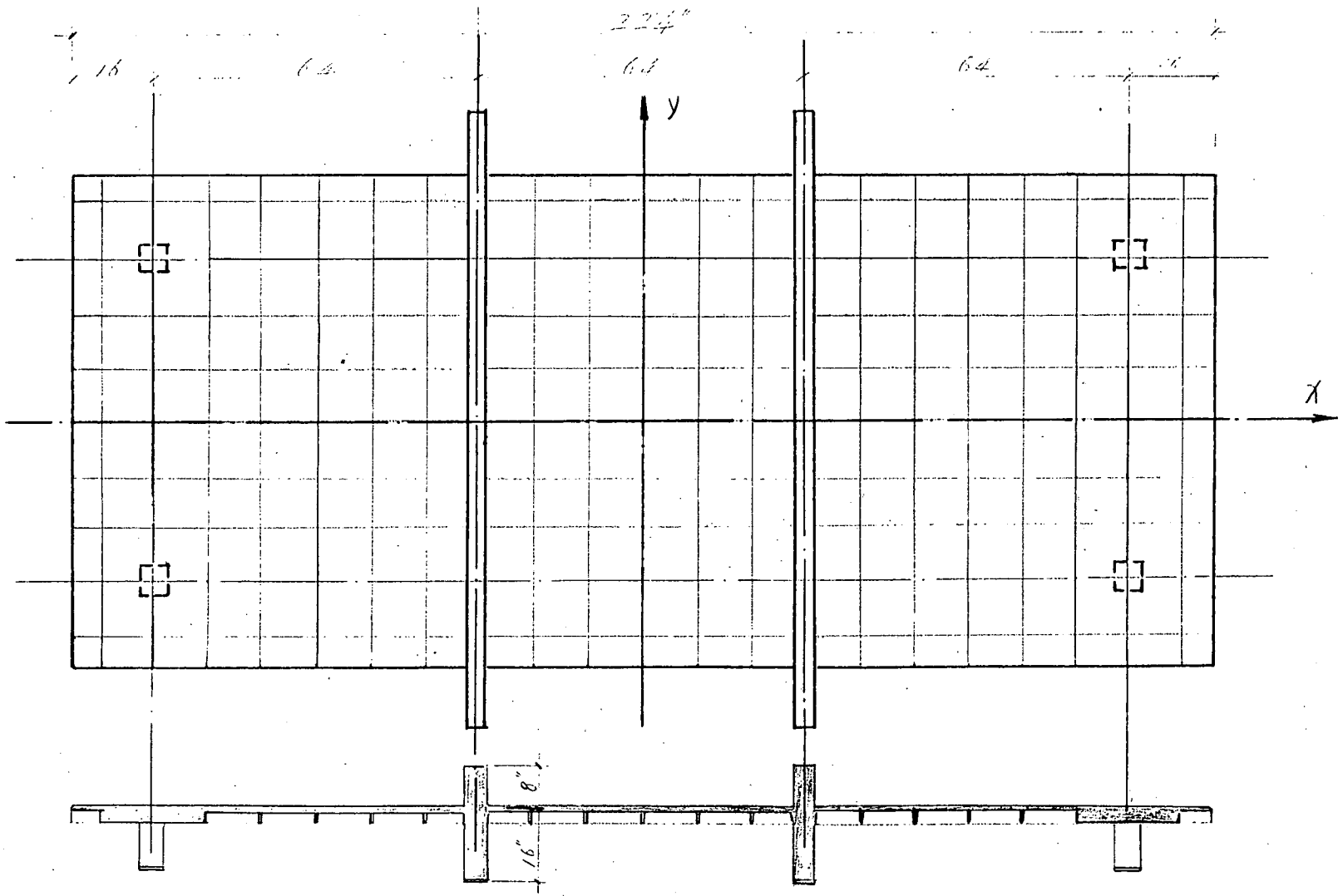

Fig 2.1 Dimensions of waffle slab specimen

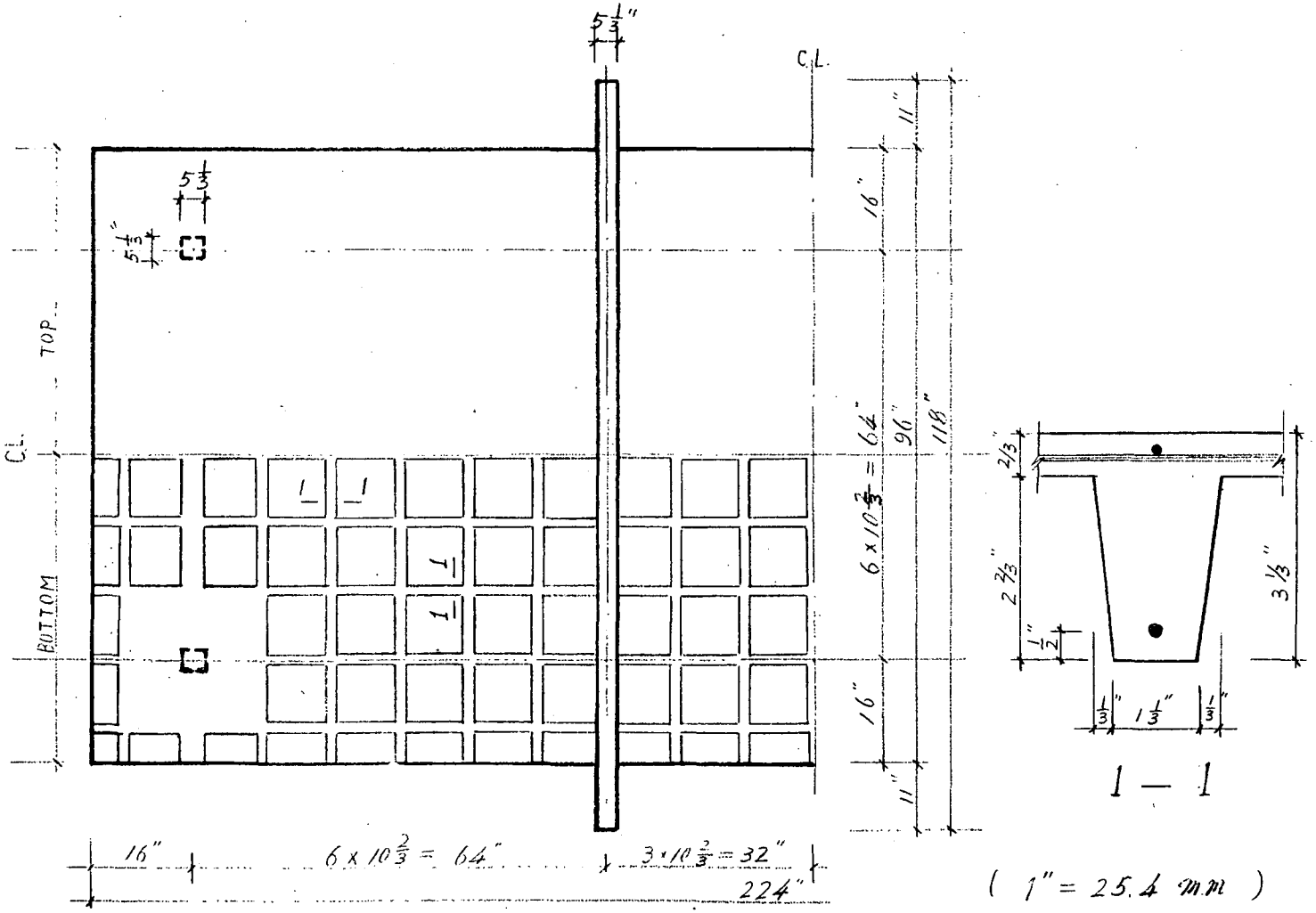

Fig 2.2 DETAILS OF THE WAFFLE SLAB SPECIMEN

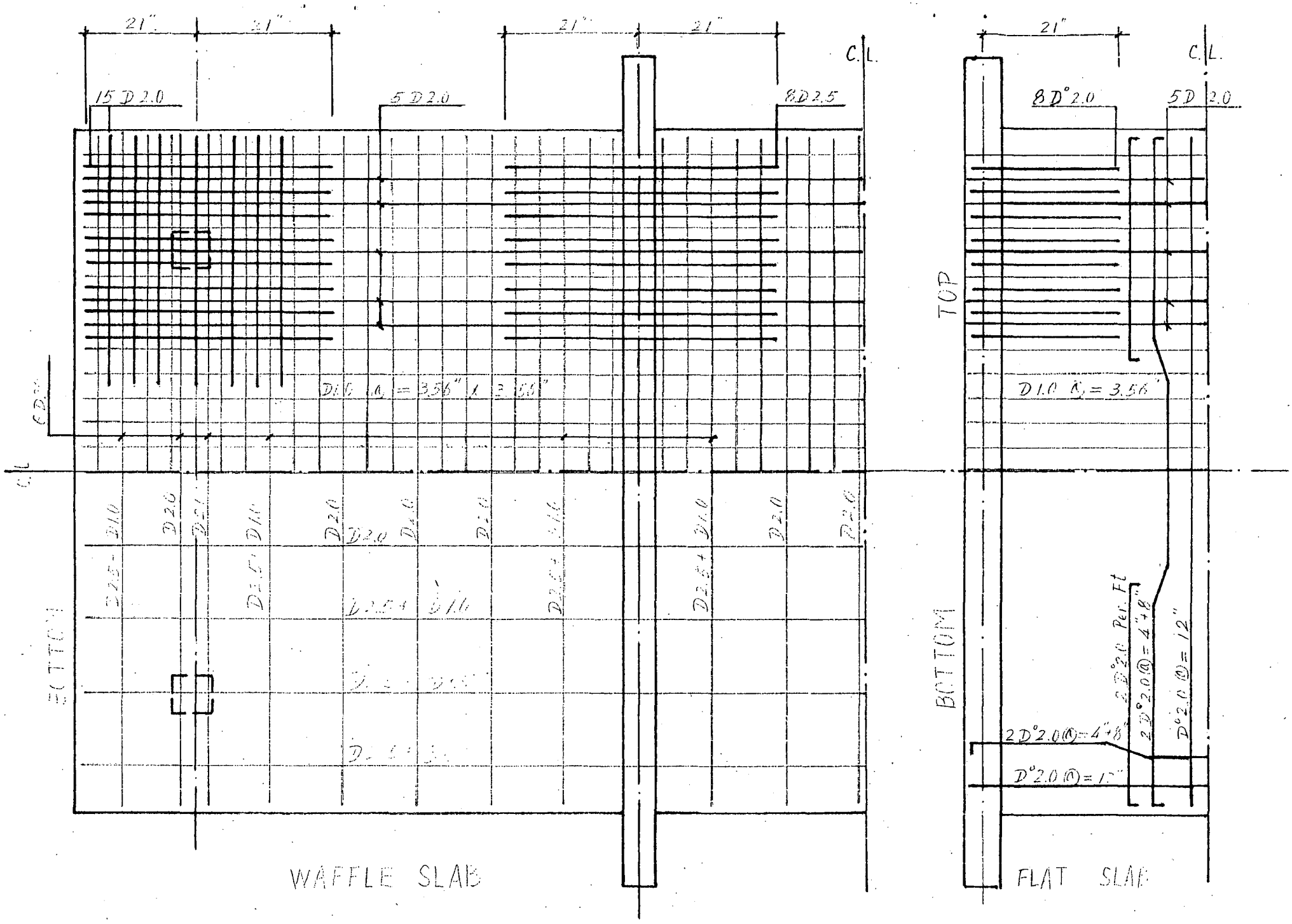
21"
21"
21"
21"
C.L.
15 D 2.0
5 D 2.0
8 D 2.5
C.L.
BOTTOM
WAFFLE SLAB
21"
C.L.
8 D° 2.0
5 D 2.0
TOP
D1.0 @ = 3.56"
BOTTOM
2 D° 2.0 @ = 4"
D° 2.0 @ = 12"
2 D° 2.0 @ = 4"
D° 2.0 @ = 1"
FLAT SLAB

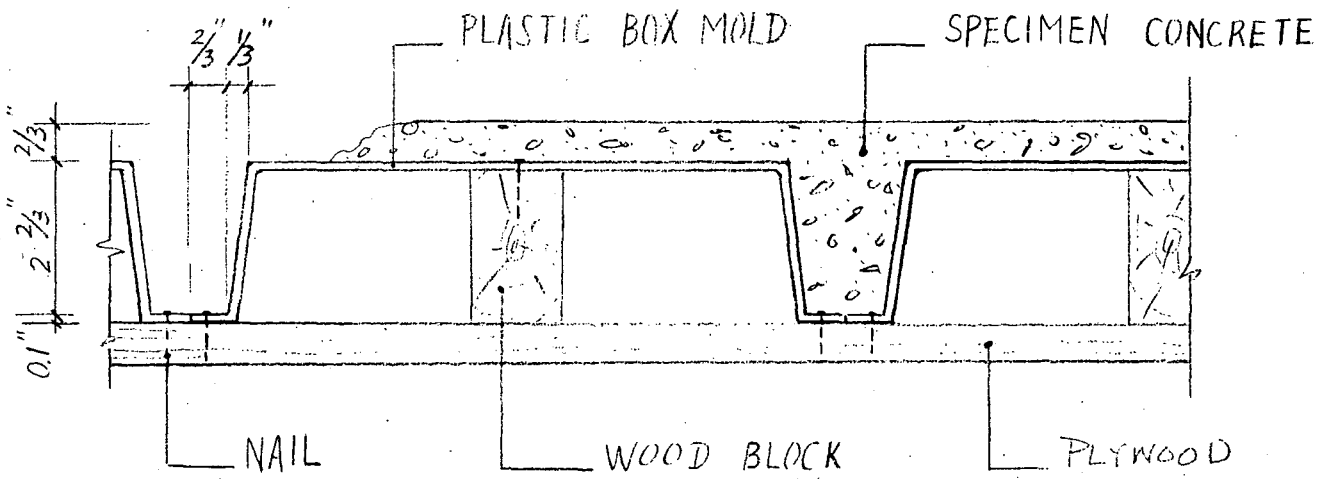

Fig 2.4 The Formwork for Waffle Dome (1"=25.4 mm)

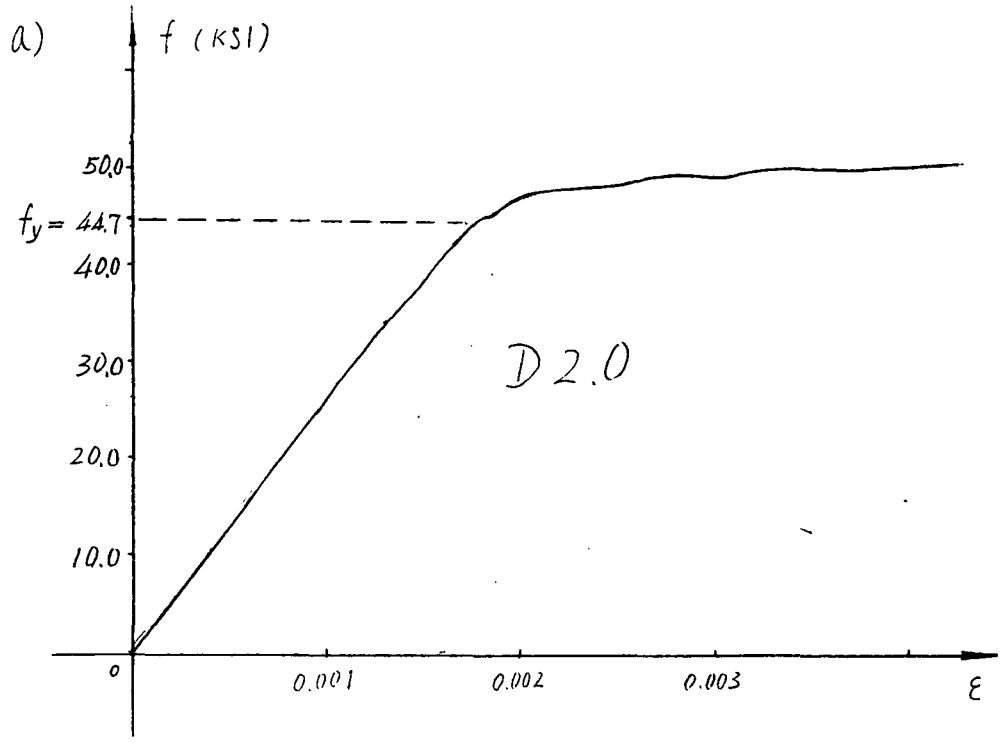

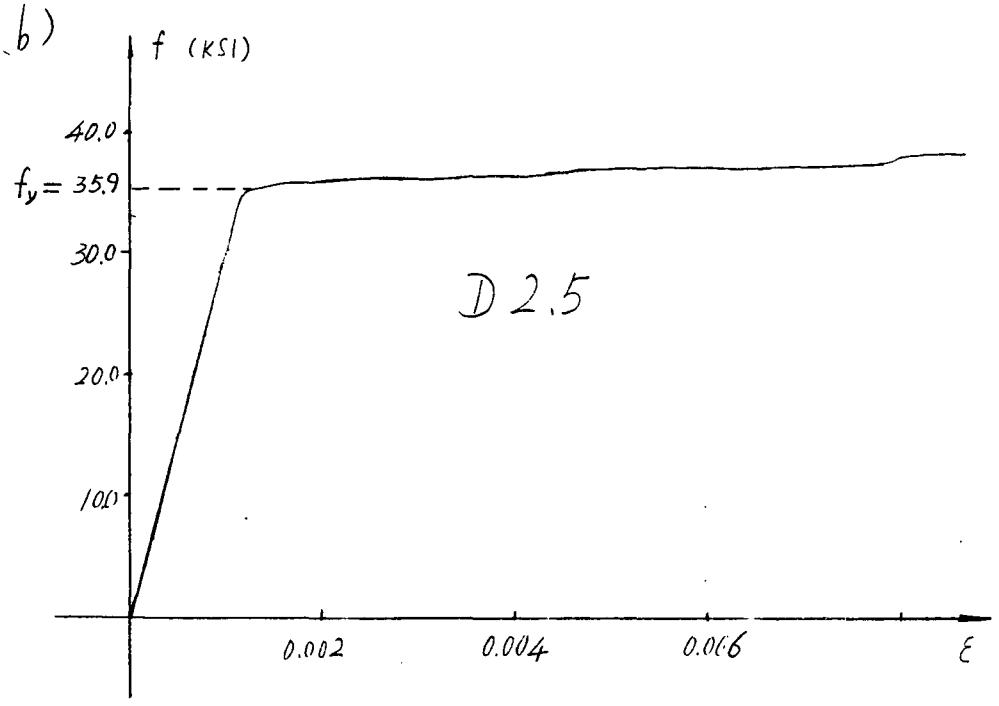

Fig. 3.1 Typical stress-strain curve of annealed bars (1 KSI = 6.89 MPa)

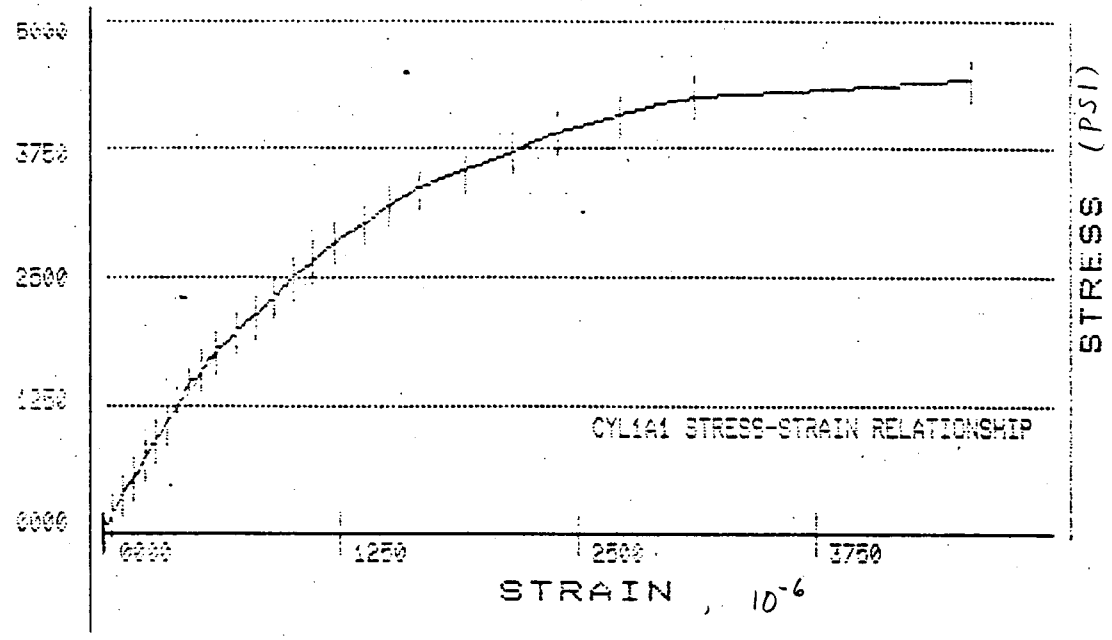

Fig 3.2 A Typical stress-strain relationship of concrete cylinder

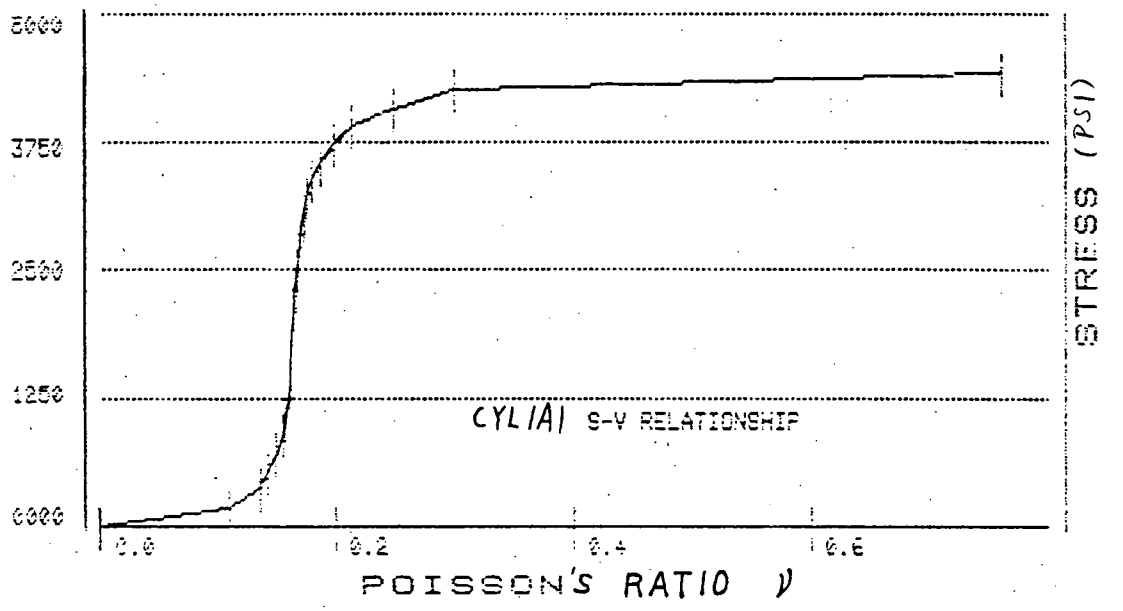

Fig. 3.3 A Typical stress-poisson's ratio relationship of concrete cylinder

(1 PSI = 6.89 KPa)

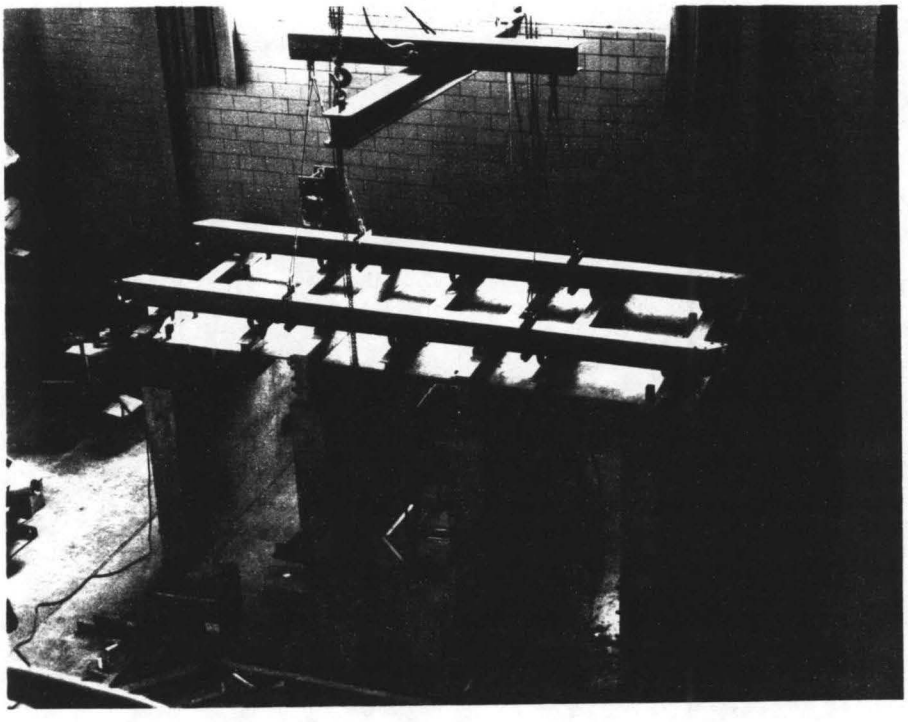

Fig 41 The reinforced concrete pedestals

Fig 42 Shear wall to pedestal Condition

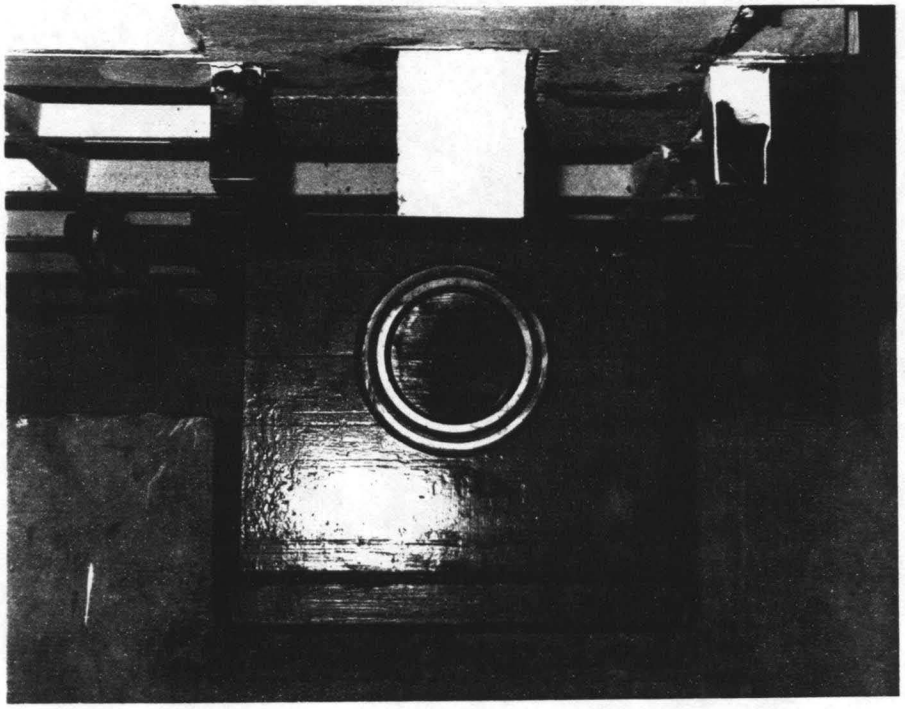

Fig. 4.3 The column base fixture

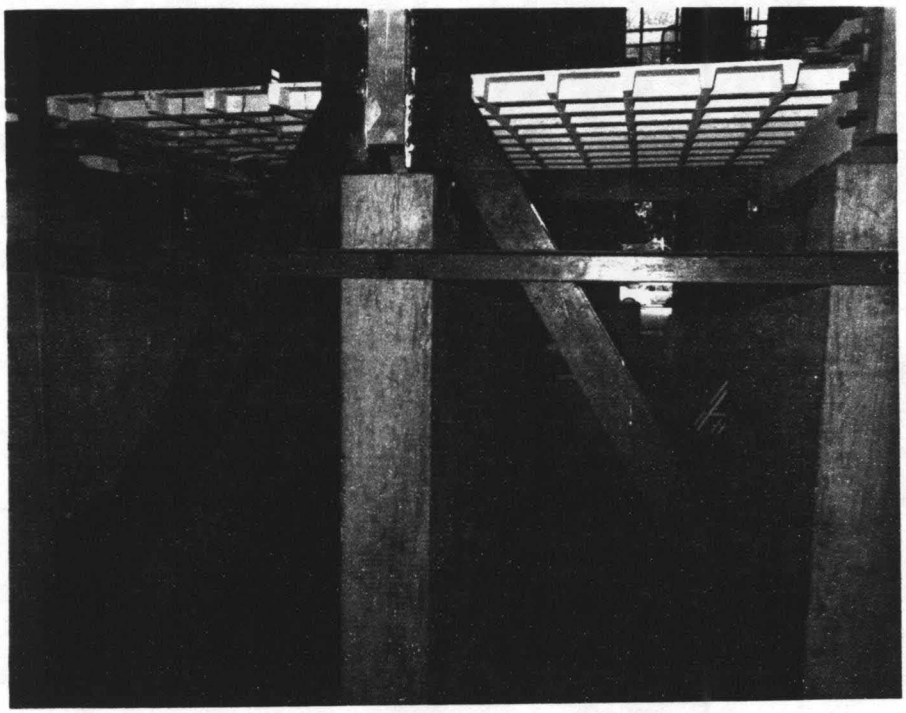

Fig. 4.4 The bracings of shear wall

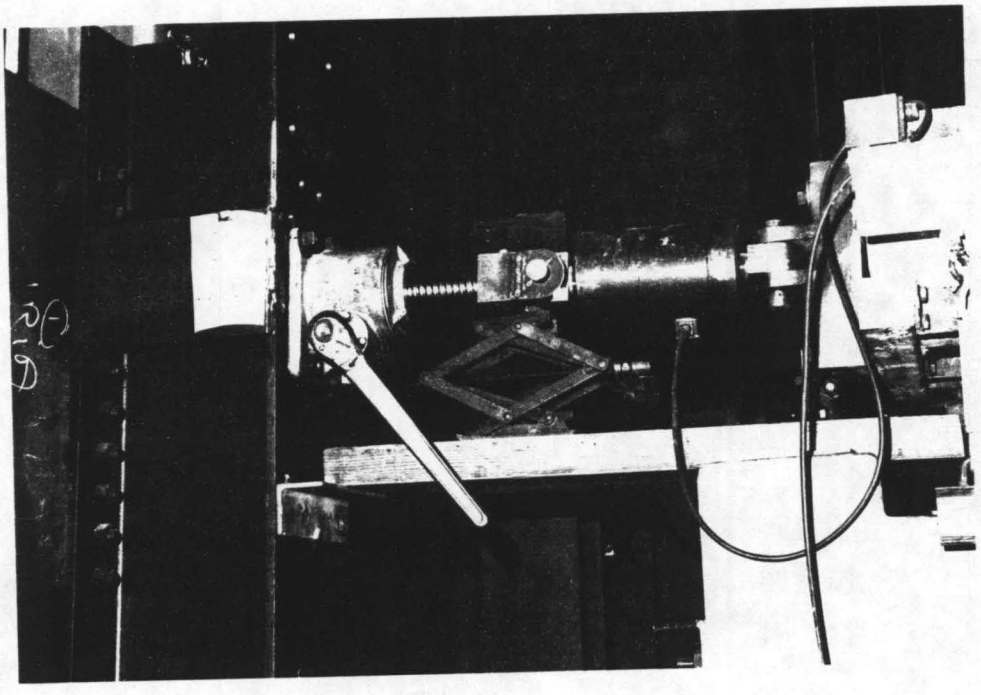

a)

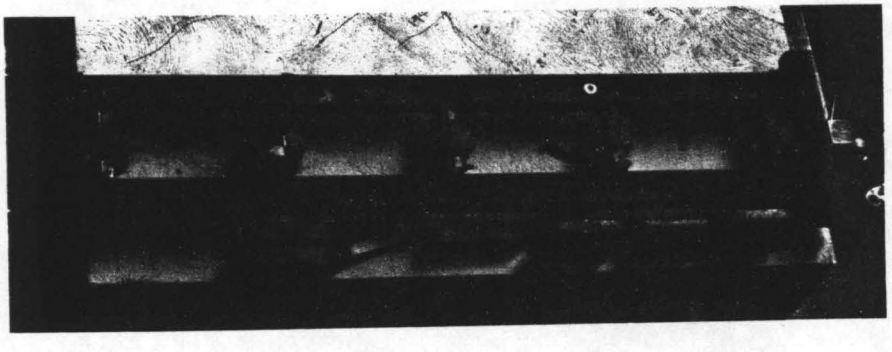

b)

Fig 4.5 The in-plane loading system

a) The mechanical jack and load cell.

b) The horizontal steel frame and studs.

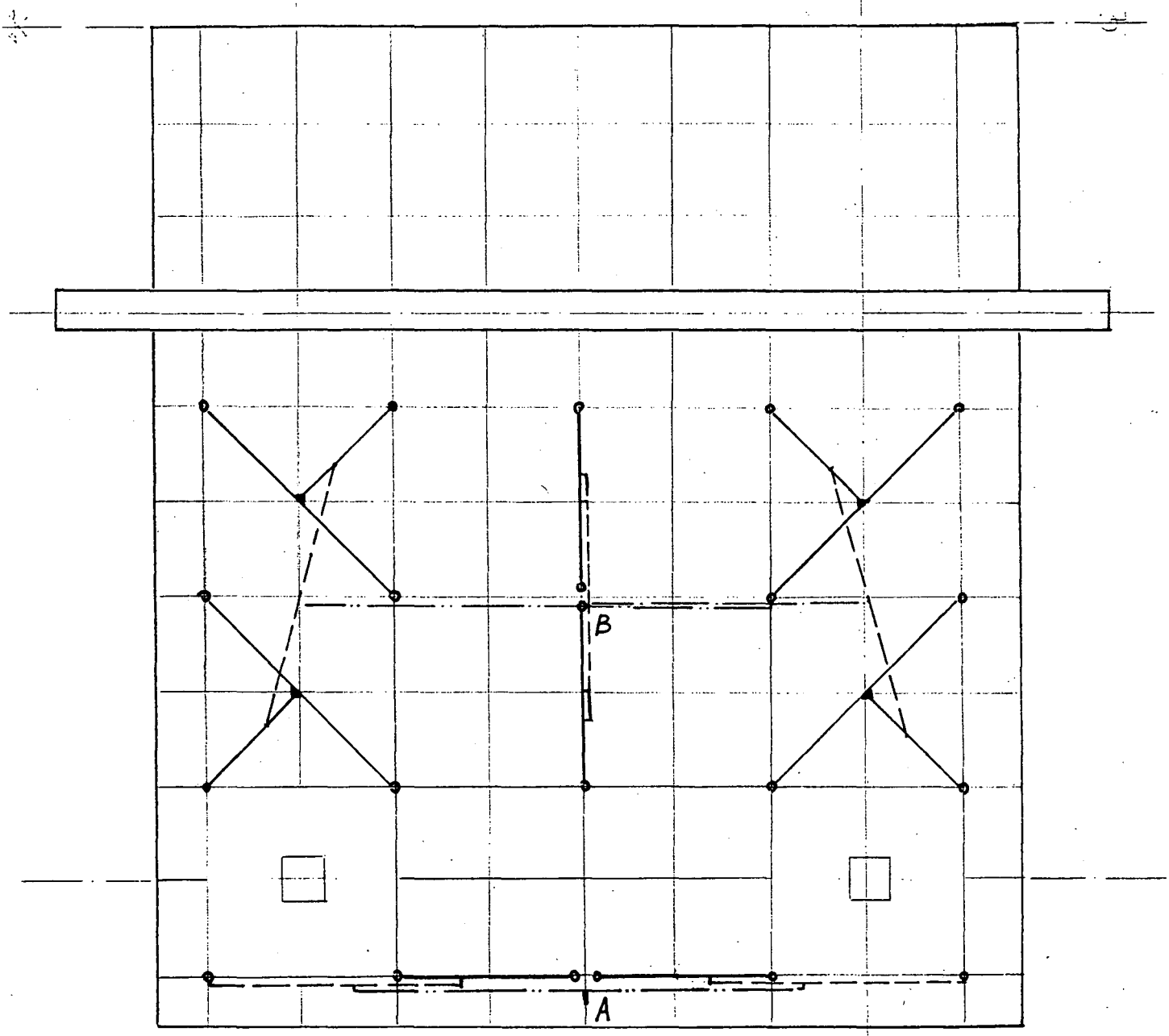

Fig.4.6 THE DISTRIBUTION BEAMS OF VERTICAL LOADING

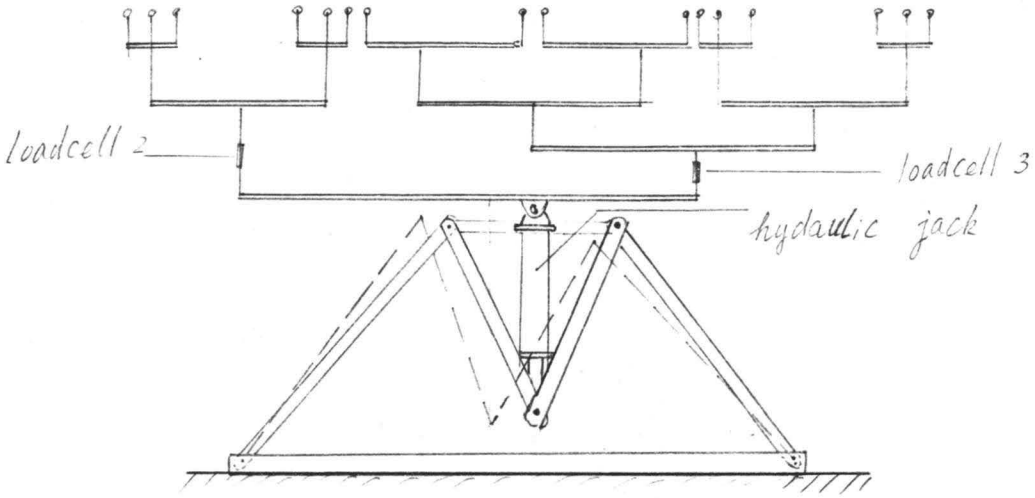

a.

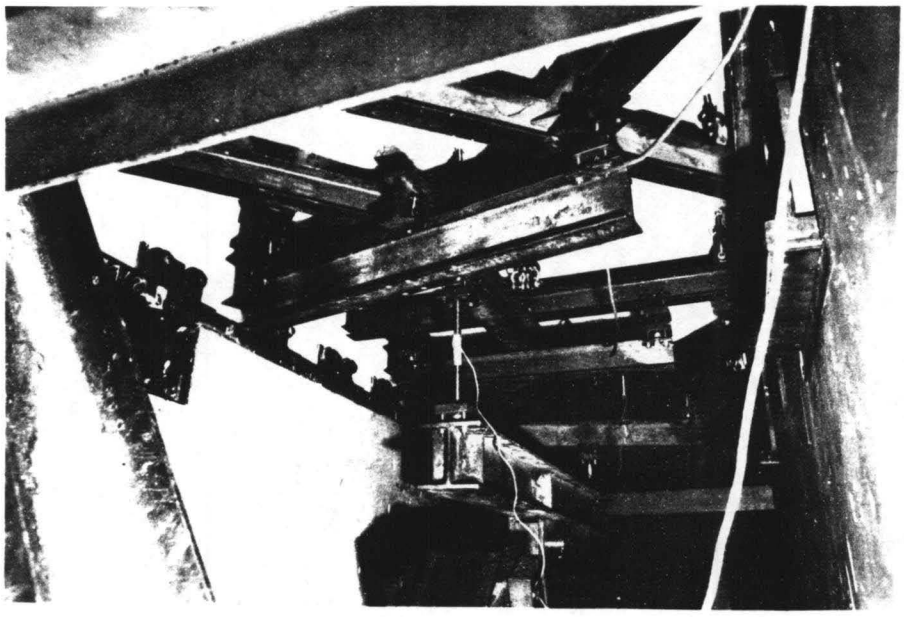

b.

Fig. 4.7 The Vertical loading System
(1) Interior Panel

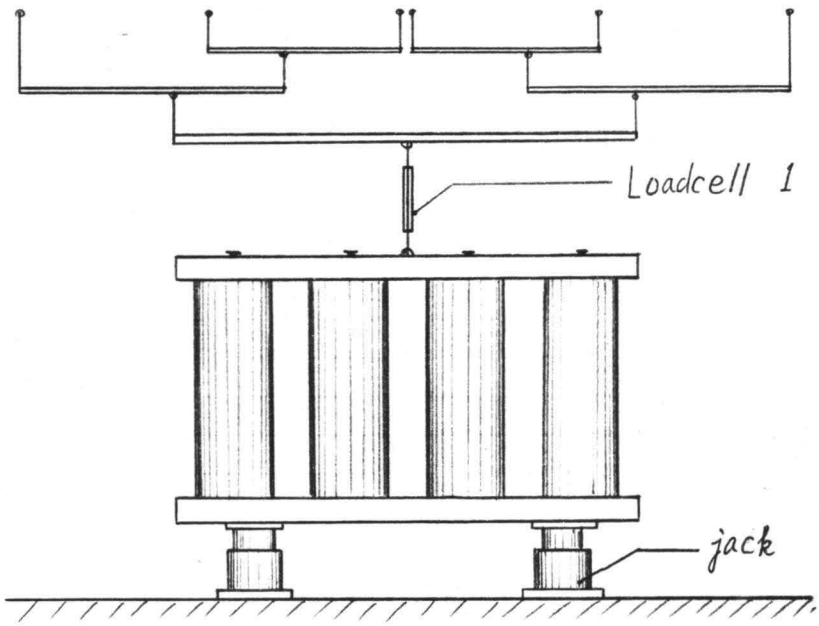

a.

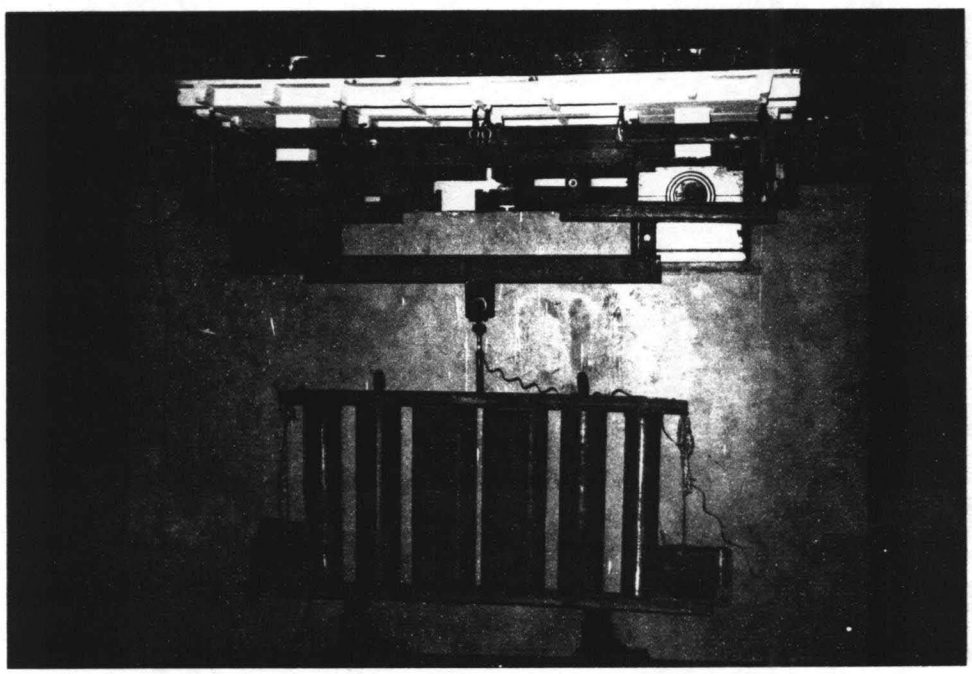

b.

Fig. 4.8 The Vertical loading System

(2) End extension

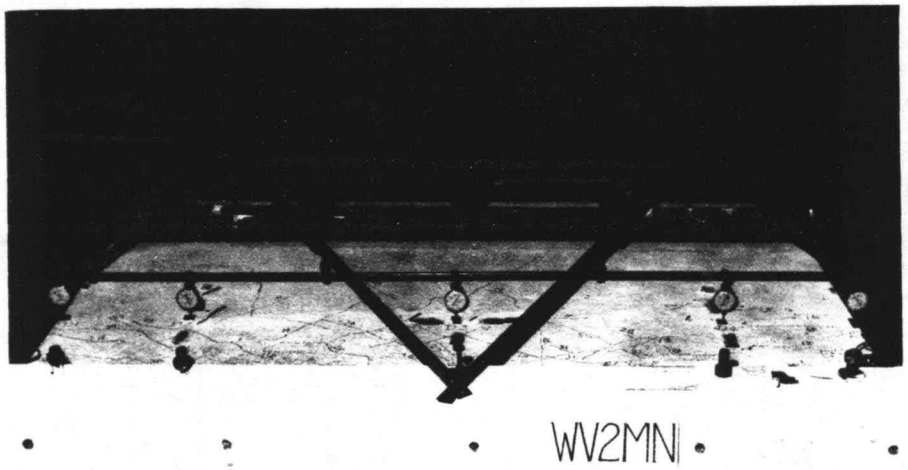

Fig 4.9 The measurement of vertical deflection

— Strain gauge on concrete surface

-- Strain gauge on rebar in the top of rib

Strain gauge on rebar in the bottom of rib

LVDT ○ dail gauge

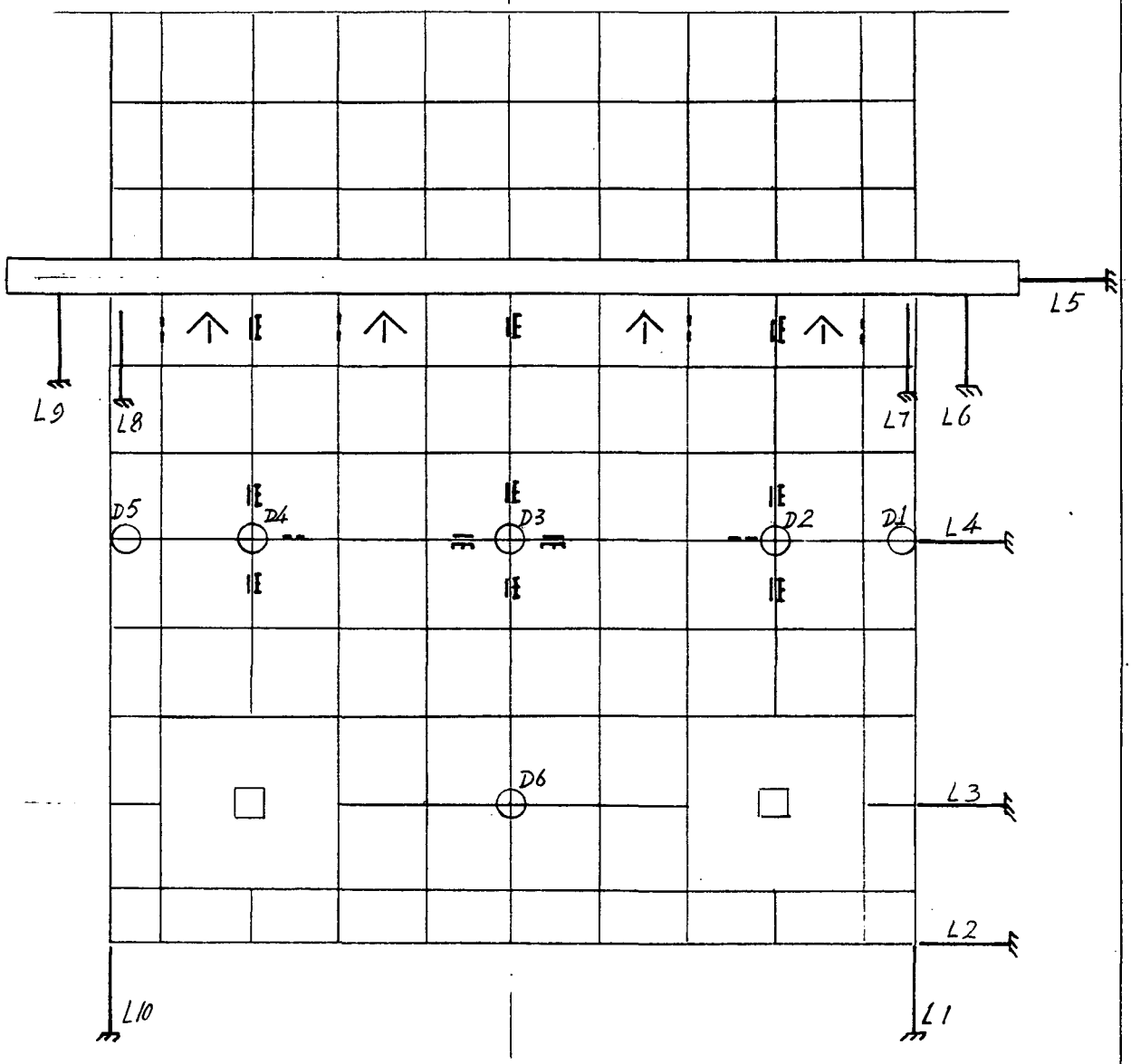

Fig. 4.10 A Typical Arrengement of Instrumentation

Fig. 5.1 TEST SETUP OF WS-1

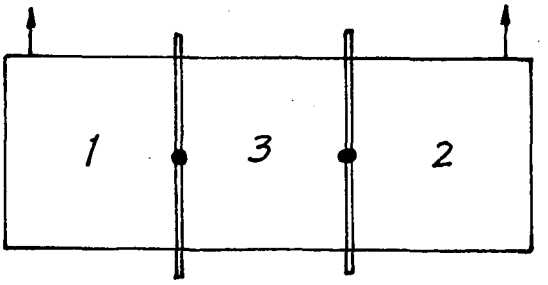

1. WH6SS

Stiffness test, symmetrical loading.

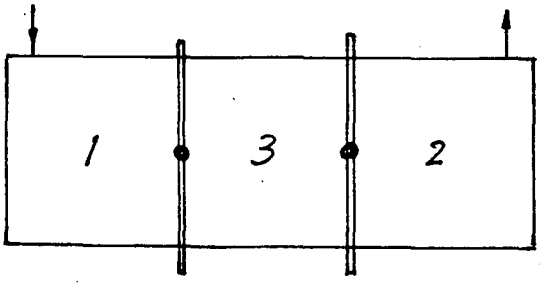

2. WH6SA

Stiffness test, anti-symmetrical loading.

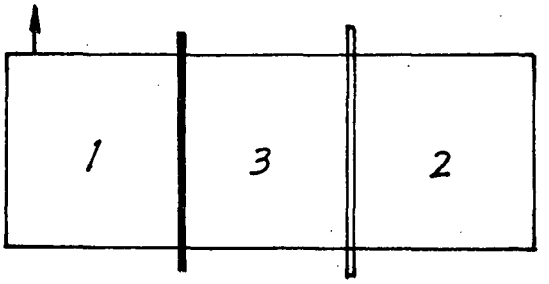

3. WH1MN

Strength test, monotonic loading without vertical load. M/Q = 64".

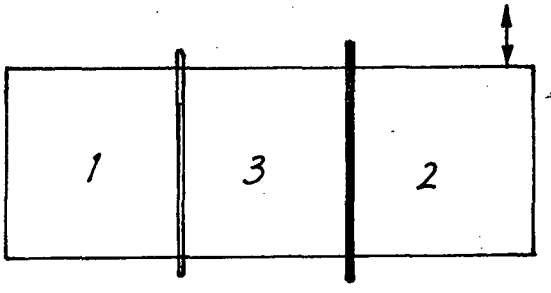

4. WH2CY

Strength test, cyclic loading without vertical load. M/Q = 64".

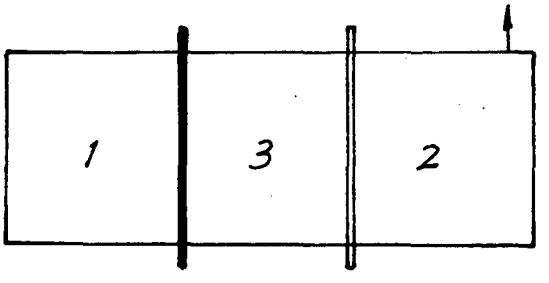

5. WH5MN

Strength test, monotonic loading without vertical load. M/Q = 128".

Fig. 5.2 TEST SEQUENCE OF WS-2

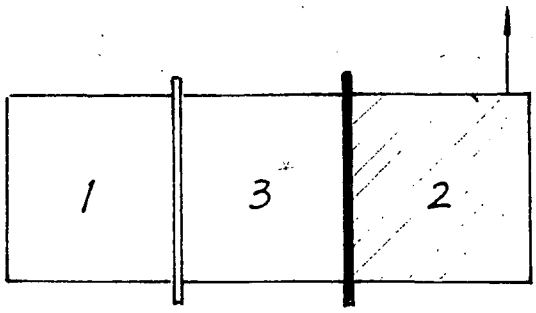

6. WV2MN

Strength test, monotonic loading with vertical load. M/Q = 64"

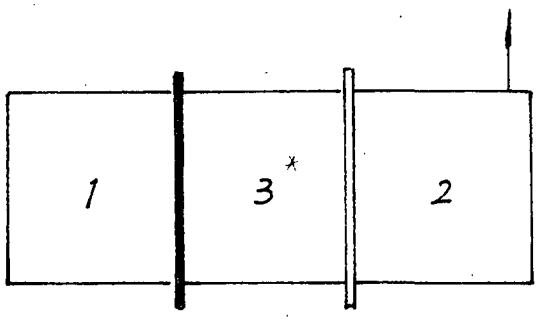

7. FH5MN

Strength test, monotonic loading without vertical load. M/Q = 128"

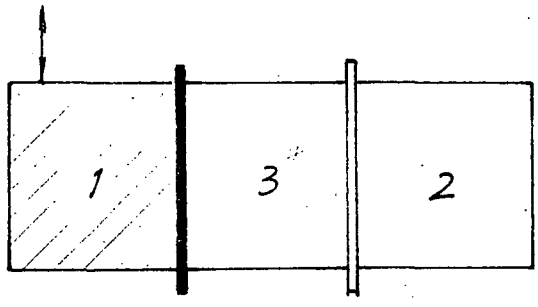

8. WV1CY

Strength test, cyclic loading with vertical load. M/Q = 64"

* Panel 3 is a flat slab

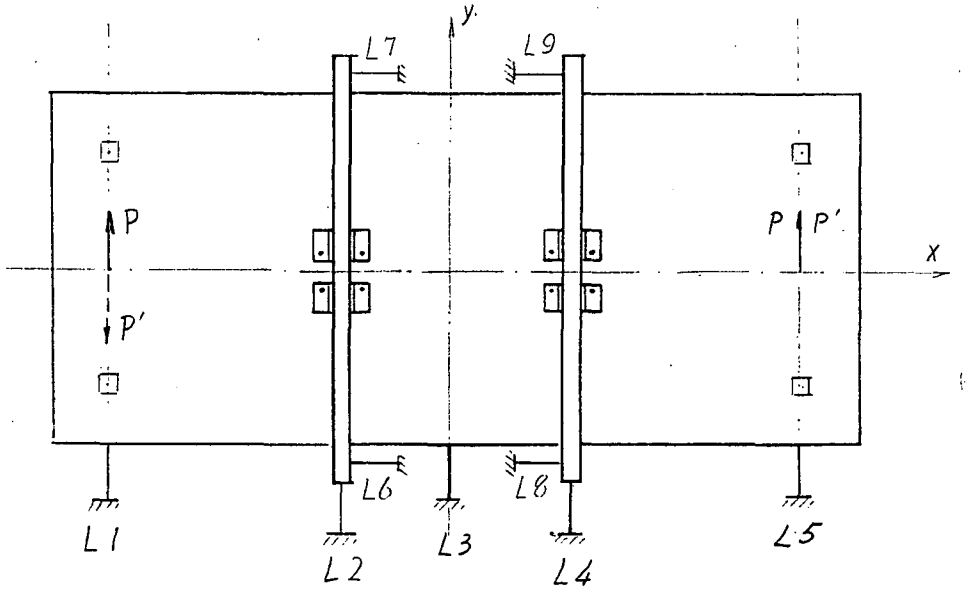

LVDT

P — SYMMETRICAL

P' — ANTI-SYMMETRICAL LOAD

ANCHOR BOLT

Fig. 5.3 STIFFNESS TESTS

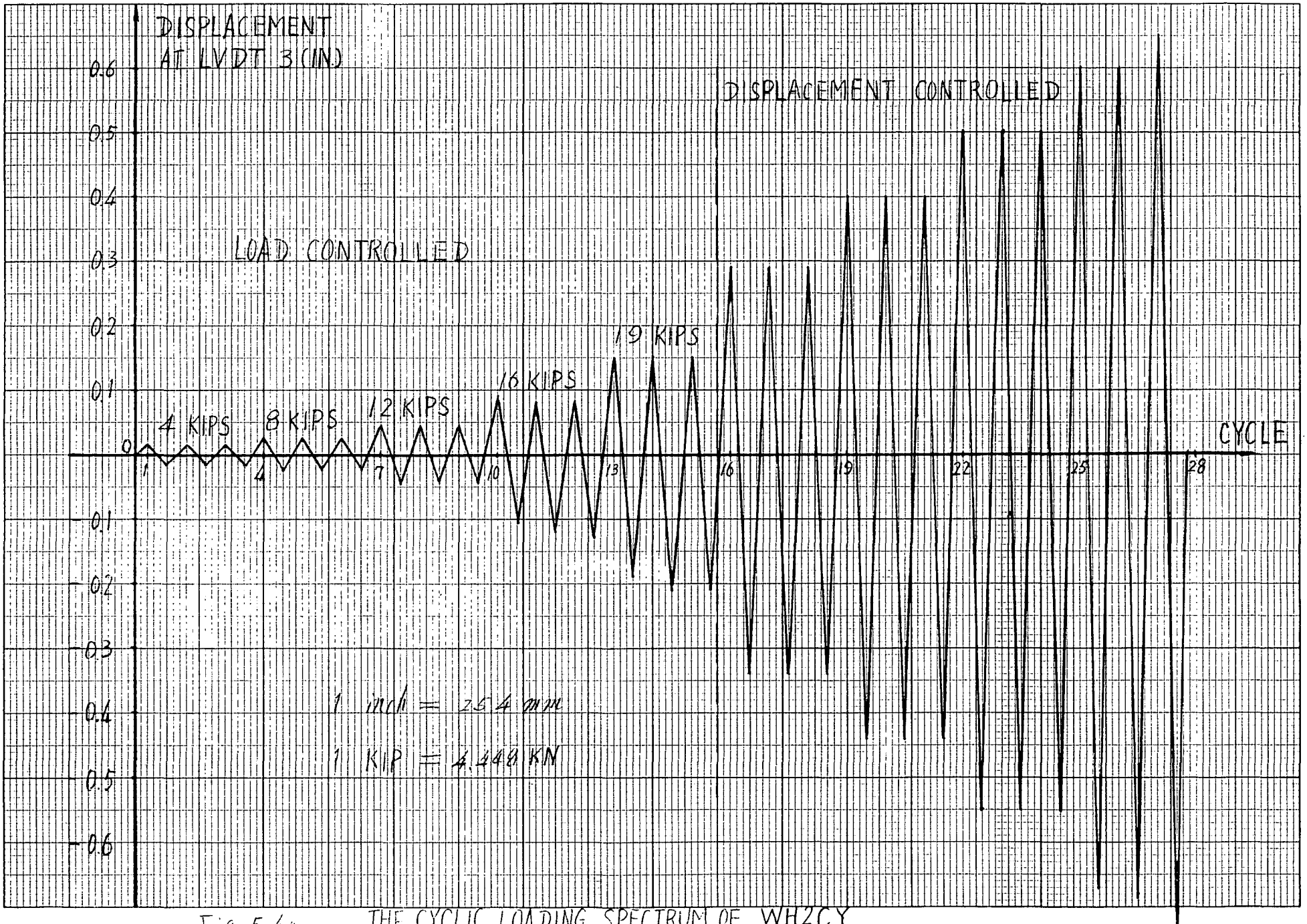

Fig. 5.4a THE CYCLIC LOADING SPECTRUM OF WH2CY

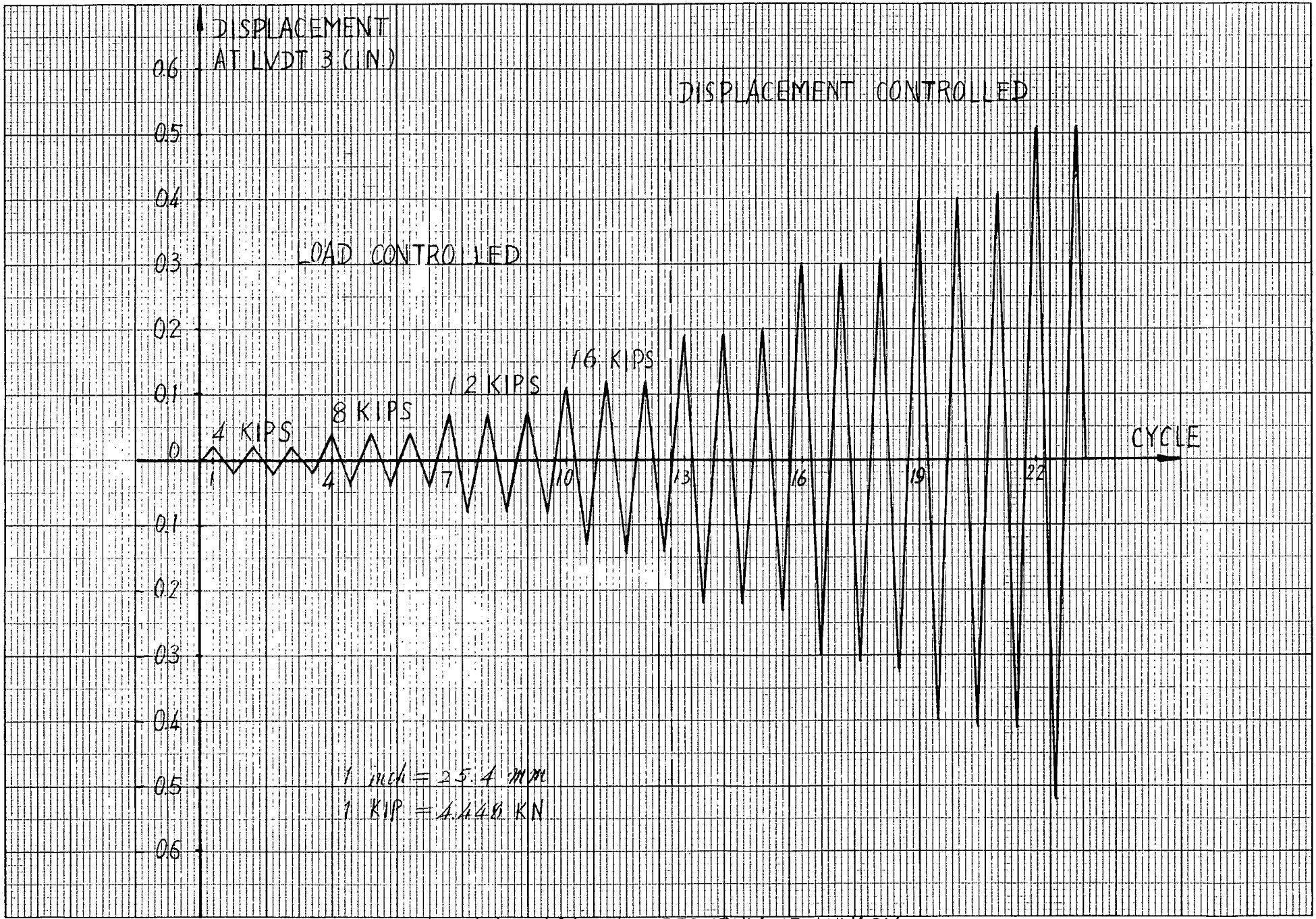

Fig. 5.4b THE CYCLIC LOADING SPECTRUM OF WVICY

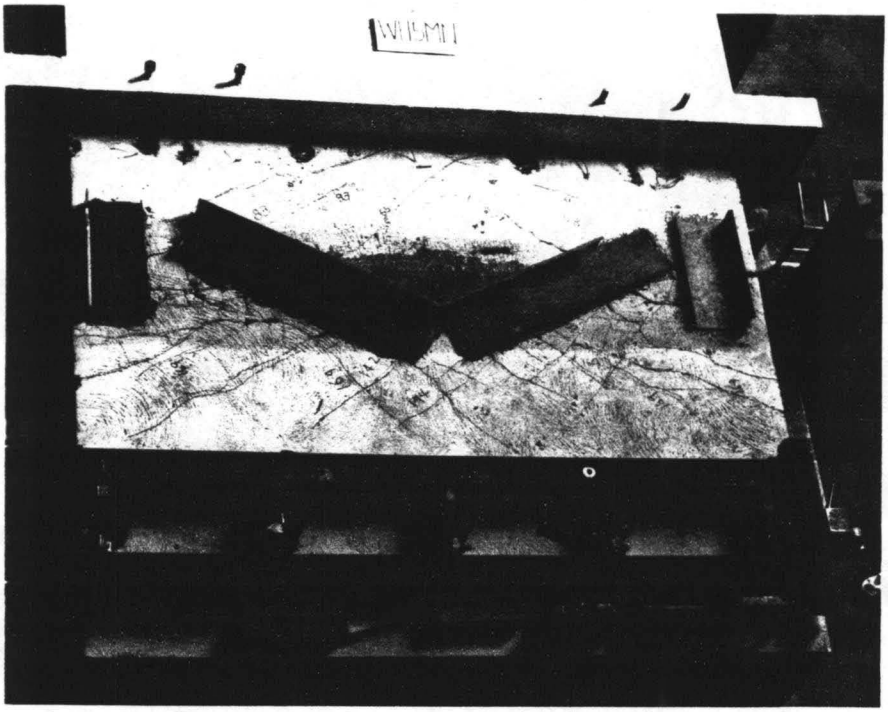

Fig 5.5 The repair of panel 2.

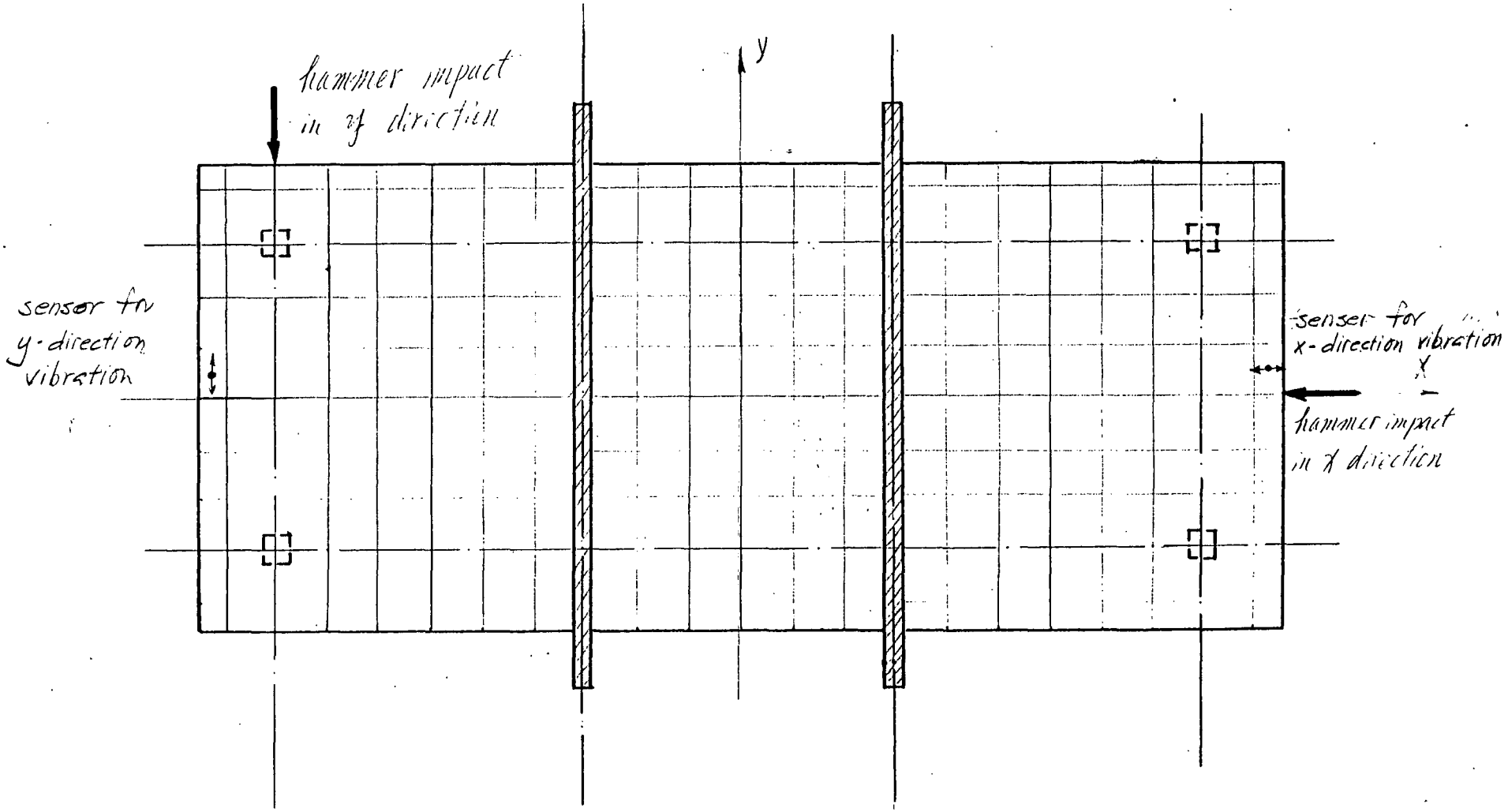

Fig 5.6 In plane free Vibration tests

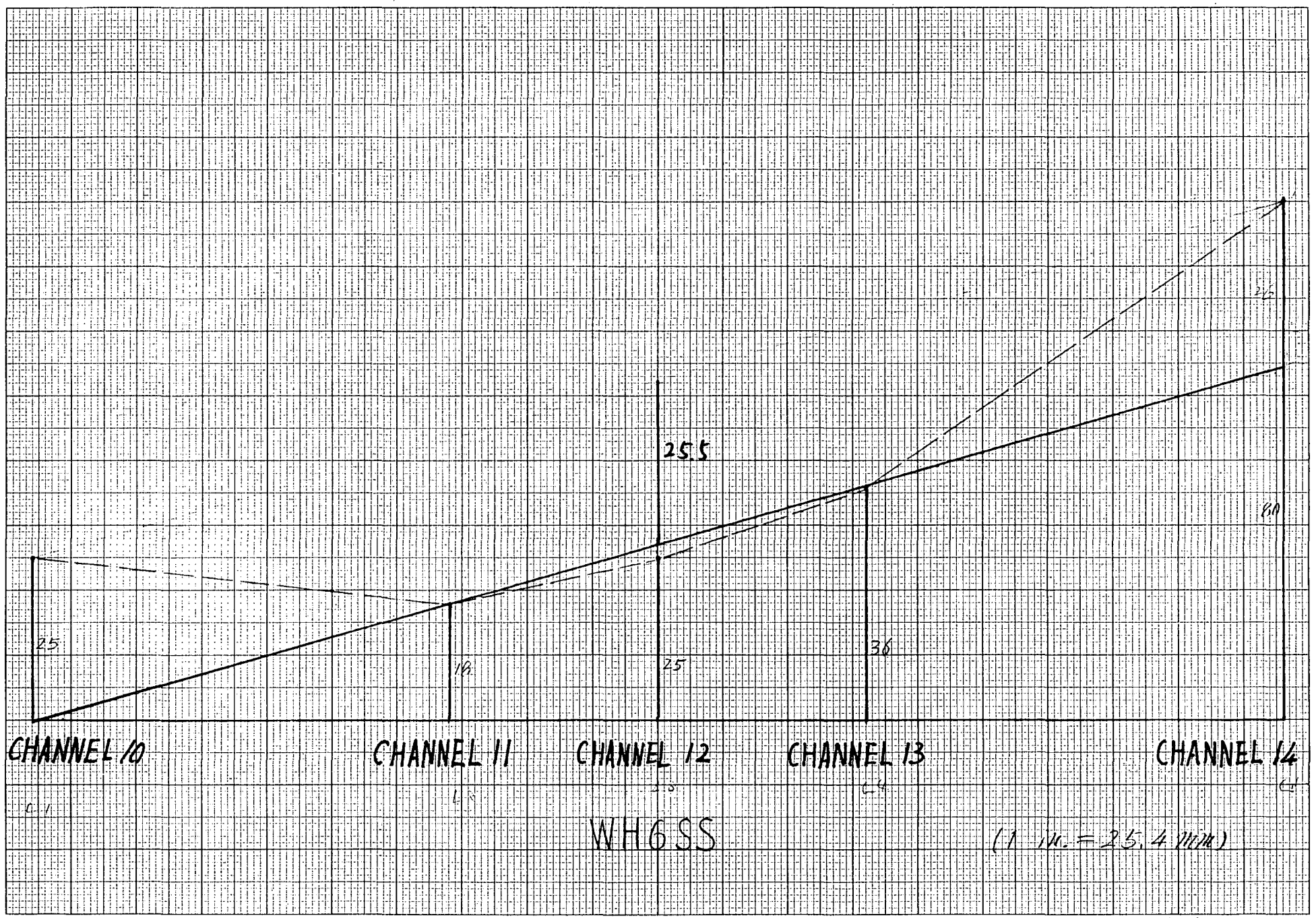

Fig 6.1 DISPLACEMENT (10^{-4} in.) UNDER SYMMETRICAL IN-PLANE LOAD 2 KIPS (8.9 KN)

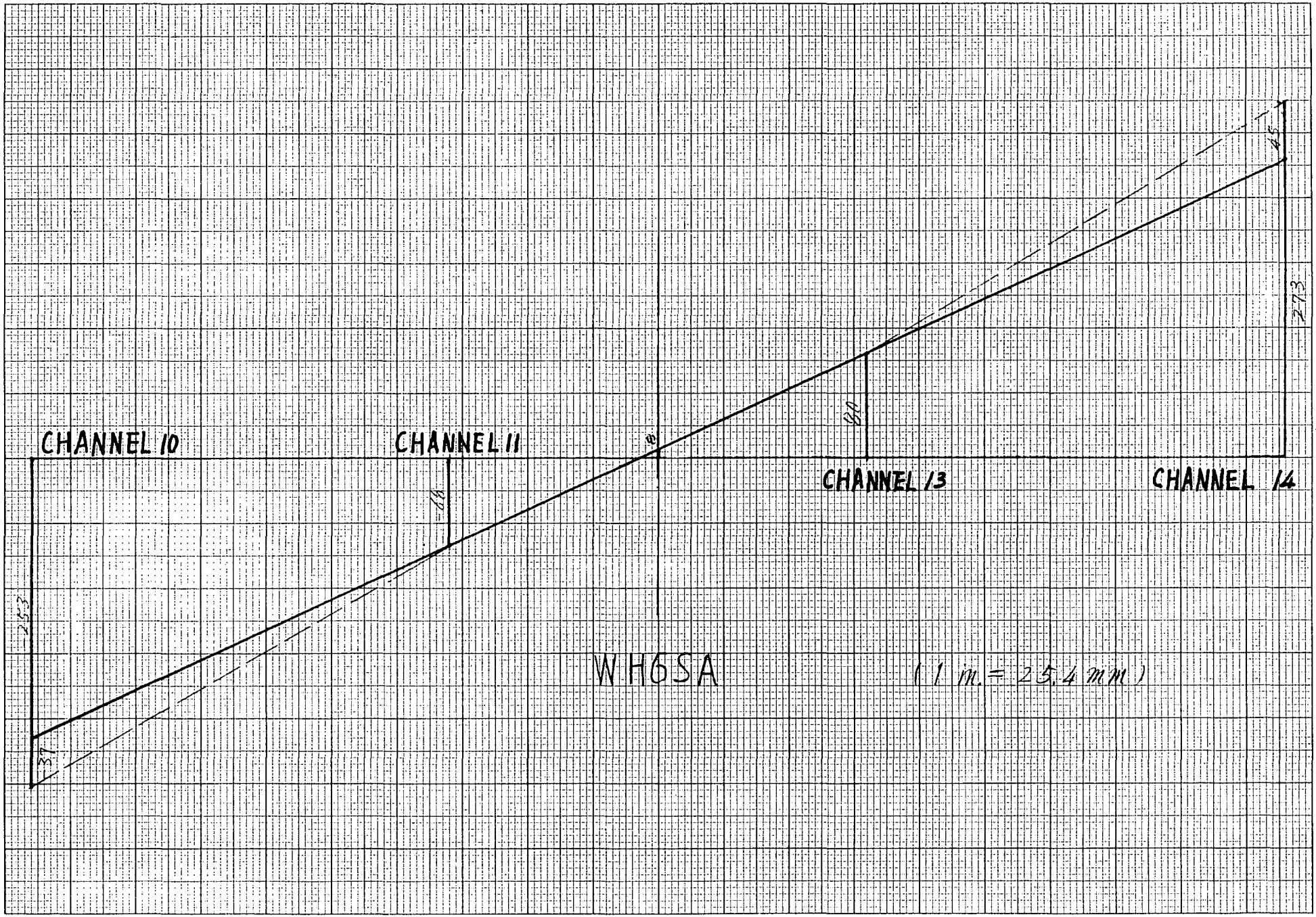

Fig. 6.2 DISPLACEMENT (10^{-4} in.) UNDER ANTI-SYMMETRICAL IN-PLANE LOAD STEPS

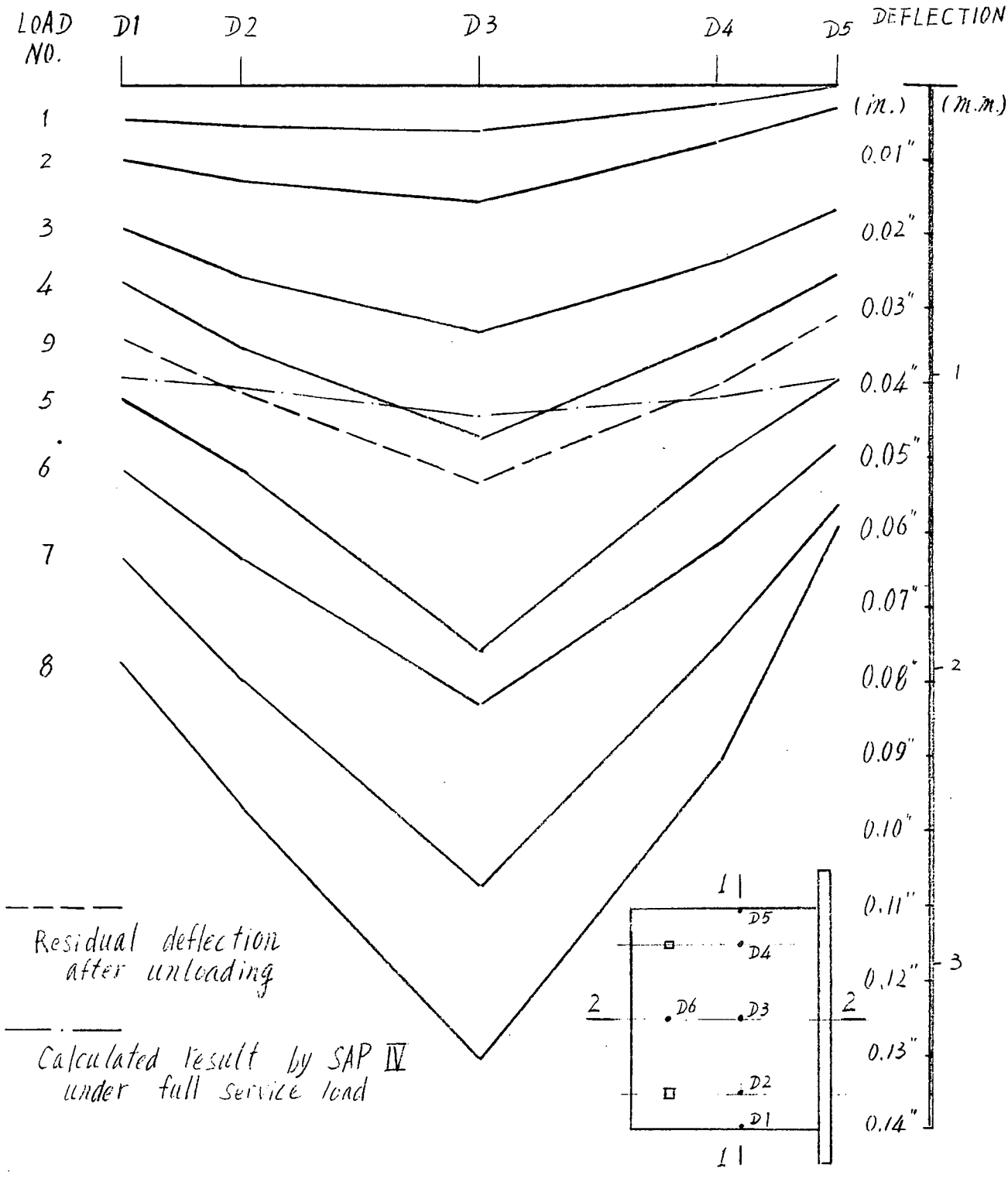

Fig 6.3 VERTICAL DEFLECTION OF WVICY DUE TO VERTICAL LOADING (1 - 1)

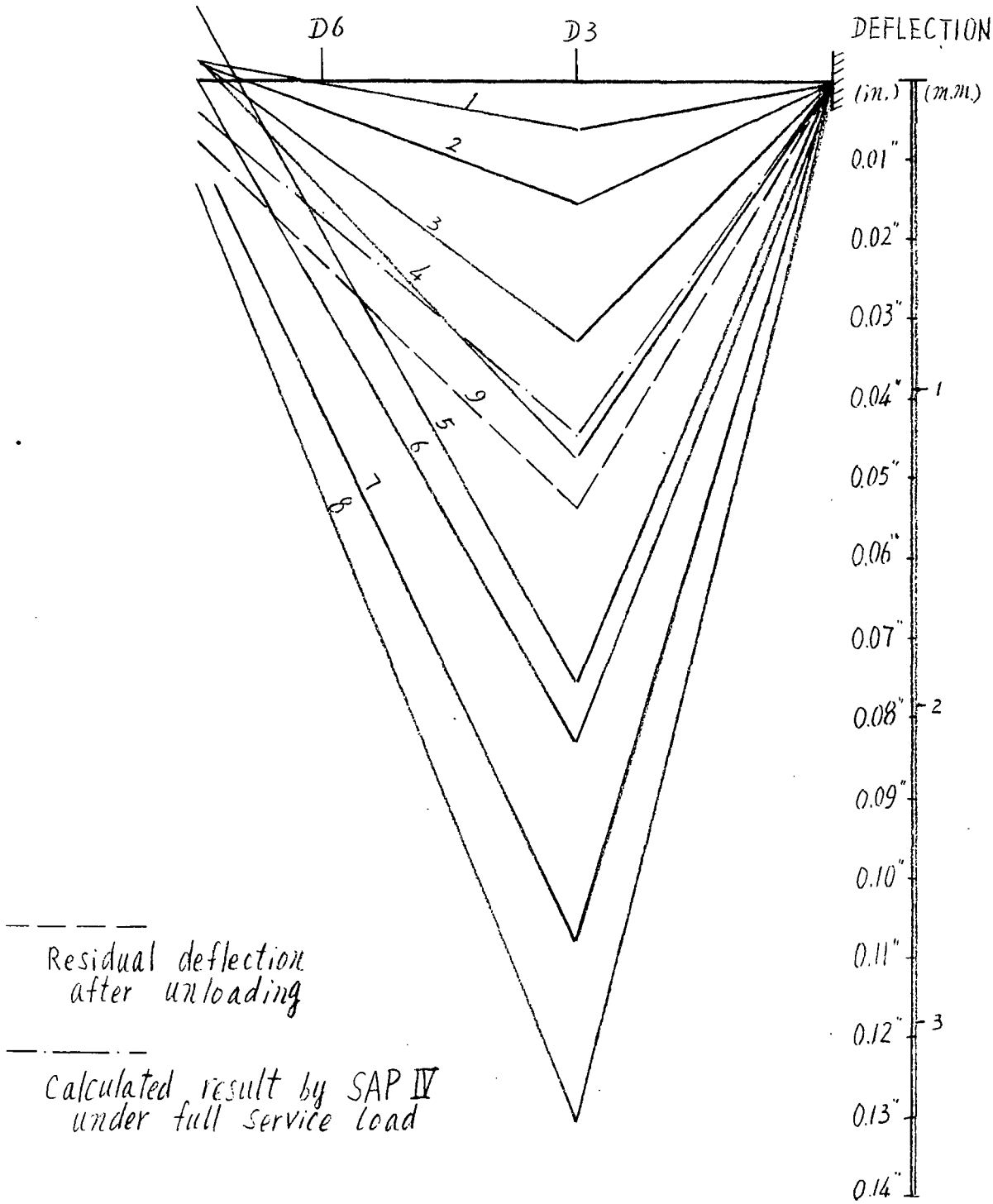

Fig. 6.3 VERTICAL DEFLECTION OF WVICY DUE TO VERTICAL LOADING (2-2)

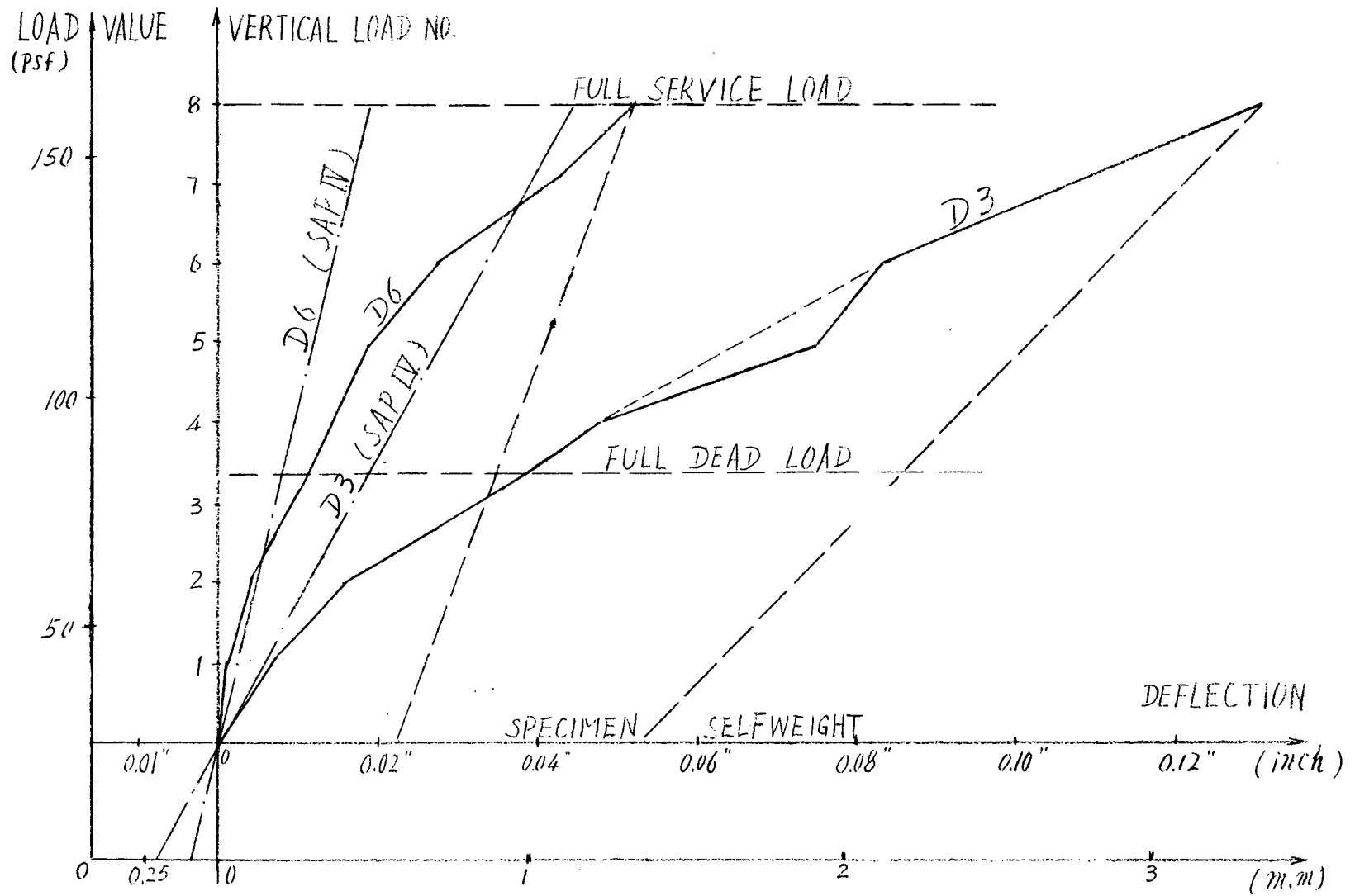

Fig. 6.5 THE VERTICAL LOAD – VERTICAL DEFLECTION CURVE OF WV1C Y

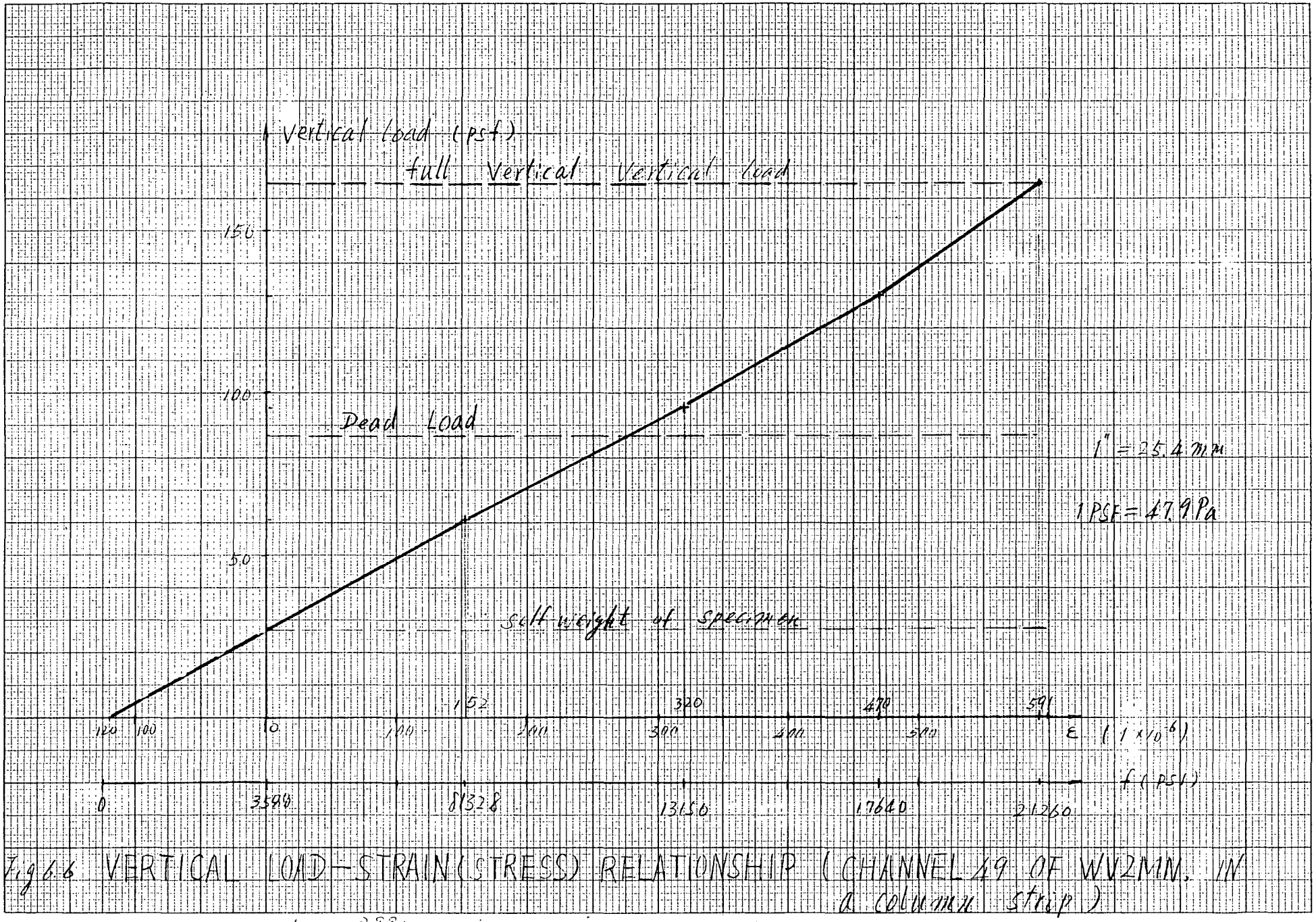

Fig 66 VERTICAL LOAD-STRAIN(STRESS) RELATIONSHIP (CHANNEL 49 OF WV2MN. IN a column strip)

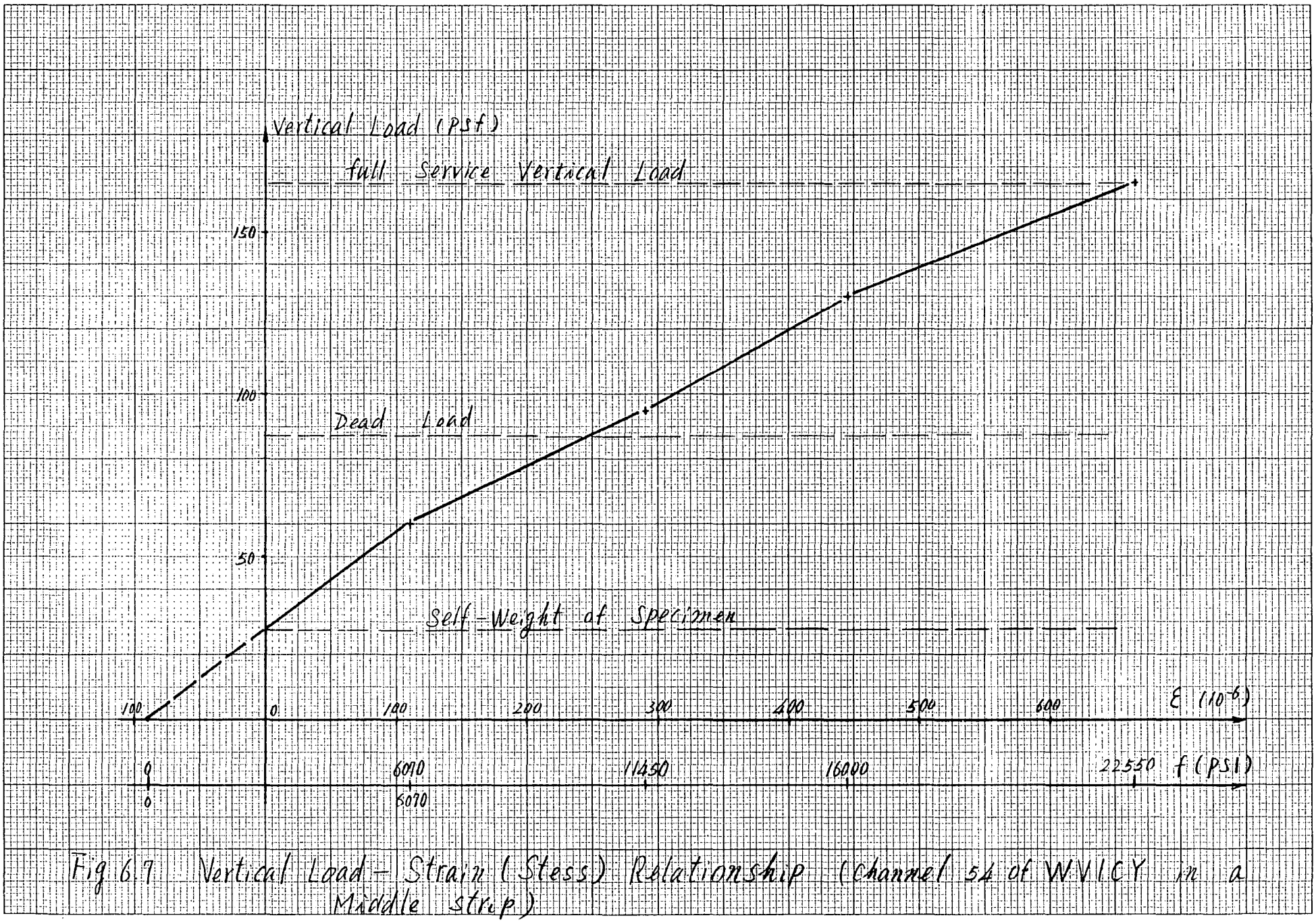

Fig 6.7 Vertical Load – Strain (Stess) Relationship (Channel 54 of WVICY in a Middle Strip)

1" = 100 x 10⁻⁶ → ≈990 psi

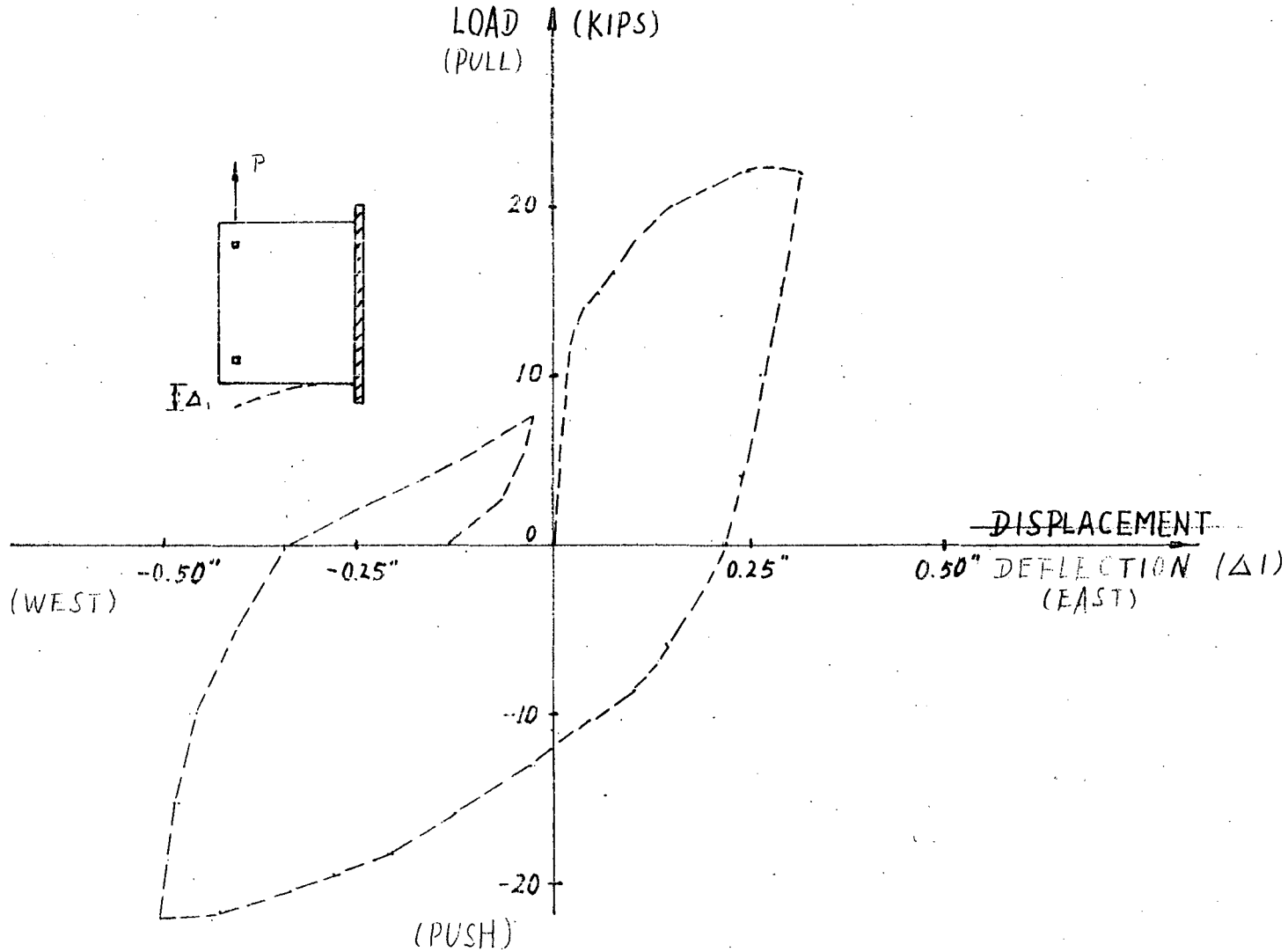

Fig 65 Load - Deflection Curve of WHIMN, Monotonic loading without Vertical load

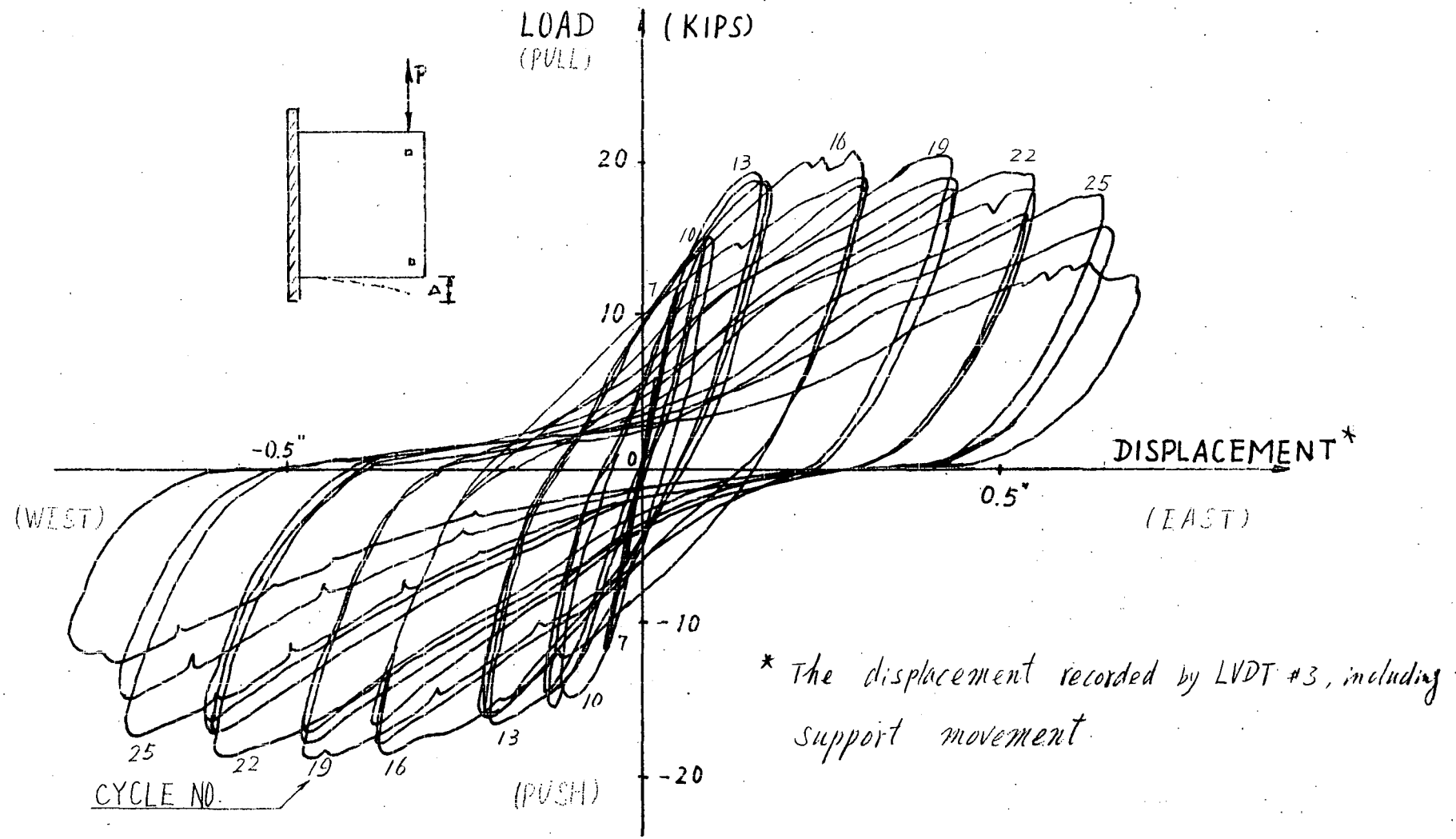

Fig 6.9 Load-Displacement Curve of WH2CY, Cyclic loading without Vertical load

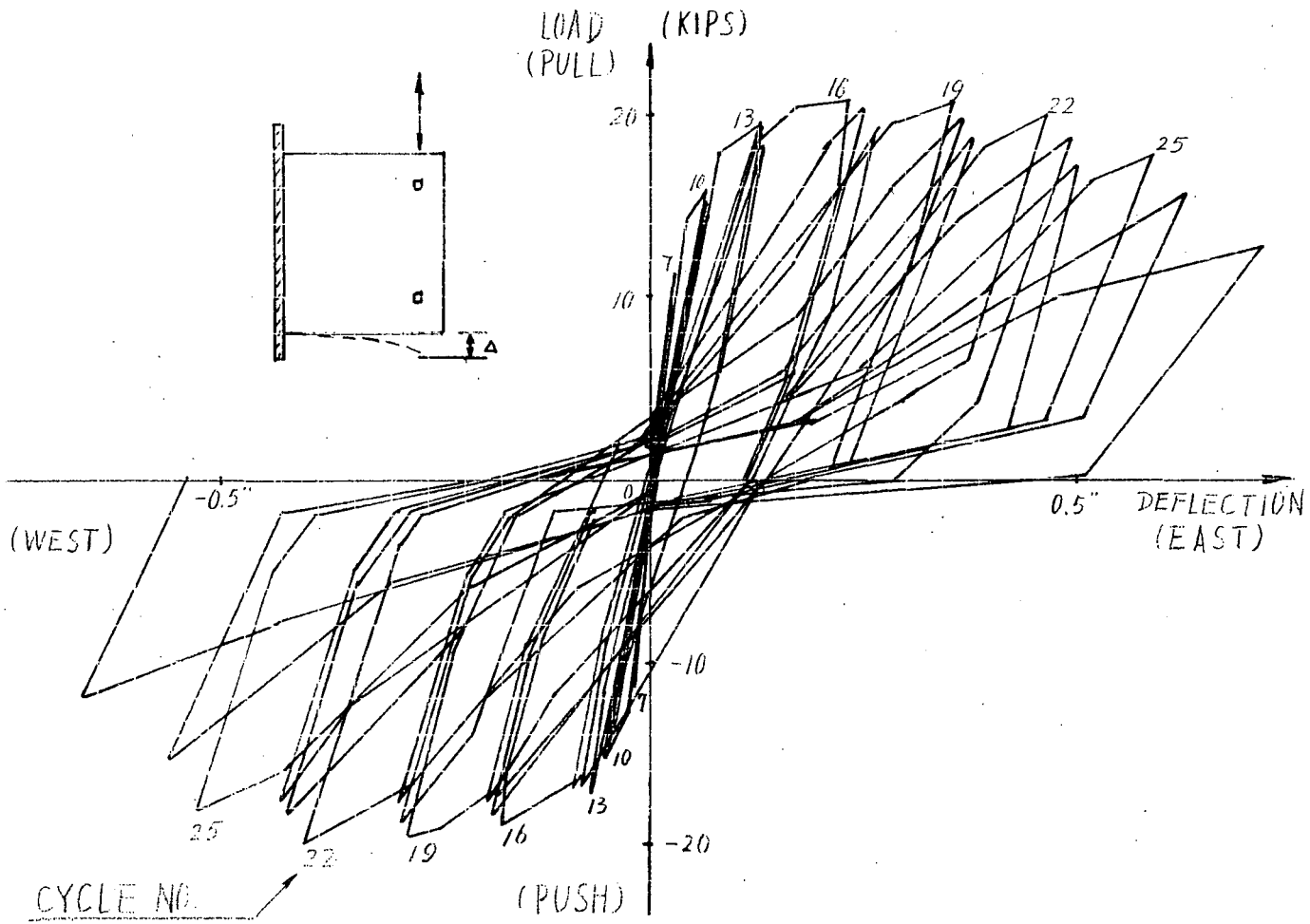

Fig 6.10 Load-Deflection Curve of WH2CY. Cyclic loading without Vertical Load

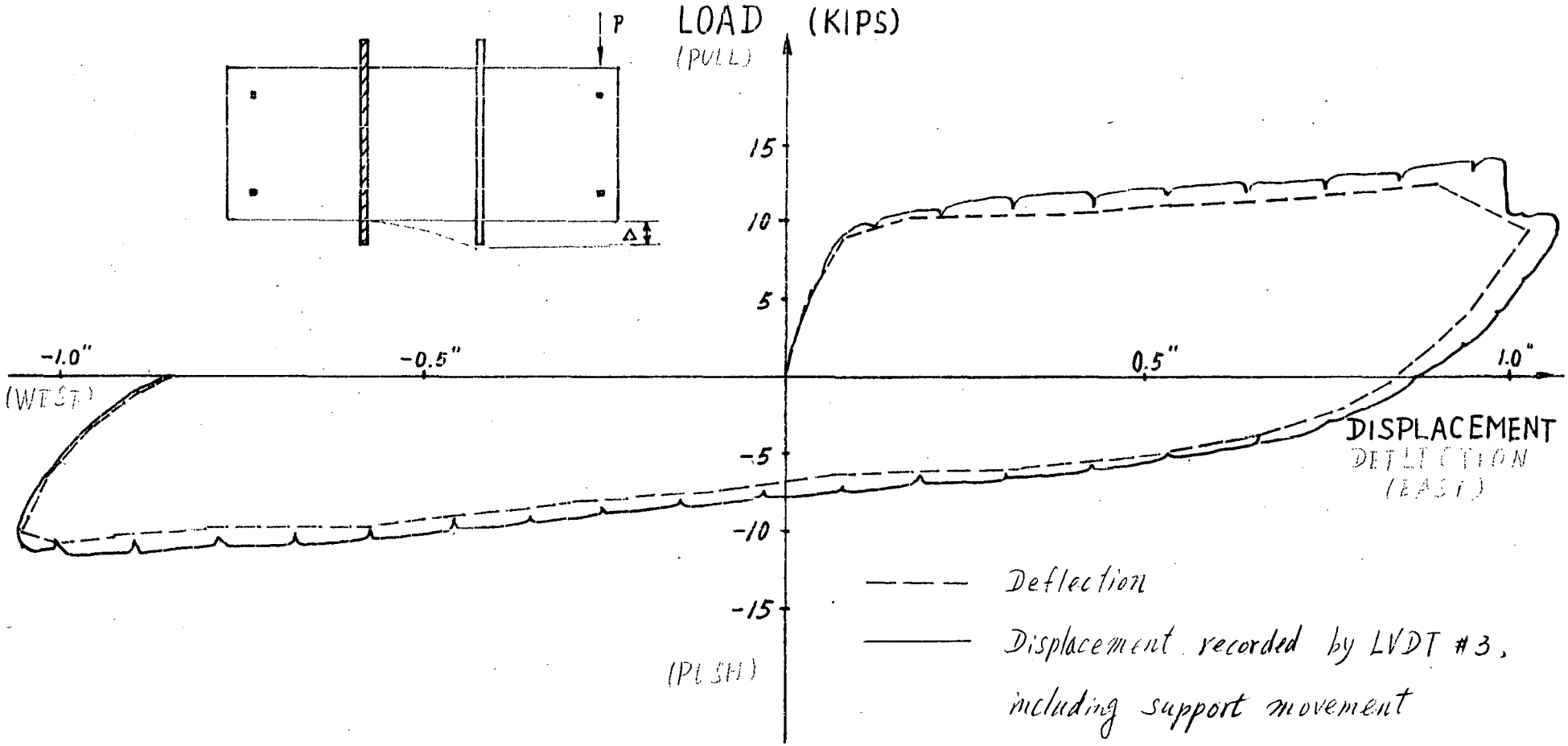

Fig 6.11 Load - Deflection and Load Displacement Curves of WH5MN, Monotonic loading without Vertical load

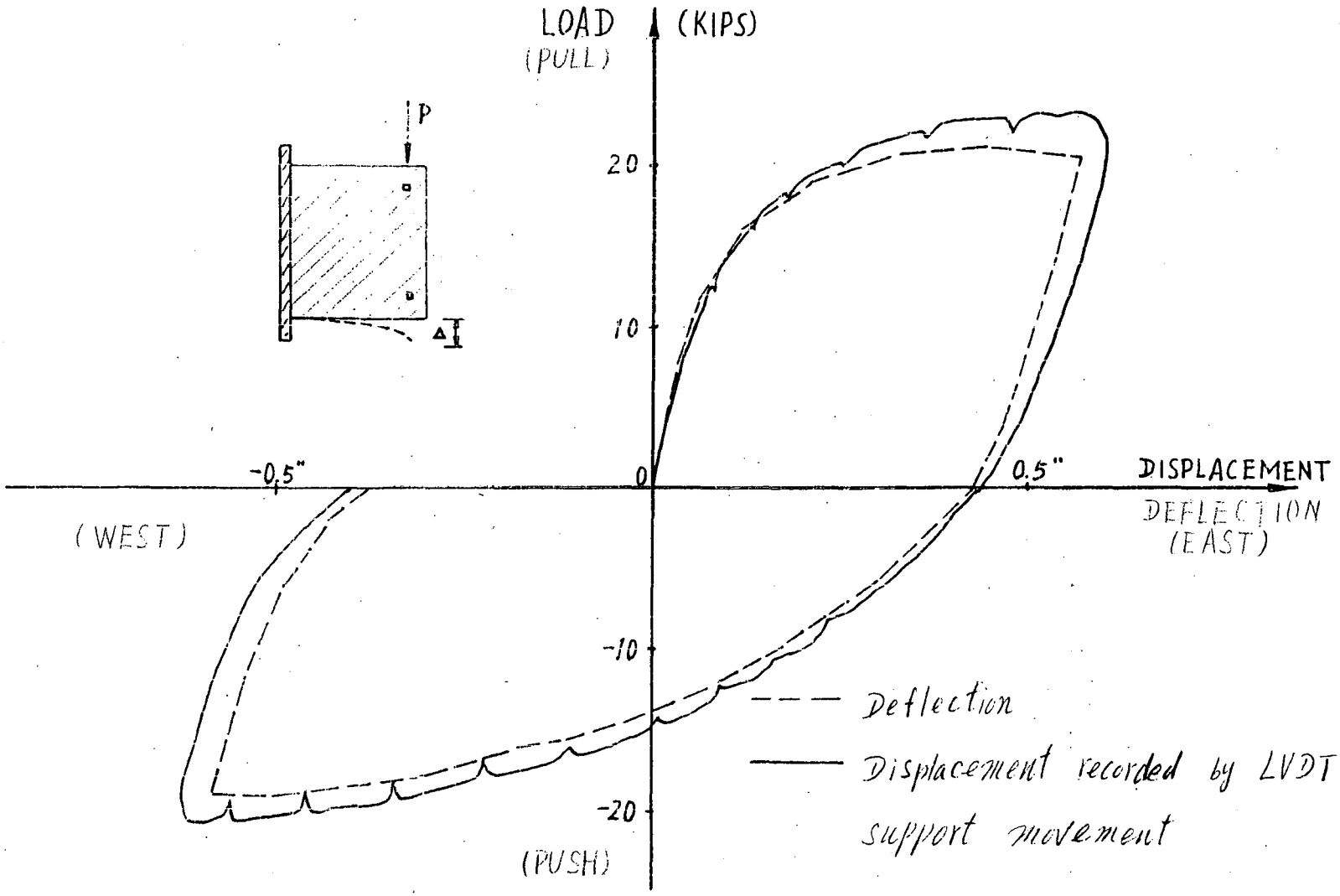

Fig 6.12 Load - Deflection and Load - Displacement Curves of WV2MN, Monotonic Loading With Vertical load

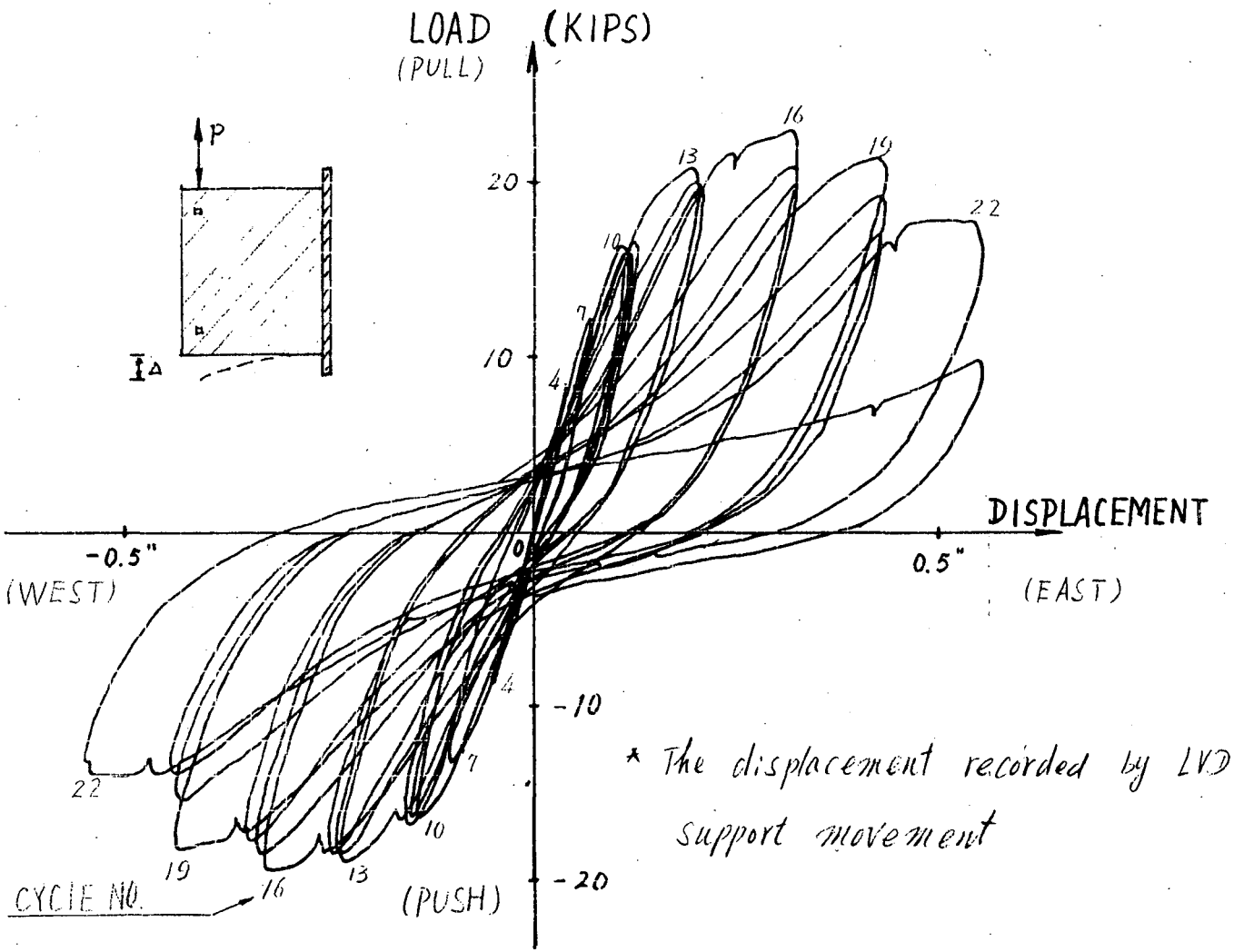

Fig 6.13 Load - Displacement Curve of WVICY, Cyclic loading with vertical Load

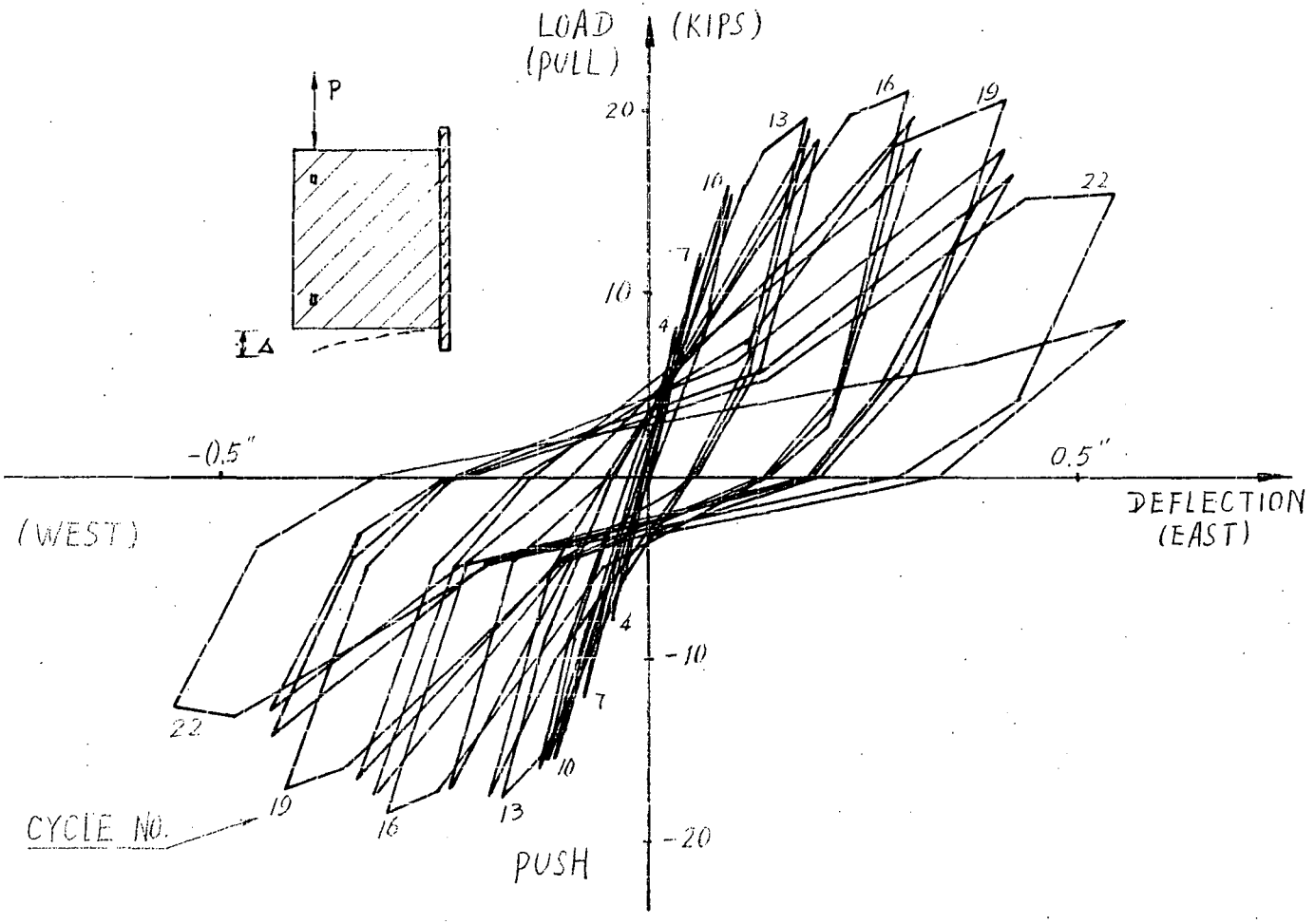

Fig 6.14 Load-Deflection Curve of WVICY. Cyclic loading with Vertical load

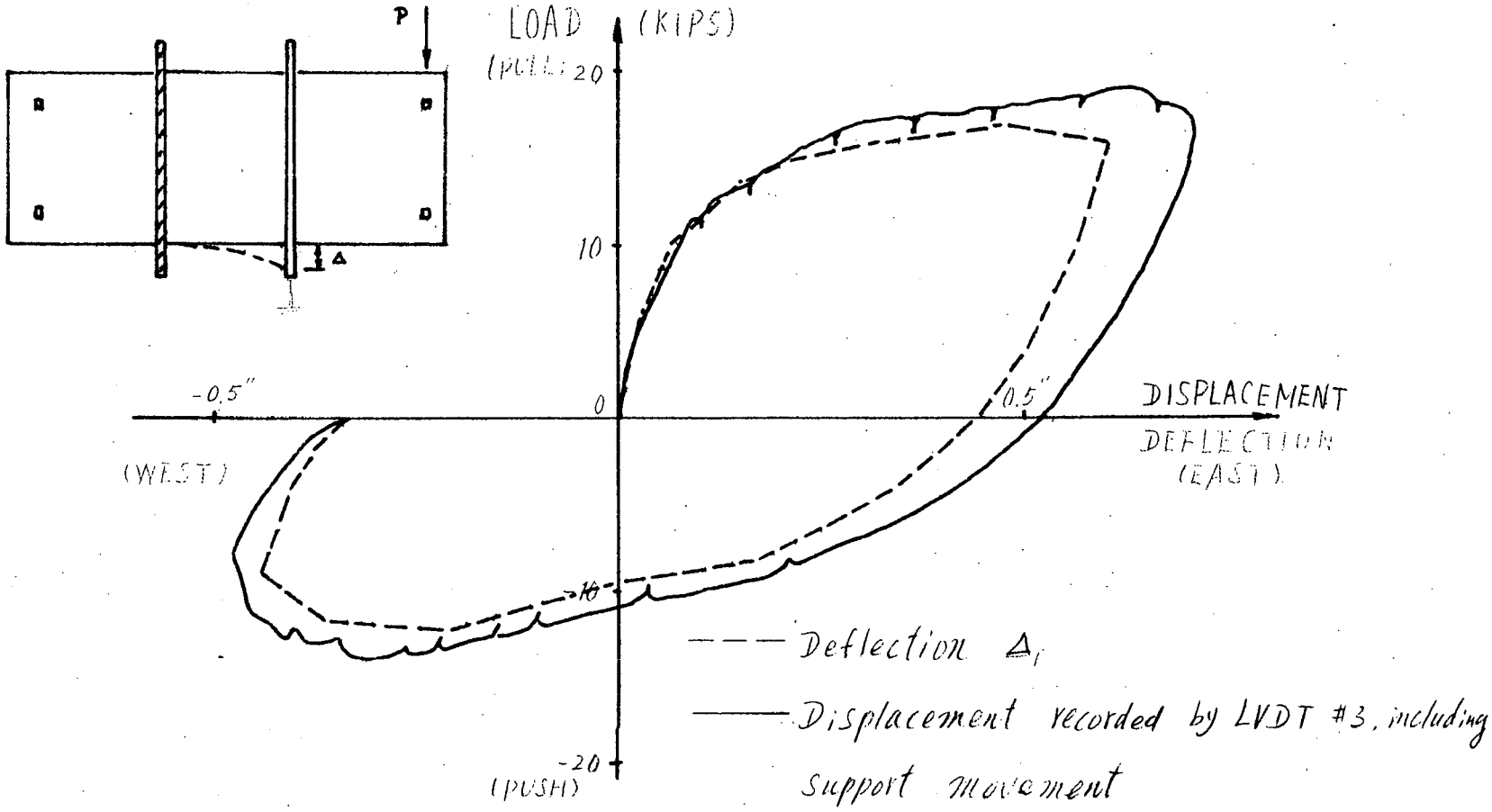

Fig 6.1C Load - Deflection and Load - Displacement Curve of FH5MN, Monotonic loading without vertical load

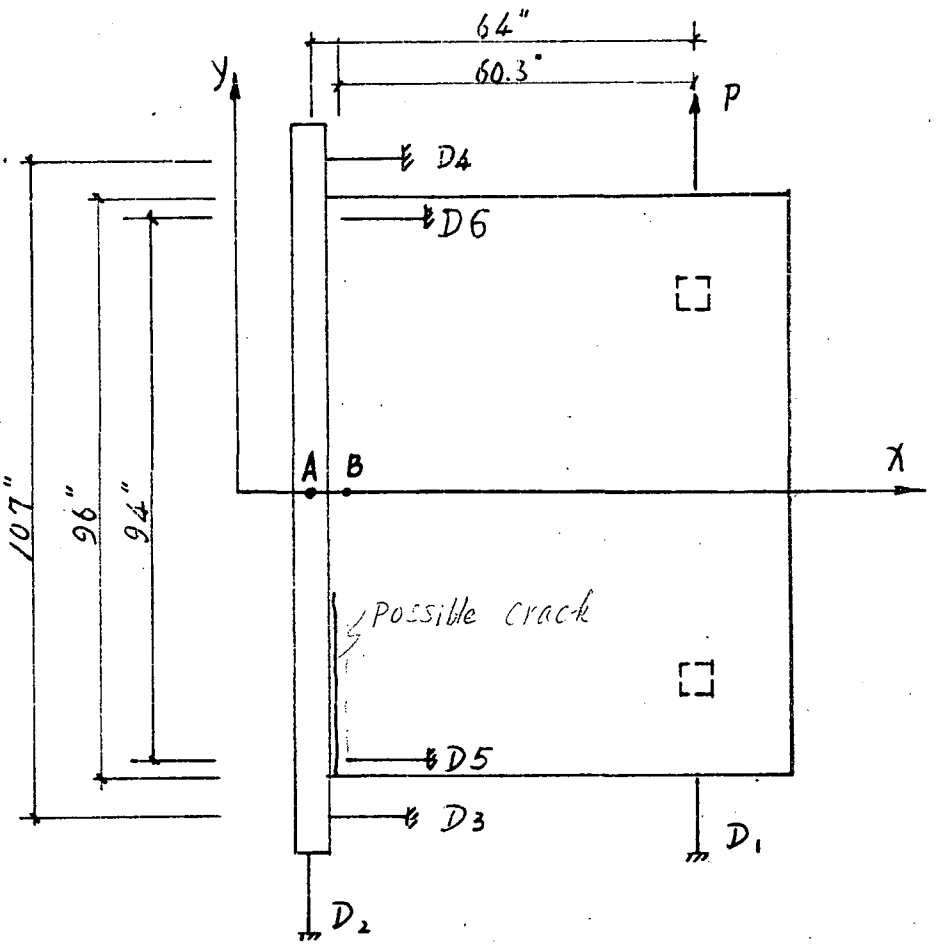

$$\theta_1 = \frac{D3 - D4}{107"} \qquad \theta_2 = \frac{D5 - D6}{94}$$

$$\Delta 1 = D1 - D2 - \theta 1 \cdot 64"$$

$$\Delta 2 = D1 - D2 - \theta 2 \cdot 60.3"$$

Here: D1 to D6 — displacements recorded by LVDT's

$\theta 1$ — the rotation at point A (shear wall)

$\theta 2$ — the rotation at point B which was 1 inch away from panel-shear wall junction.

$\Delta 1$ — principel deflection based on tangent at point A

$\Delta 2$ — principel deflection based on tangent at point B

Fig 6.16. Principel Deflections $\Delta 1$ and $\Delta 2$

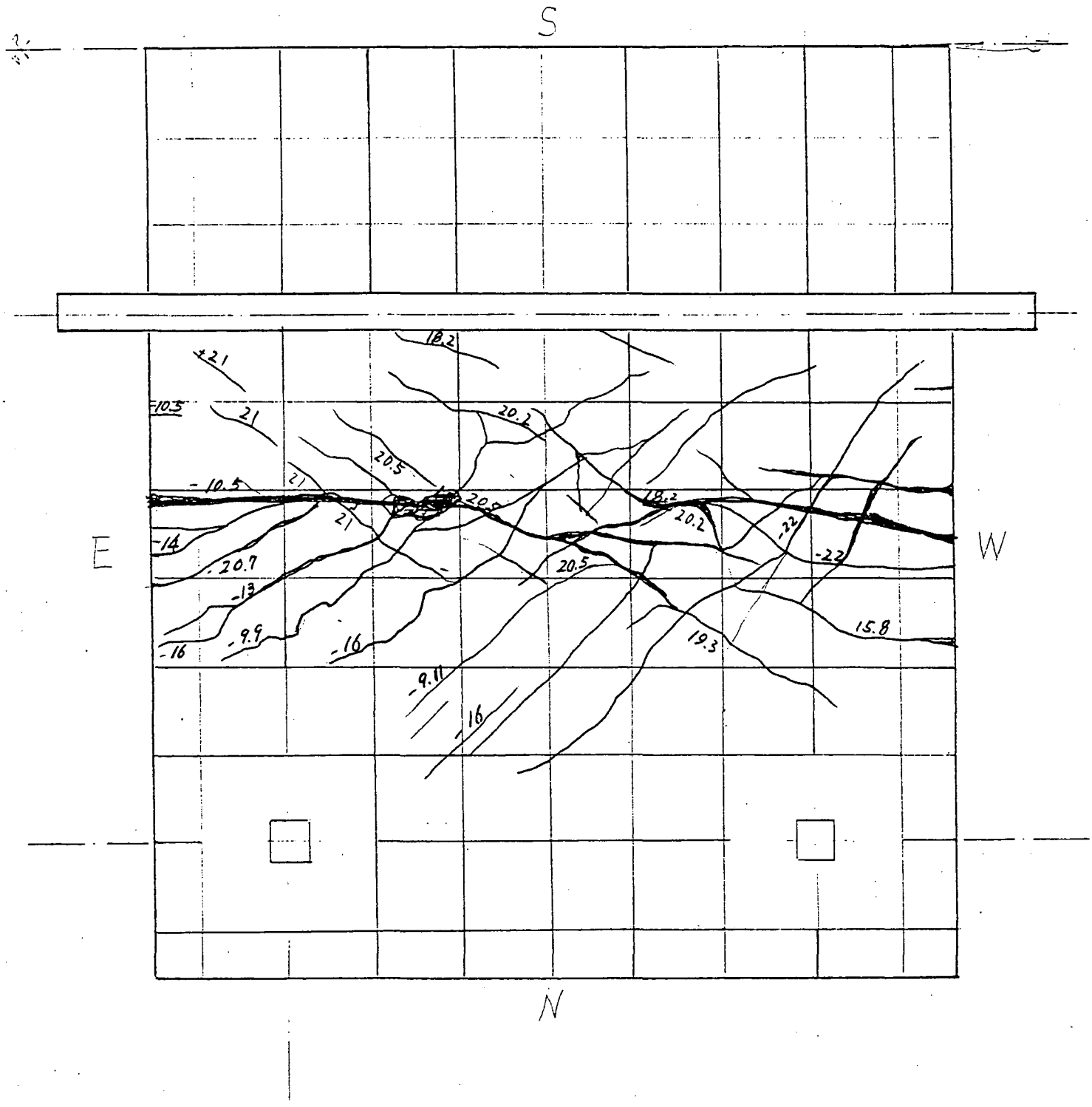

Fig 6.17 cracking pattern of WHIMN (TOP) ~~After strength Test~~

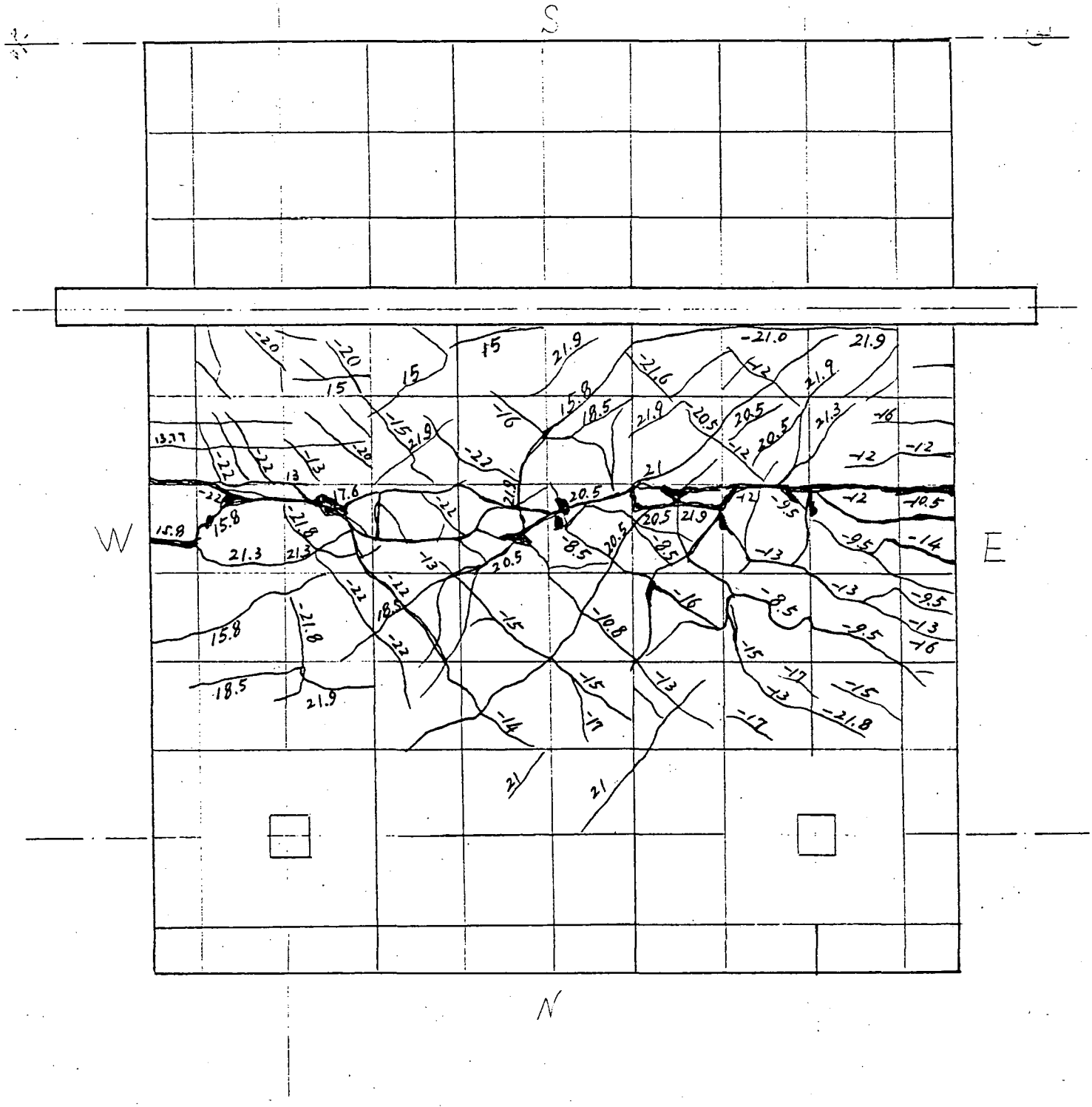

Fig 6.18 Cracking pattern of WHIMN (BOTTOM) ~~After Strength Test~~

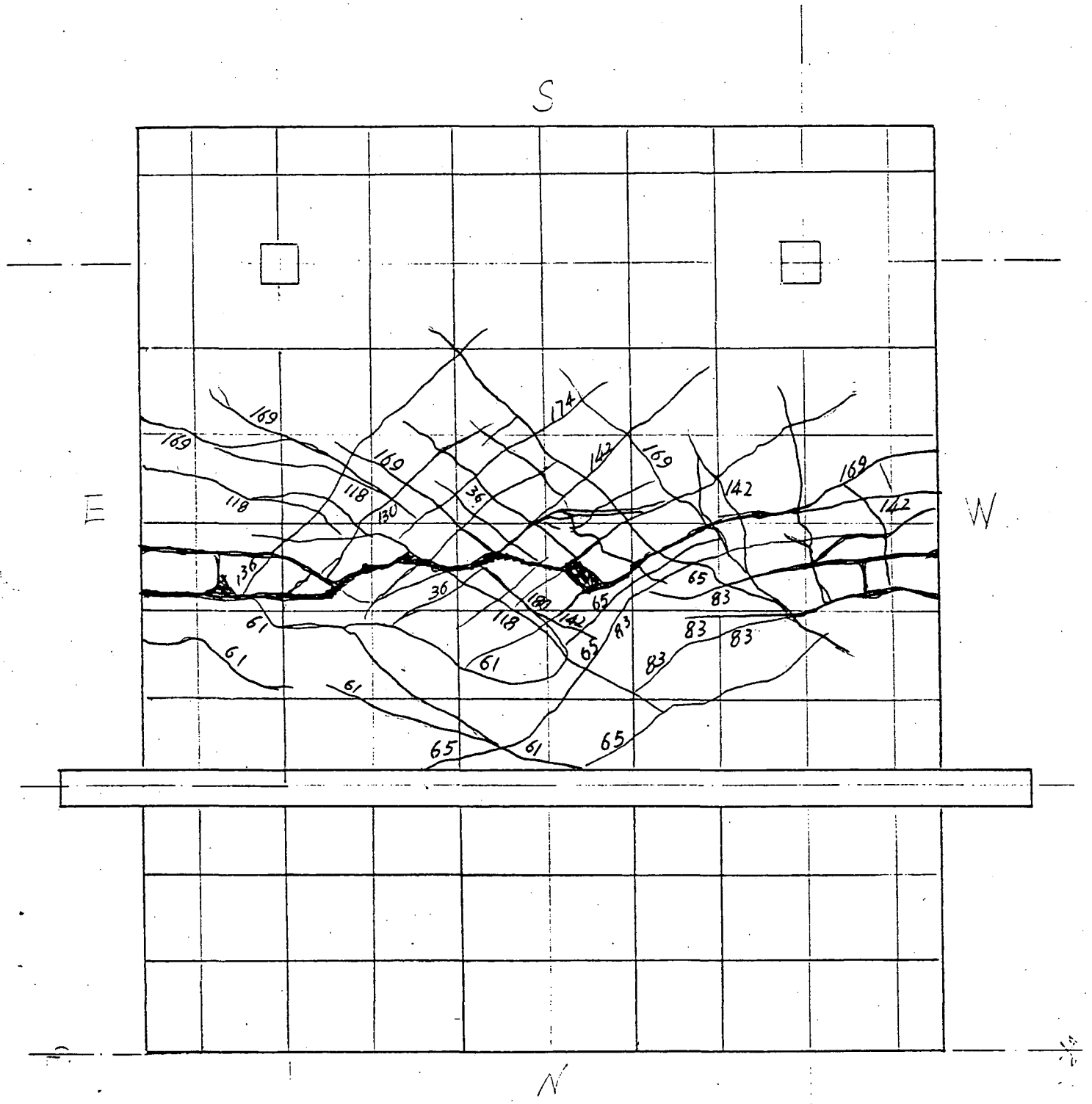

Fig 6.19 Cracking pattern of WH2CY (TOP) After Strength Test

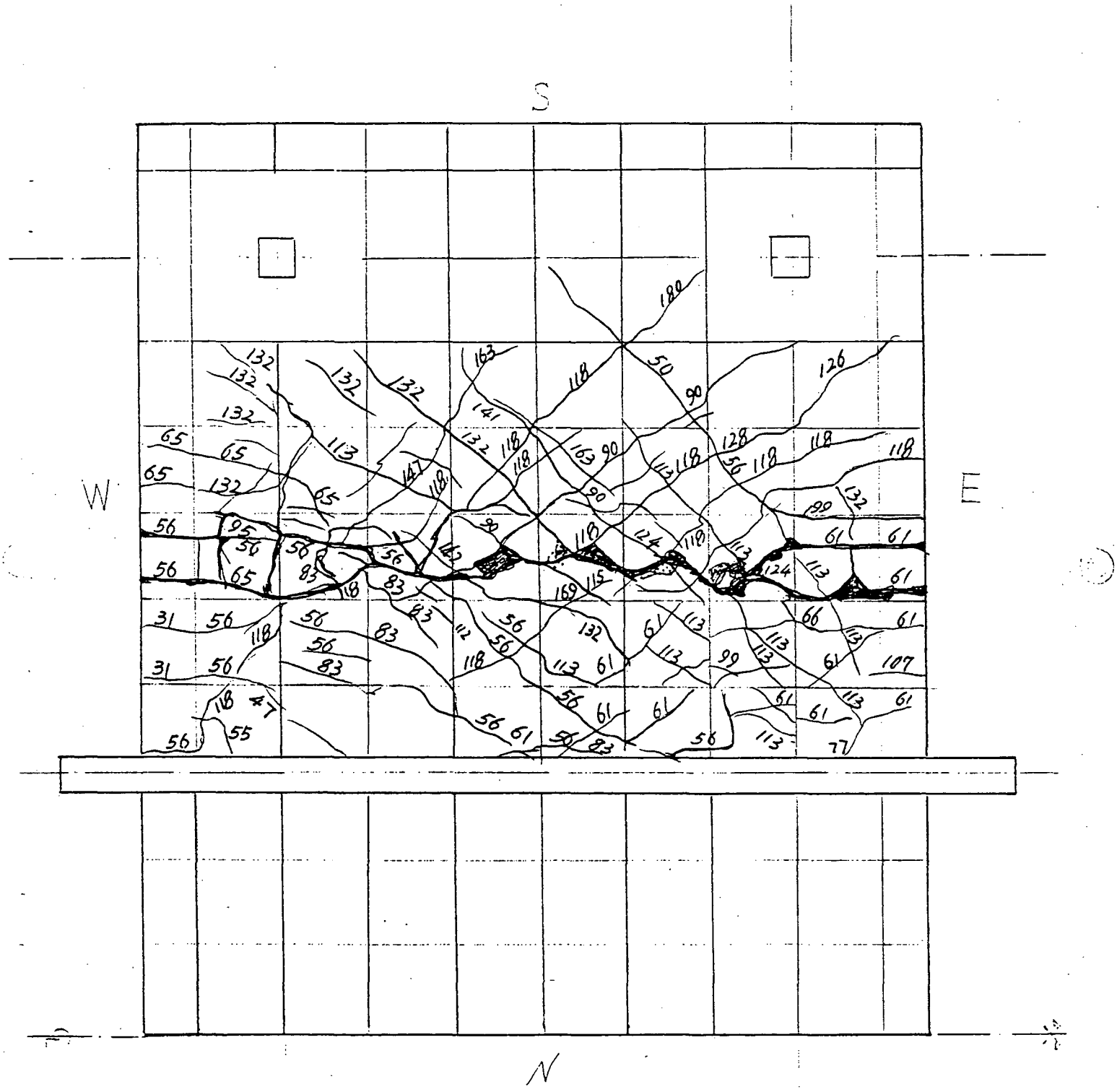

Fig 6.20 Cracking Pattern of WH2CY (BOTTOM) After Strength test

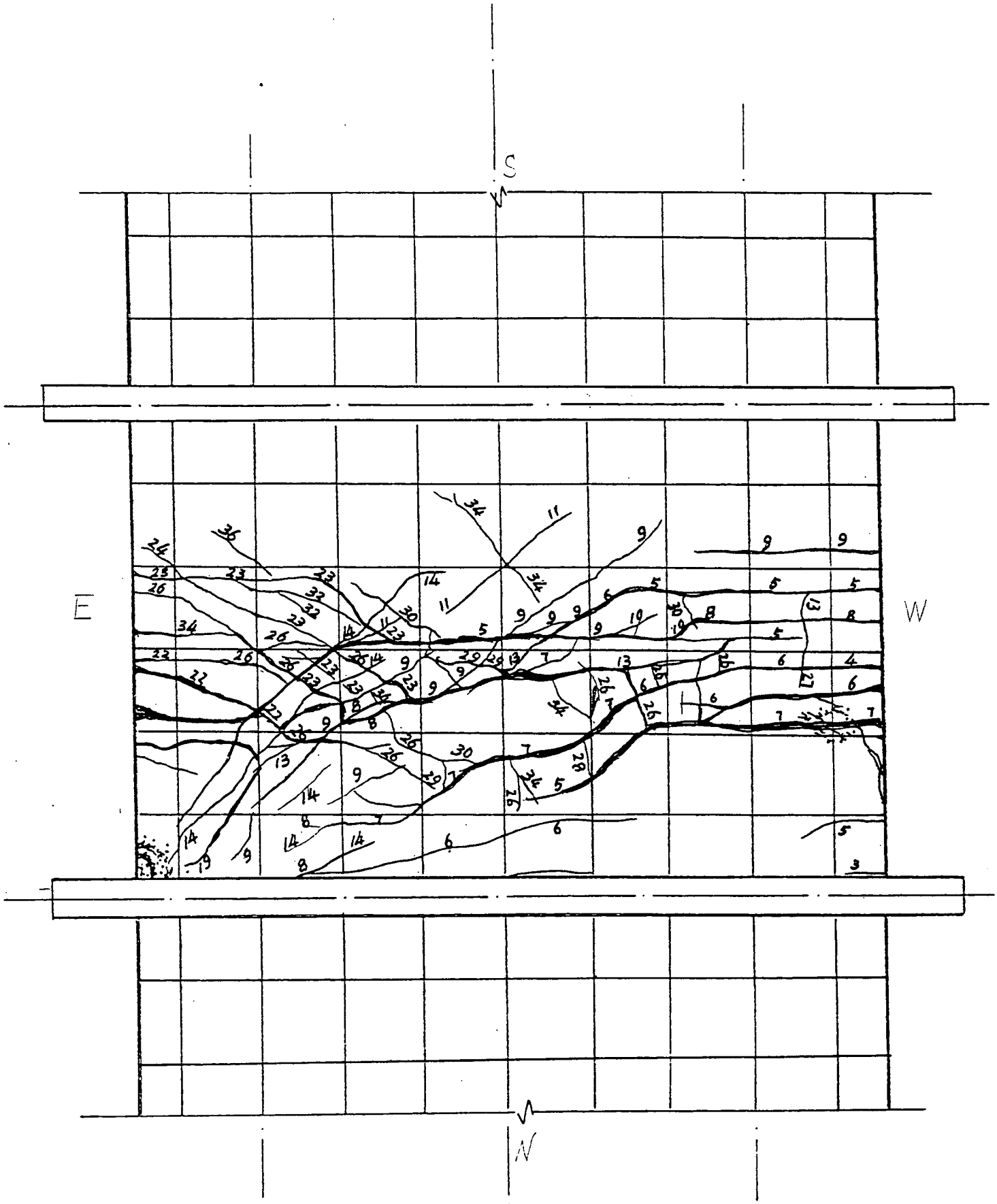

Fig 6.21 Cracking pattern of WH5MN (TOP) After Strength Test

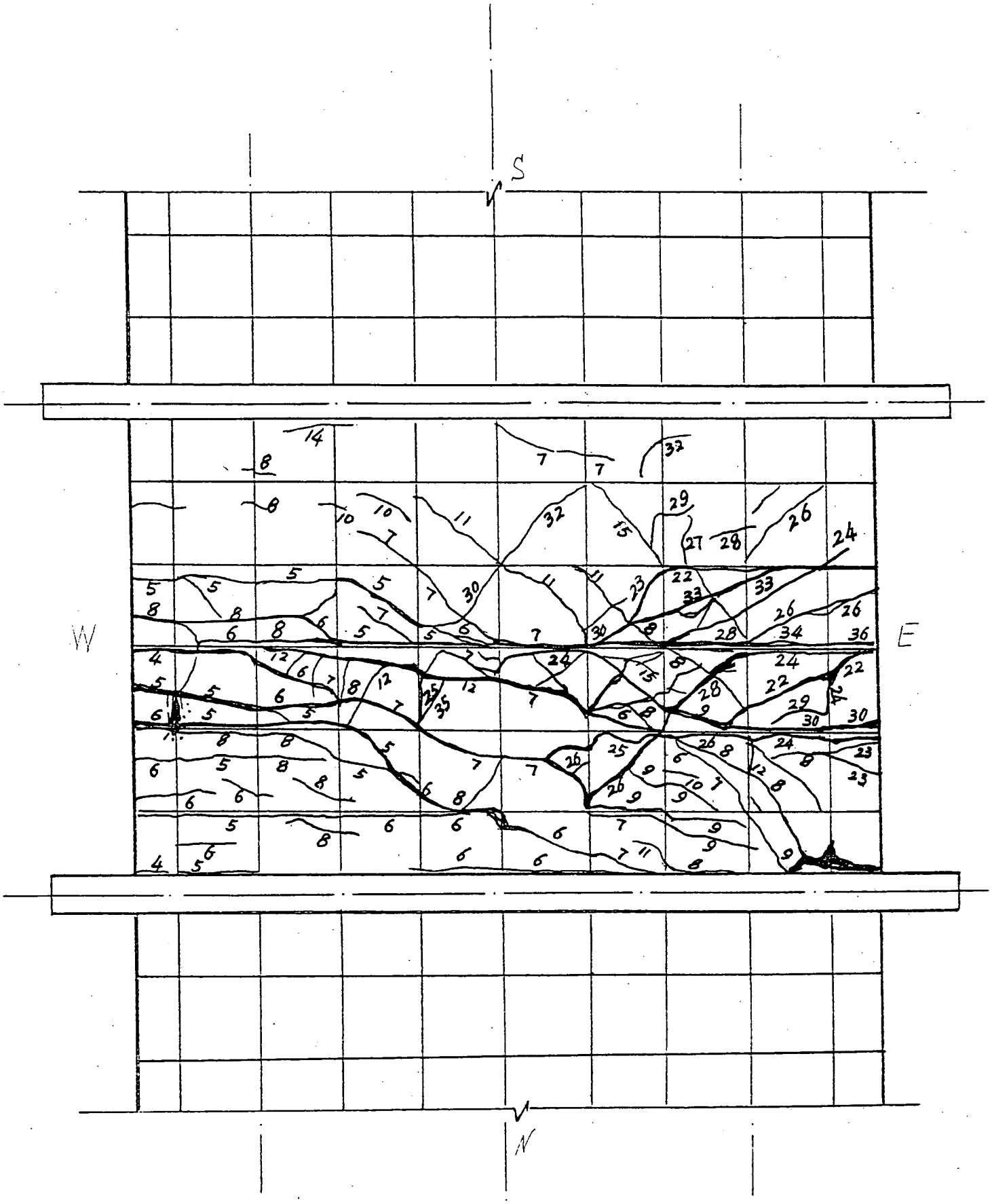

Fig 6.22 Cracking Pattern of WH5MN (BOTTOM) After Strength test

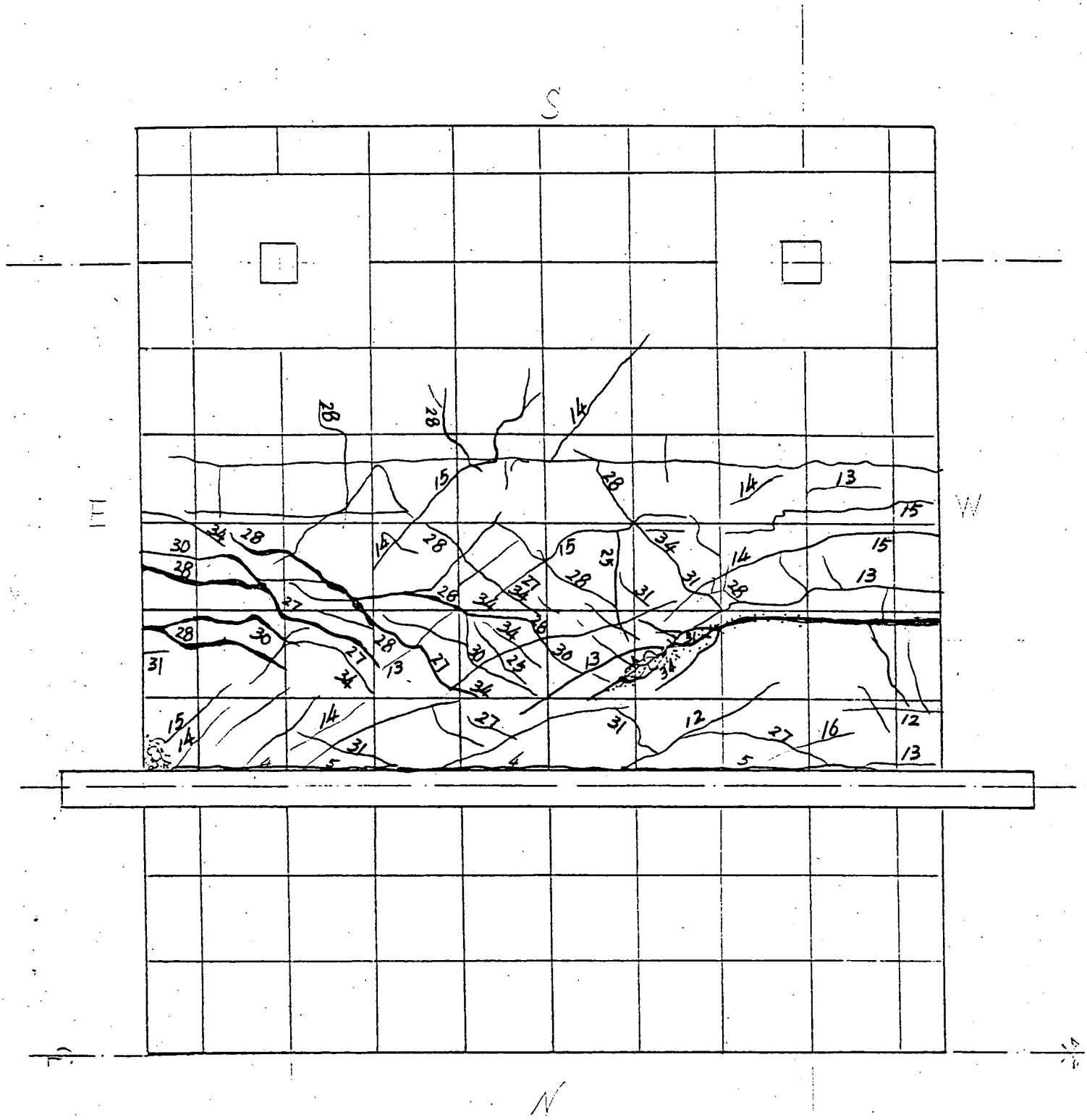

Fig 6.23 Cracking Pattern of W12MN (TOP) After Strength Test

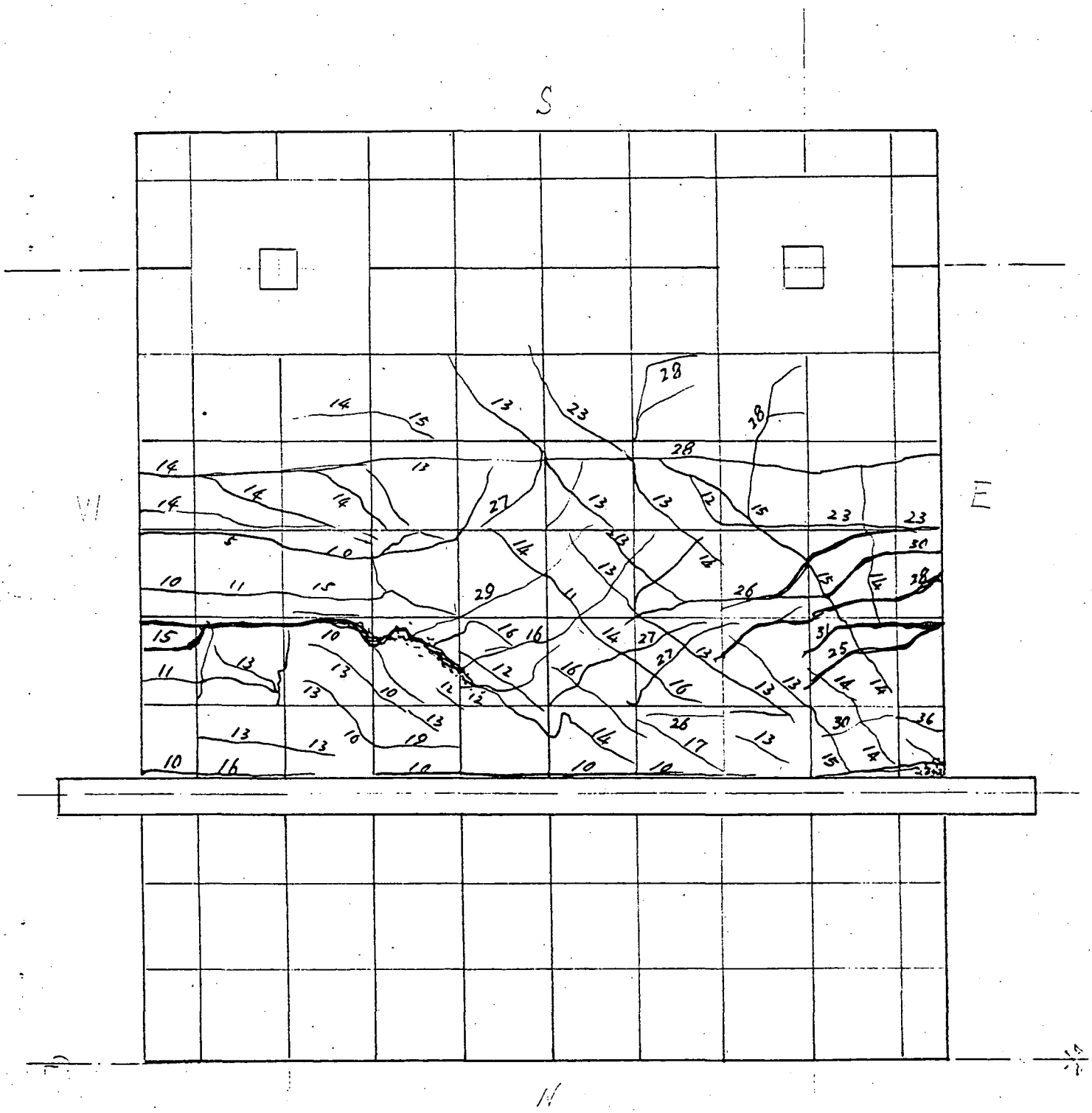

Fig 6.24 Cracking Pattern of WV2MN (BOTTOM) After Strength Test

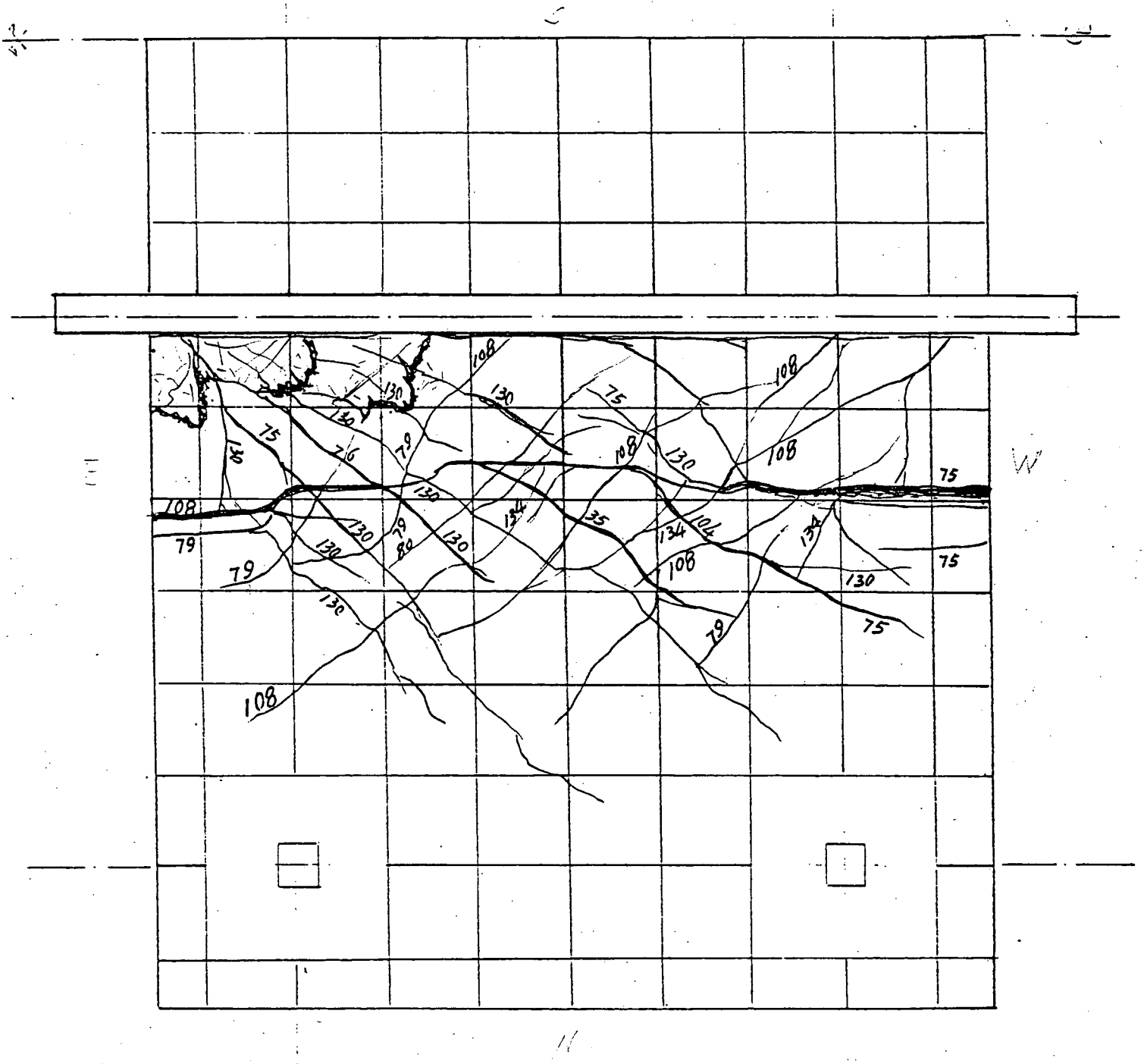

Fig 6.25 Cracking Pattern of WW1CY (TOP) After Strength Test

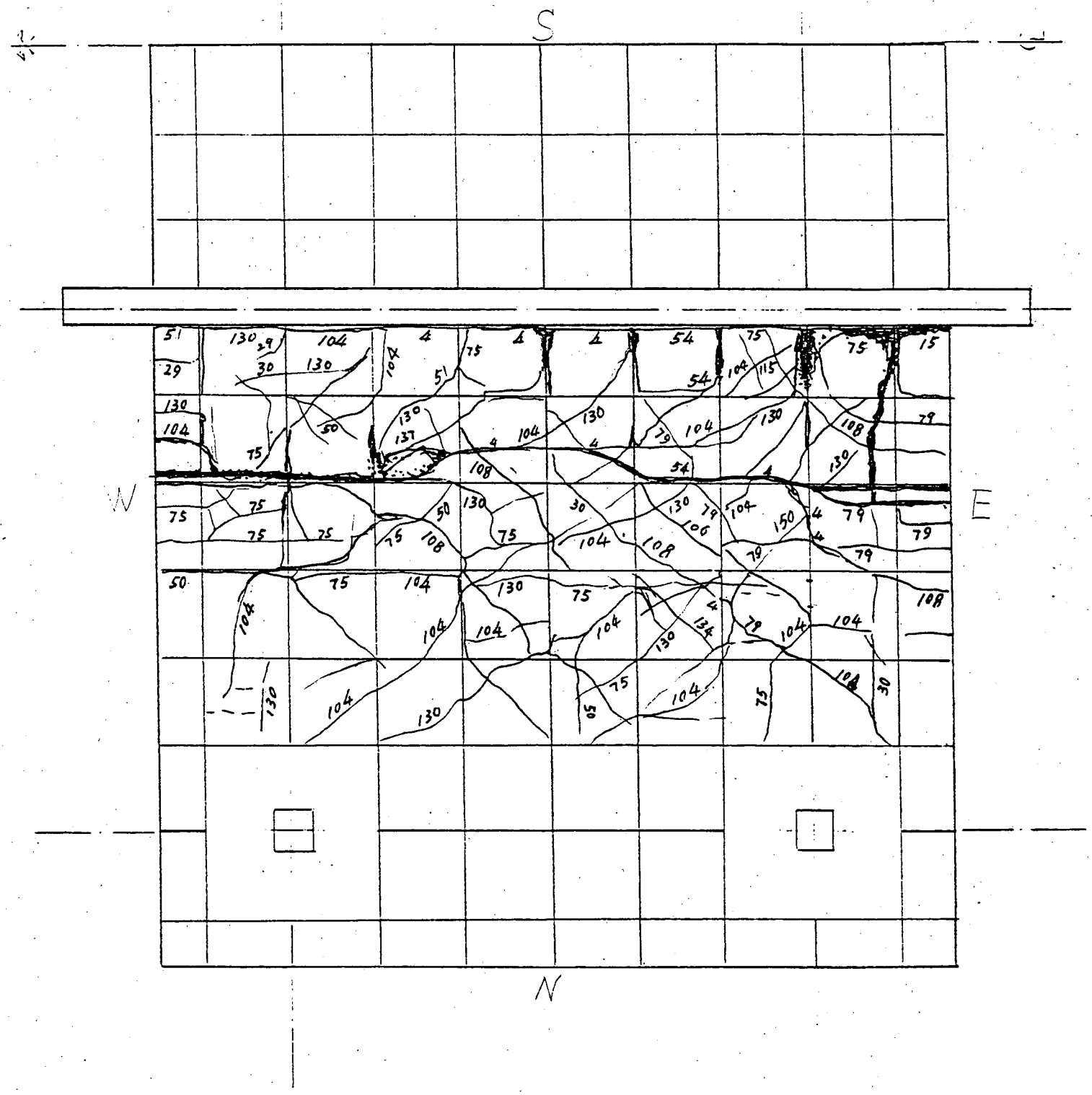

Fig 6.26 Cracking Pattern of WVICY (BOTTOM) After Strength Test

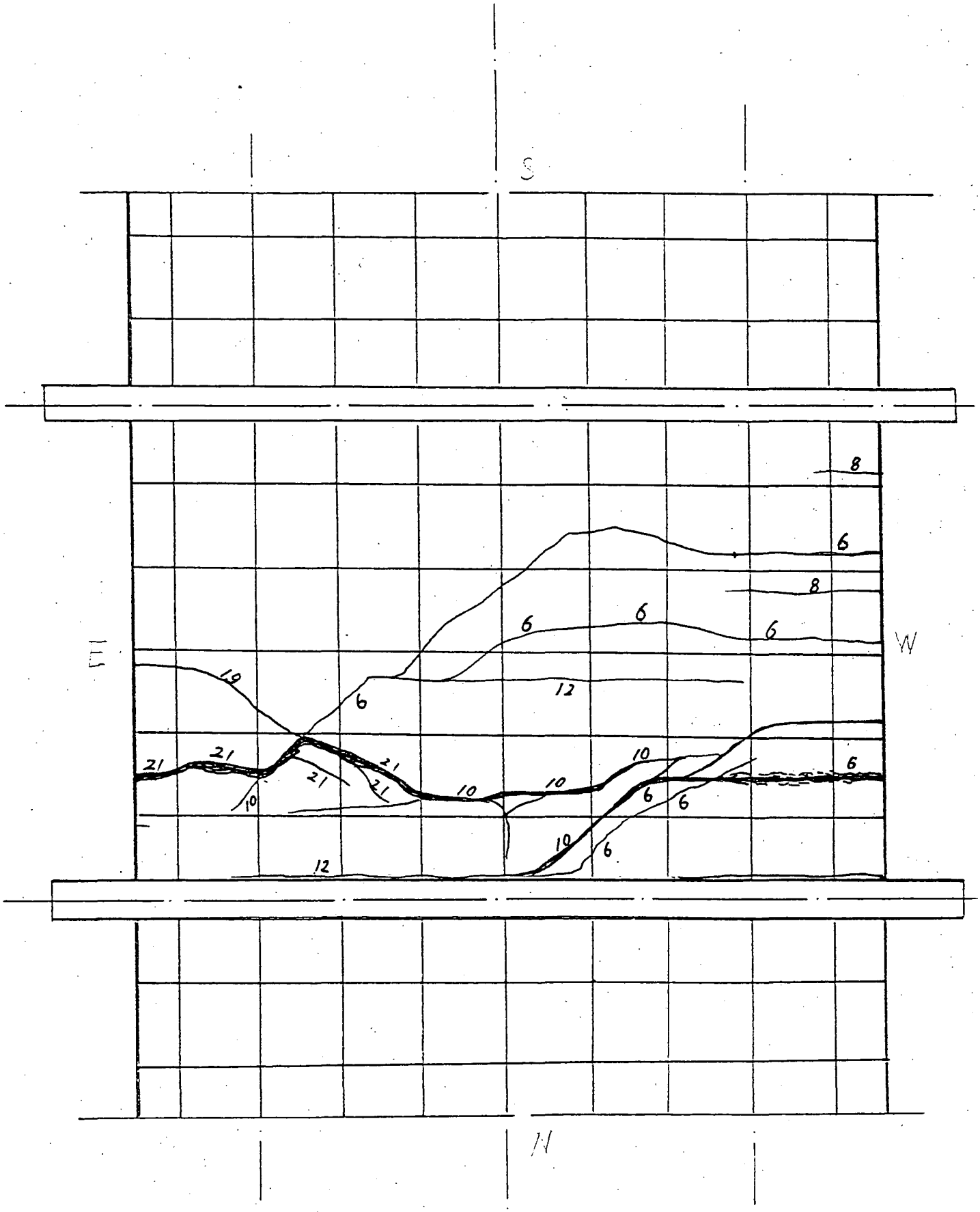

Fig 6.27 Cracking Pattern of FH5MN (TOP) After Strength Test

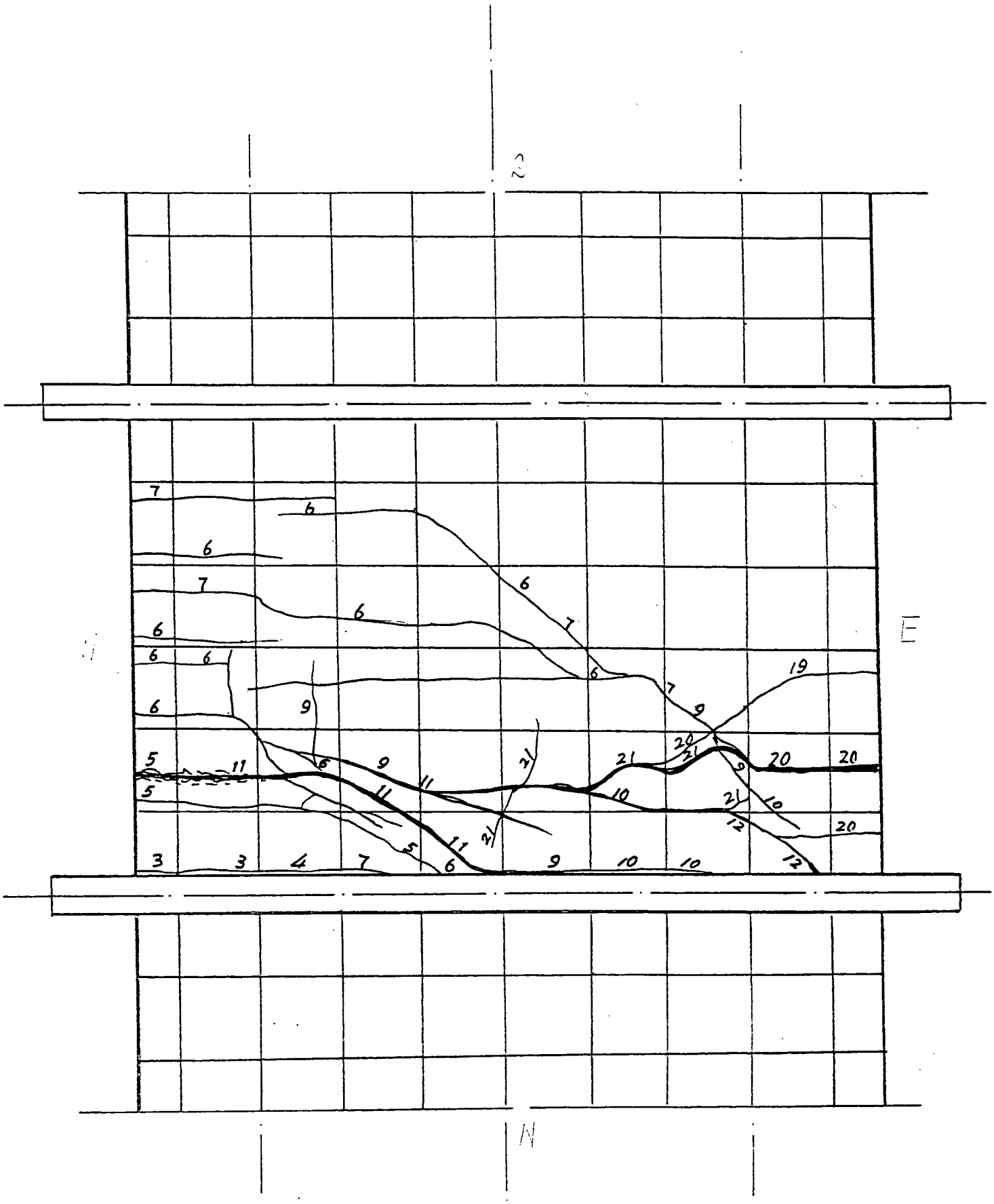

Fig 6.28 Cracking Pattern of FH5MN (BOTTOM) After Strength Test

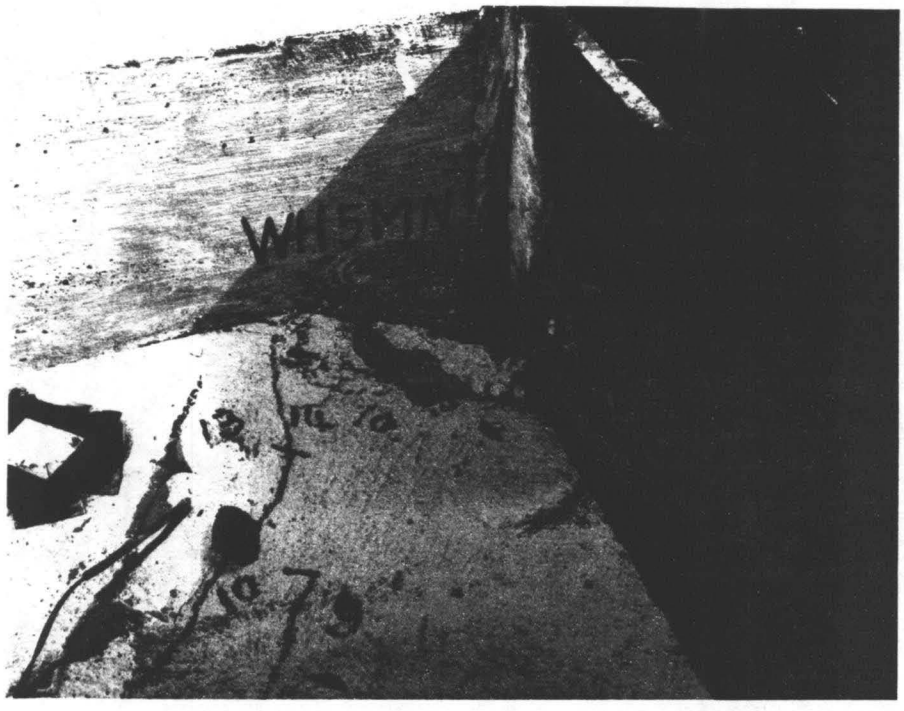

a. from top

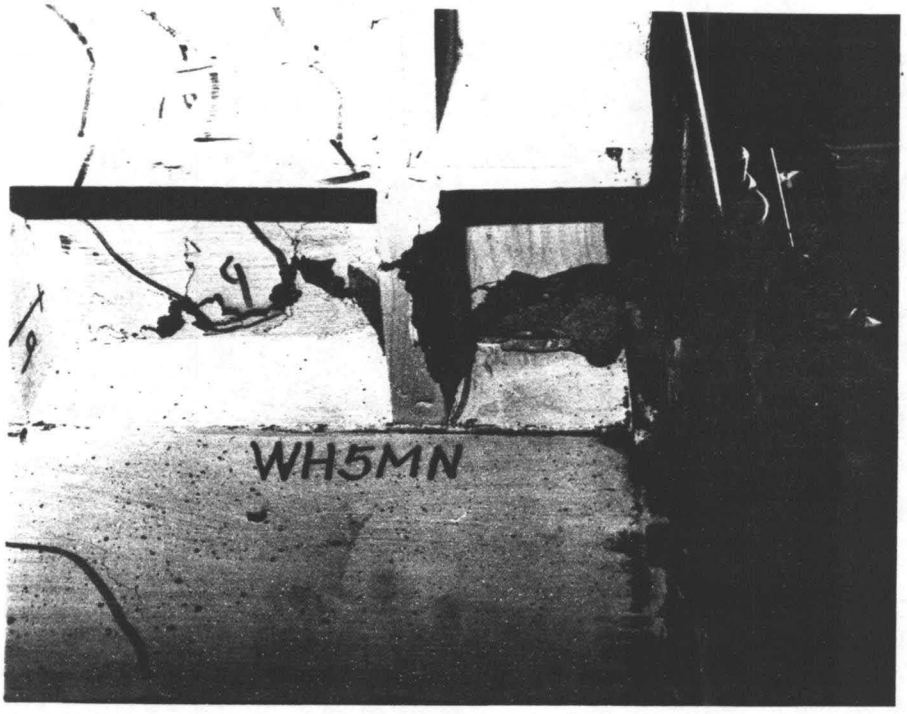

b. from bottom

Fig 6.29 Concrete Crushing at the Compressive Corner

Fig 6.30 Concrete Crushing at the Compressive Corner

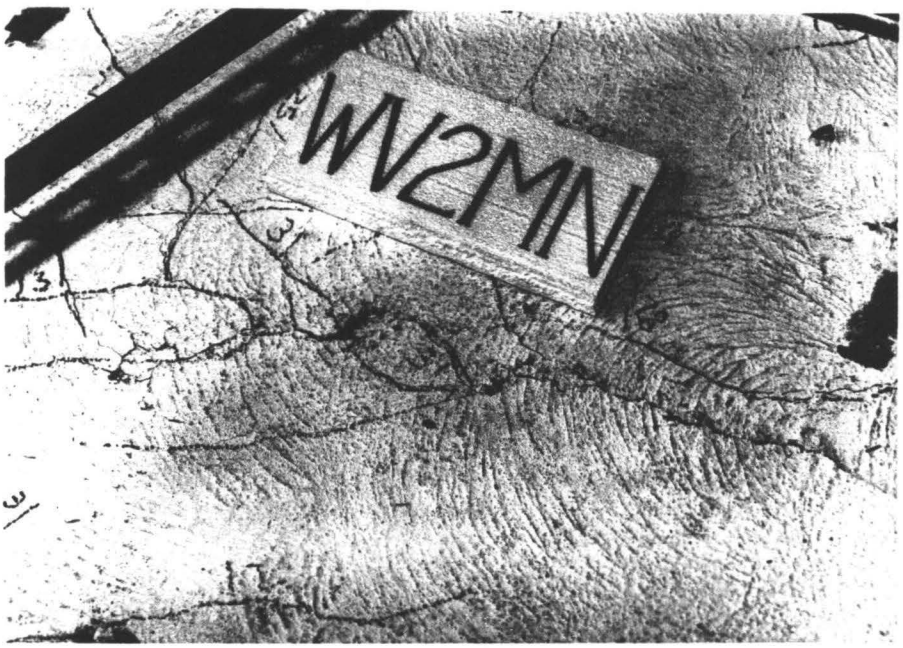

Fig 6.31 Concrete Crushing in the middle of closed major crack which developed under previous positive loading

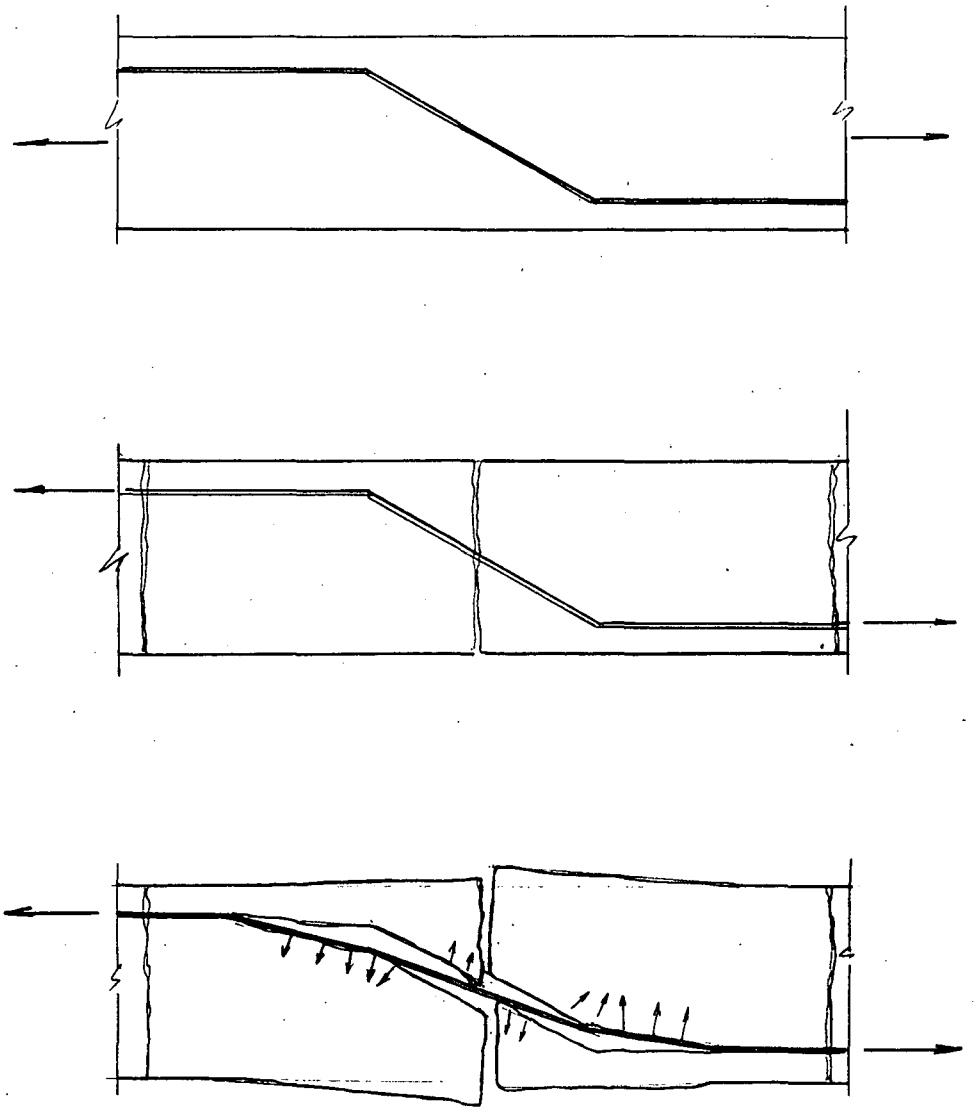

Fig 6.32 The reinforcement with continuative bent bars under in-plane load

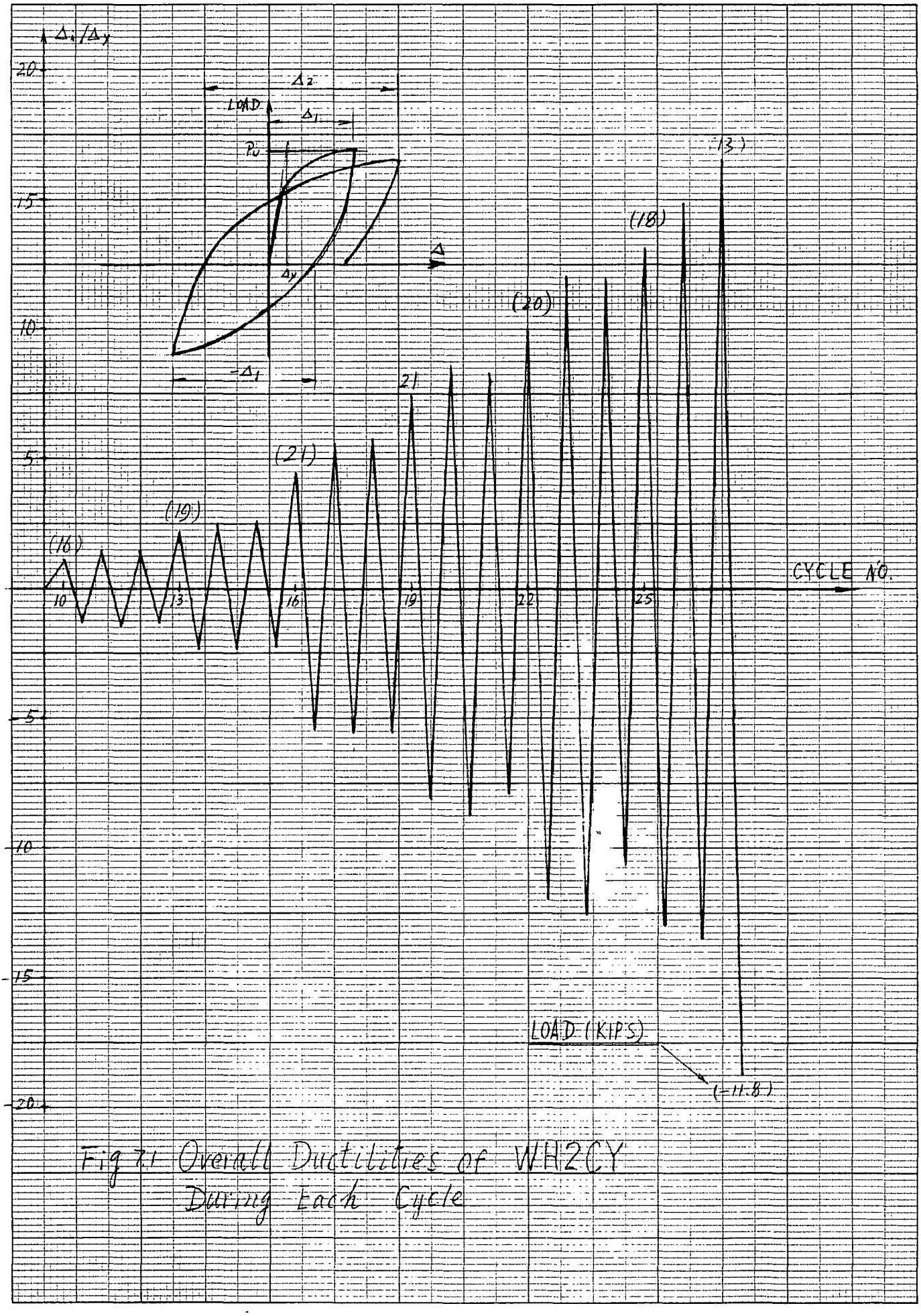

Fig 7.1 Overall Ductilities of WH2CY During Each Cycle

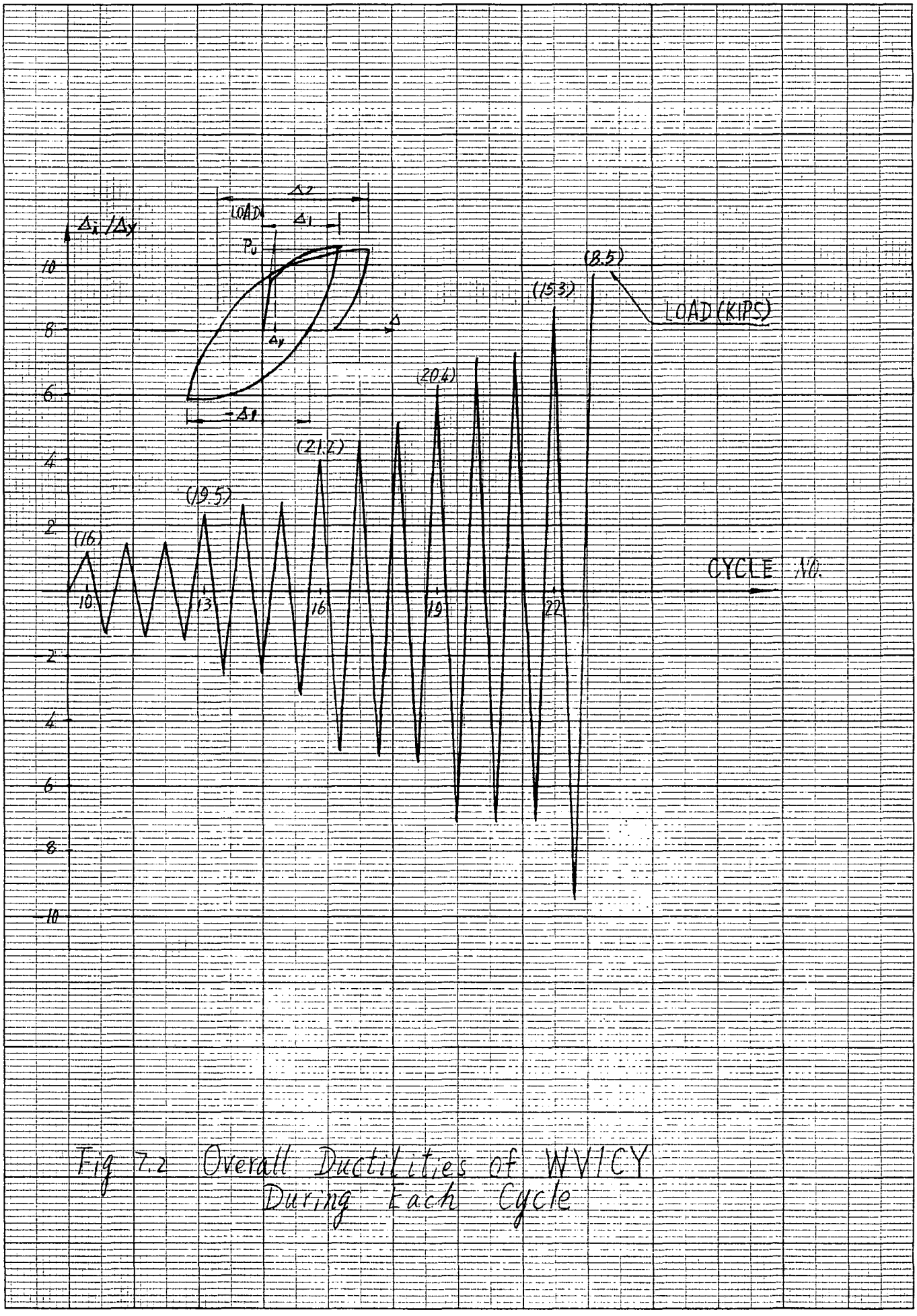

Fig 7.2 Overall Ductilities of WV1CY During Each Cycle

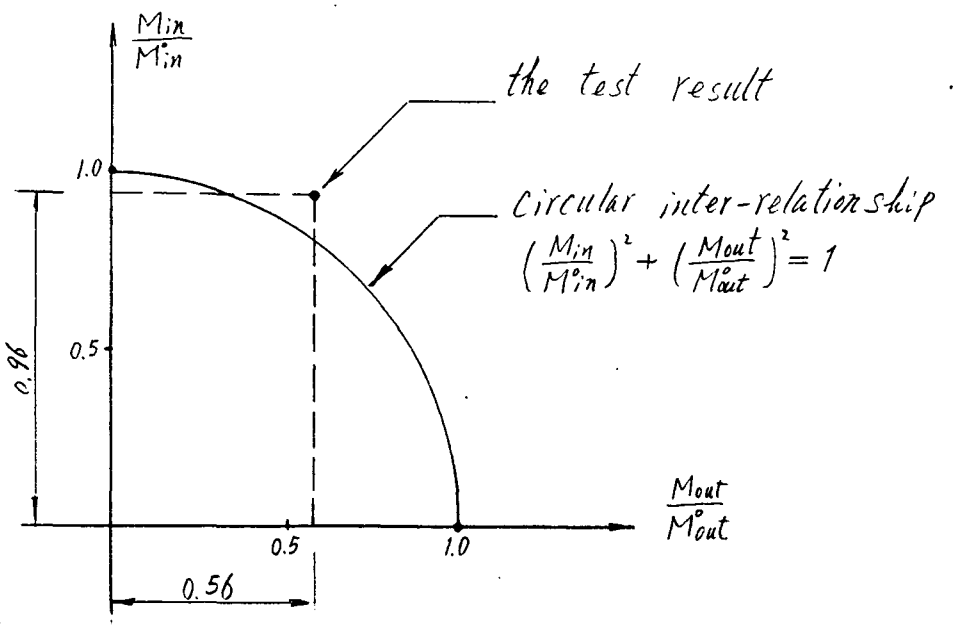

here: M°_{in} — in-plane resistance without out-of-plane load.

M°_{out} — out-of-plane resistance without in-plane load.

M_{in} — in-plane moment with certain moment due to out-of-plane load.

M_{out} — the certain moment due to out-of-pland load.

Fig 7.3 The inter-relationship between in-plane resistance and out-of-plance resistance.

APPENDIX

Calculated Ultimate in-Plane Resistance of Waffle slab specimen

1. Main Crack pattern.

According to the reinforcement, there are three posibilities of main crack pattern. (See Fig A-1)

Along Crack I there was maximum in-plane bending moment. and the additional negative reinforcemet would carry more bending moment; Along crack II there was less in-plane bending moment. but the additional negative reinforcement would not carry the moment; Along crack III there was maximum in-plane bending moment, however, the additional negative reinforcing bars would almost carry no more bending moment. so the crack III would become the real major crack.

2. Caculated ultimate in-plane resistance.

The reinfocement along section II is used to calculate the ultimate in-plane resistance. The additional negative rebars in compression side are neglected due to its small internal arm of force

A_s: 10 D2.0 + 17 D1.0 (in top slab)

3 D2.0 + 6 D2.5 + 6 D1.0 (in ribs)

$A_s = 0.64\ in^2$

$A_c = 0.667 \times 96 + 2.66 \times 1.33 \times 9 = 96\ in^2$

$\bar{b} = \frac{A_c}{h} = \frac{96}{96} = 1\ in.$

To find the neutral axis, assumming that As distributed uniformly along the slab. (See Fig A-2)

$$a_s = \frac{A_s}{h} = \frac{0.64}{96} = 0.00667 \ in^2/in$$

$\Sigma X = 0$: $\quad C_c = C_s$

$$C_c = 0.85\, C \cdot h \cdot \bar{b} \times 0.85 f_c' = 0.85^2 \times 96 \times 1 \times 4000 = 277440\, C$$

$$C_s = a_s \cdot (1 - 2C)\, h \cdot f_s = 0.00667\,(1-2C) \cdot 96 \times 40000 = 25613\,(1-2C)$$

Let $C_s = C_c$ $\qquad C = 0.0779$ $\qquad Ch = 7.48"$

The compressive area in fact only coveres the first rib.

$$\frac{0.85Ch}{2} = 0.85 \times 7.48 \div 2 = 3.2"$$

$$Mu = 5 \times 1200(64 + 16 - 3.2) + 4 \times 350(64+16-3.2) + 9 \times 350(32+16-3.2)$$

$$+ 3 \times 1500(64 + 16 - 3.2) + 3 \times 1200(32 + 16 - 3.2) + 3 \times 350(64+16-3.2)$$

$$= 1297000 \ lb \cdot in$$

$$Pu = \frac{1297000}{64 - 0.5 \times 5.33} = 21.15 \ Kips$$

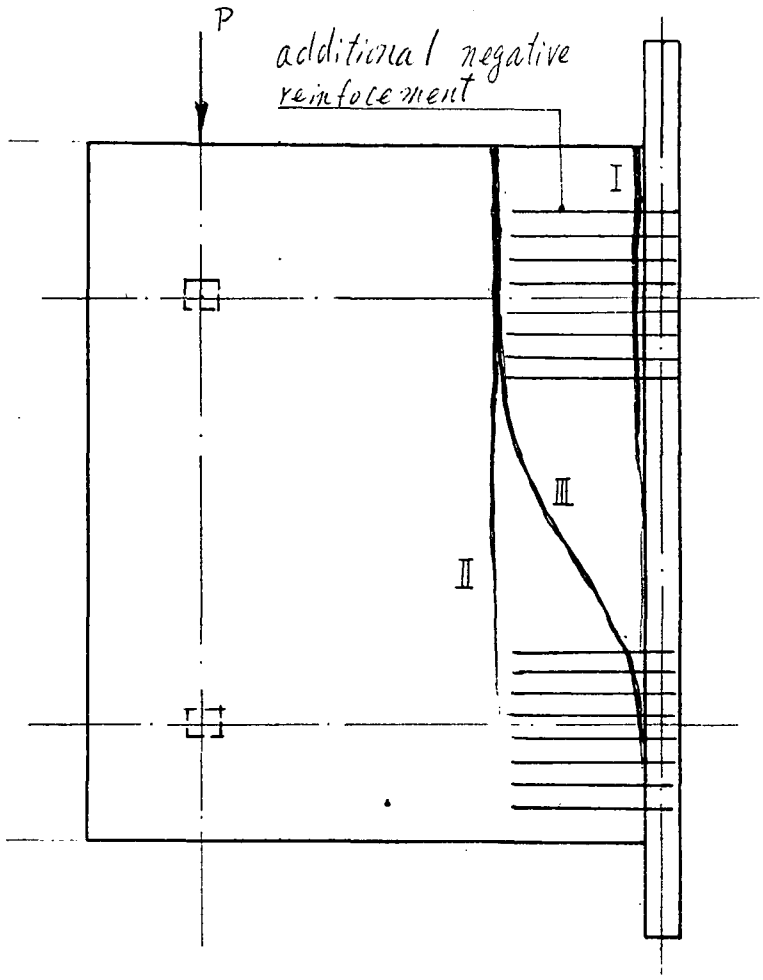

I: Maximum moment, maximum reinforcement;

II: Less moment, Less reinforcement;

III: Maximum moment, Less reinforcement.

Fig A-1 The Three Possibilities of Major Crack Pattern

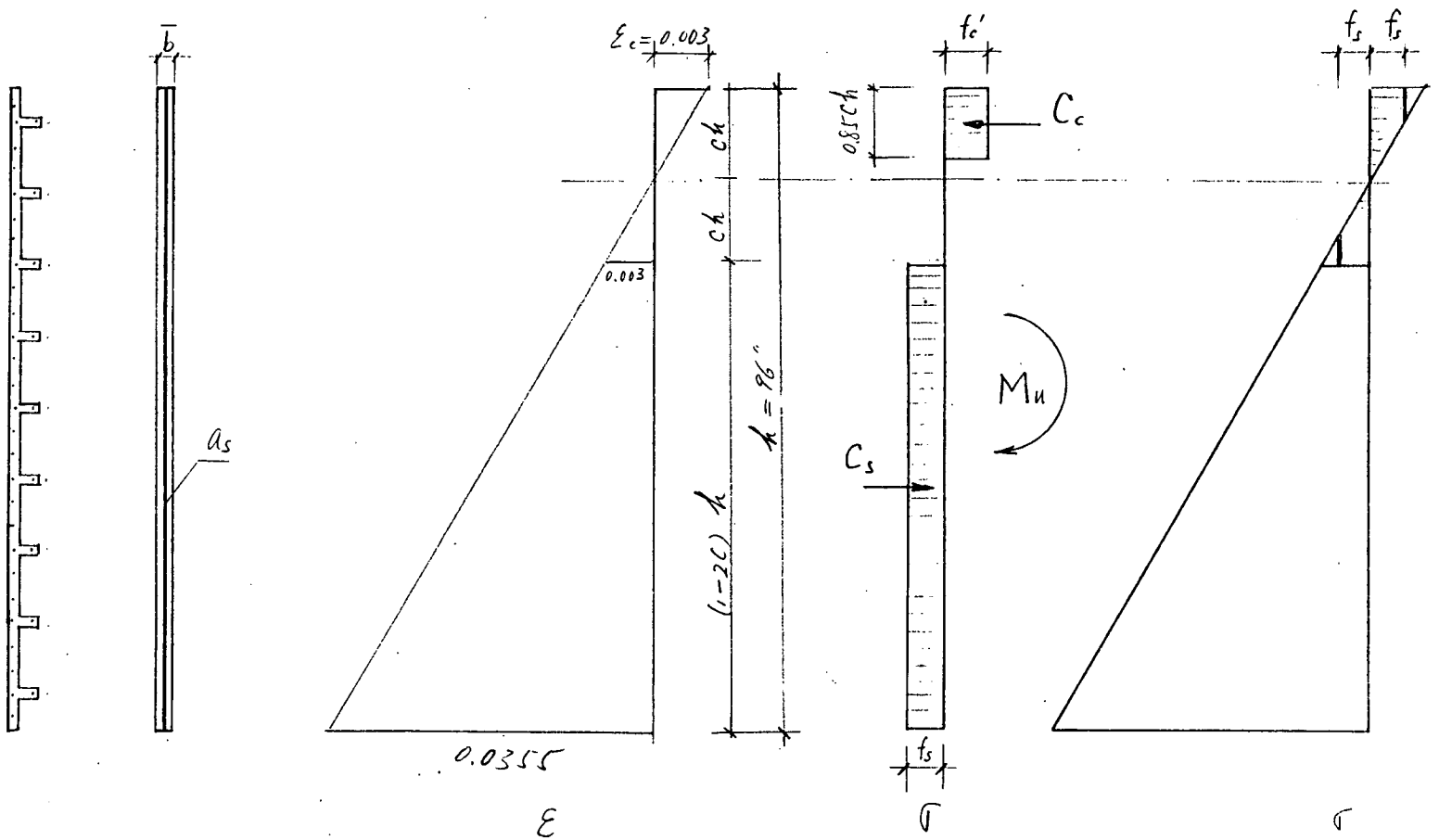

Fig A-2 Calculated Ultimate strength of waffle slab

The Flexibility of WHIMN Calculated by the Method of Equivalent Thickness

According definition the flexibility is the principal deflection of the panel under one unit in-plane load. The dimension of the waffle slab panel is shown in Fig 2.1 and 2.2. The modulus of elasticity, the Poisson's ratio and the thickness of slab are taken from measured values.

Shear force $T = 1\ \text{kip} = 1000\ \text{lb}$; Thickness of slab $t = 0.763''$

$\nu = 0.18$; $E_c = 3.47 \times 10^6\ \text{psi}$; dome side $L = 10\frac{2}{3}''$

span $H = 64''$; The width of panel $B = 96''$

1. Deflection due to Shear : Δs

$$I = \frac{1}{2} I_x = \frac{1}{2} \cdot \frac{1}{12} \cdot 2.667 \times 1.333^3 = 0.263\ \text{in}^4$$

$$I_y = \frac{1}{12} \cdot 0.763 \times 96^3 + \frac{1}{12} \times 2.667 \times 1.333^2 \times 9 + 2.667 \times 1.333 \times (1^2 + 2^2 + 3^2 + 4^2) \times 10.667^2 \times 2$$

$$= 80530\ \text{in}^4$$

$$\alpha = \frac{48 \cdot (1+\nu) \cdot 1}{L^2 t} = \frac{48 \cdot (1+0.18) \cdot 0.263}{10.667^2 \cdot 0.763} = 0.0161$$

$$\beta = 1 + 0.35\sqrt{\alpha} = 1 + 0.35\sqrt{0.0161} = 1.0444$$

$$\Delta_s = \frac{T H}{B \cdot t \cdot \beta \cdot G} = \frac{1000 \times 64 \times 2(1+0.18)}{96 \times 0.763 \times 1.0444 \times 3.47 \times 10^6} = 0.569 \times 10^{-3} \text{ in}$$

2. Deflection due to bending: Δ_b

$$B/H = 96/64 = 1.5$$

$$M = \frac{1}{1 + 0.12 (B/H)^2}\left[1 + 0.1 \times (2+\nu) \cdot (B/H)^2\right] = 1.174$$

$$\Delta_b = \frac{M T H^3}{3 E_c I_y} = \frac{1.174 \times 1000 \times 64^3}{3 \times 3.47 \times 10^6 \times 80530} = 0.367 \times 10^{-3} \text{ in}$$

3 Total Deflection (Flexibility):

$$\Delta = \Delta_s + \Delta_b = 0.936 \times 10^{-3} \text{ in} \quad (0.0238 \text{ mm})$$

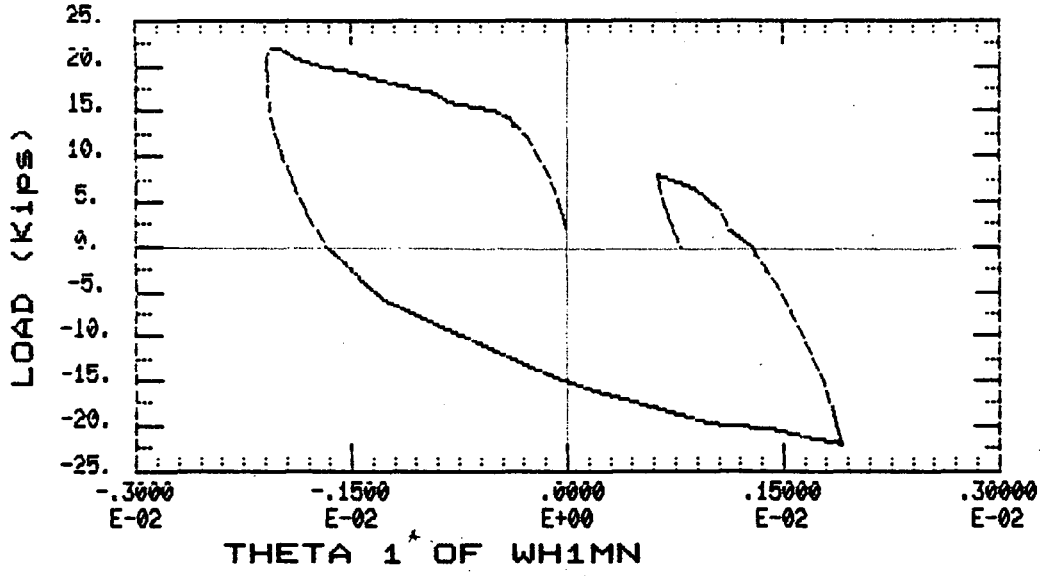

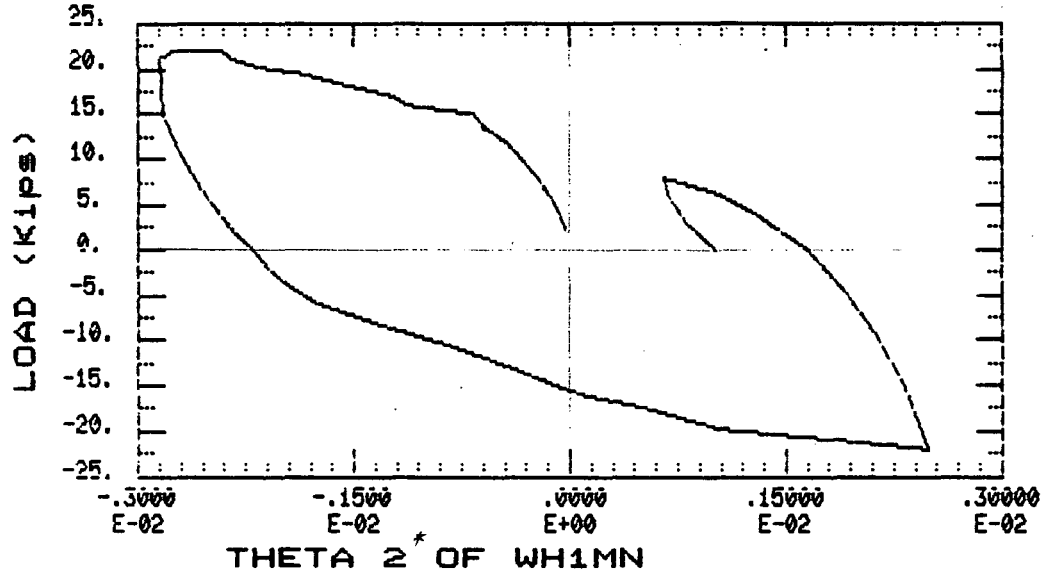

* ref. Fig 6.16 θ_1 and θ_2

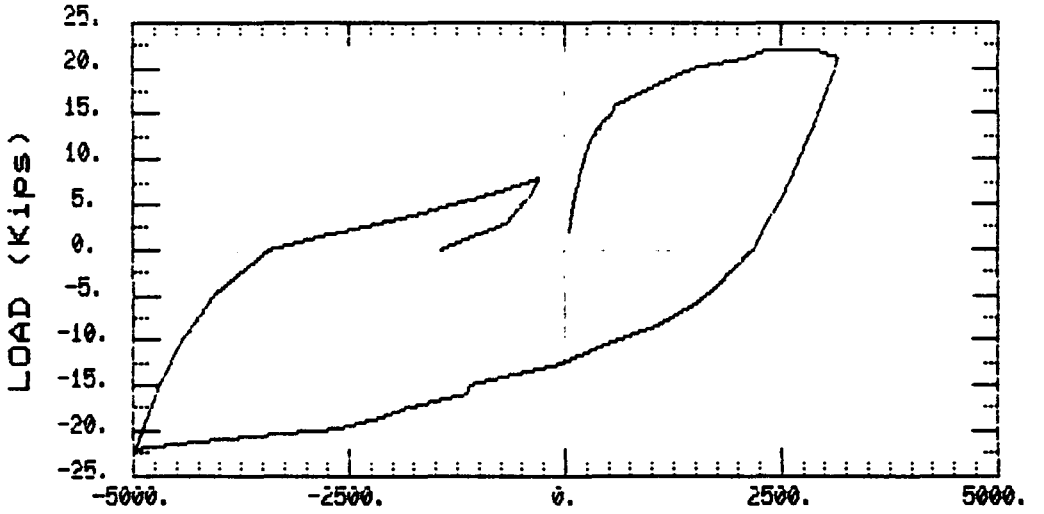

DELTA 1* OF WH1MN

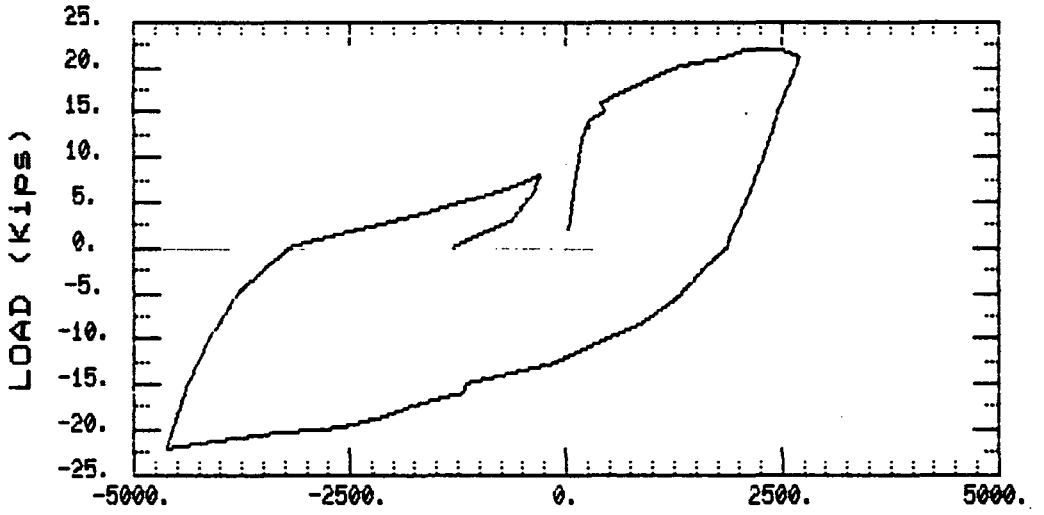

DELTA 2* OF WH1MN

* ref. Fig 6.16 $\Delta 1$ and $\Delta 2$

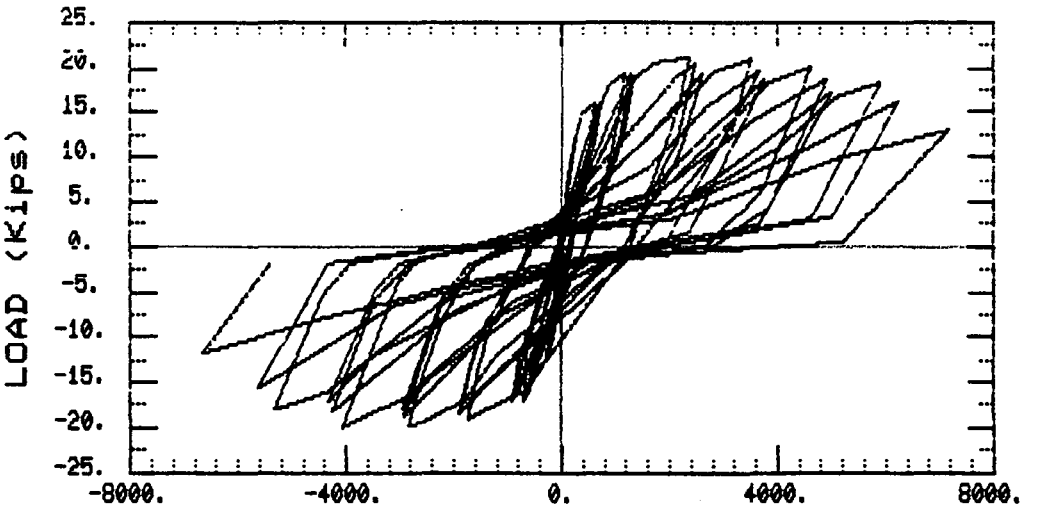

DELTA 1 OF WH2CY

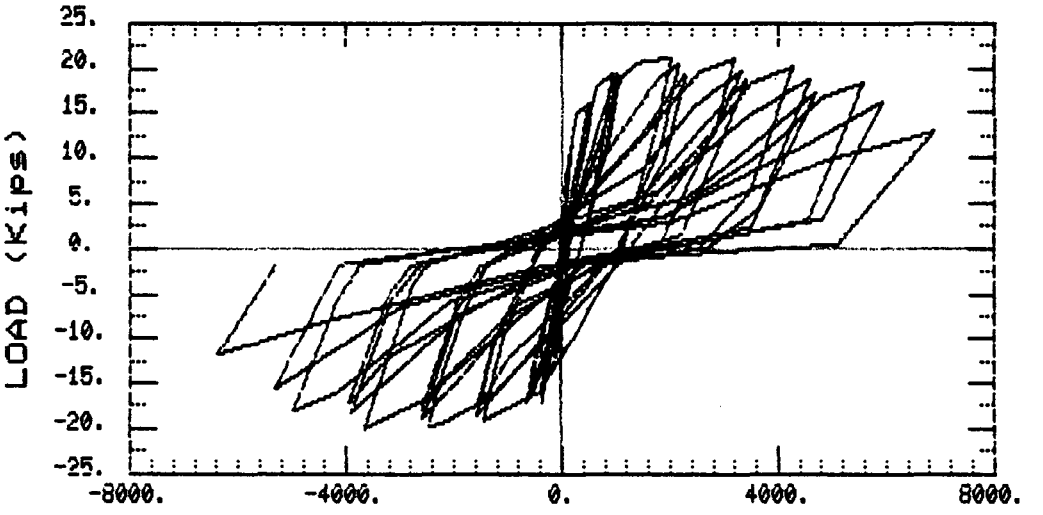

DELTA 2 OF WH2CY

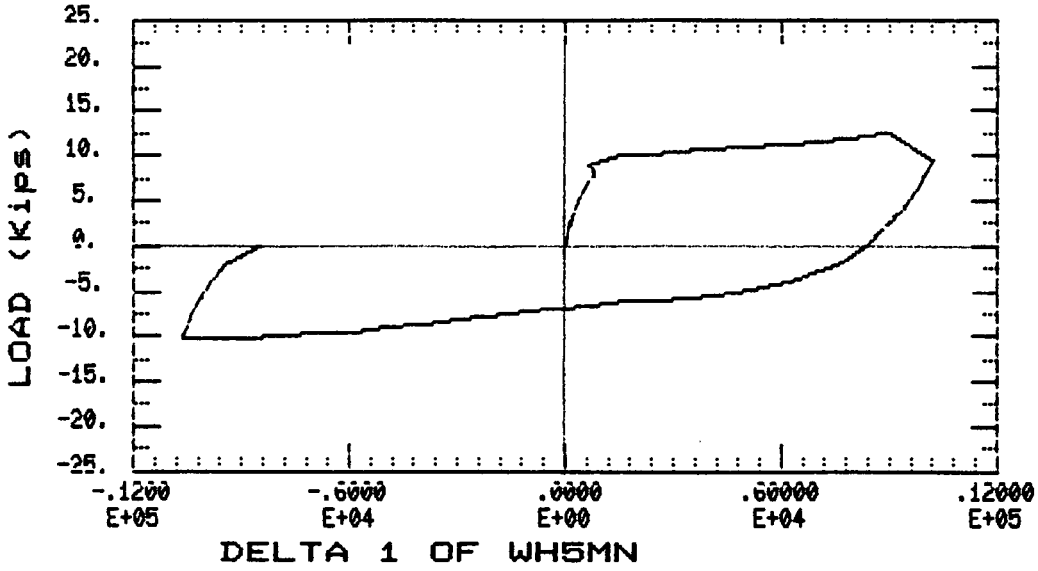
LOAD (Kips)
25.
20.
15.
10.
5.
0.
-5.
-10.
-15.
-20.
-25.
-.12000 E+05
-.60000 E+04
.00000 E+00
.60000 E+04
.12000 E+05
DELTA 1 OF WH5MN

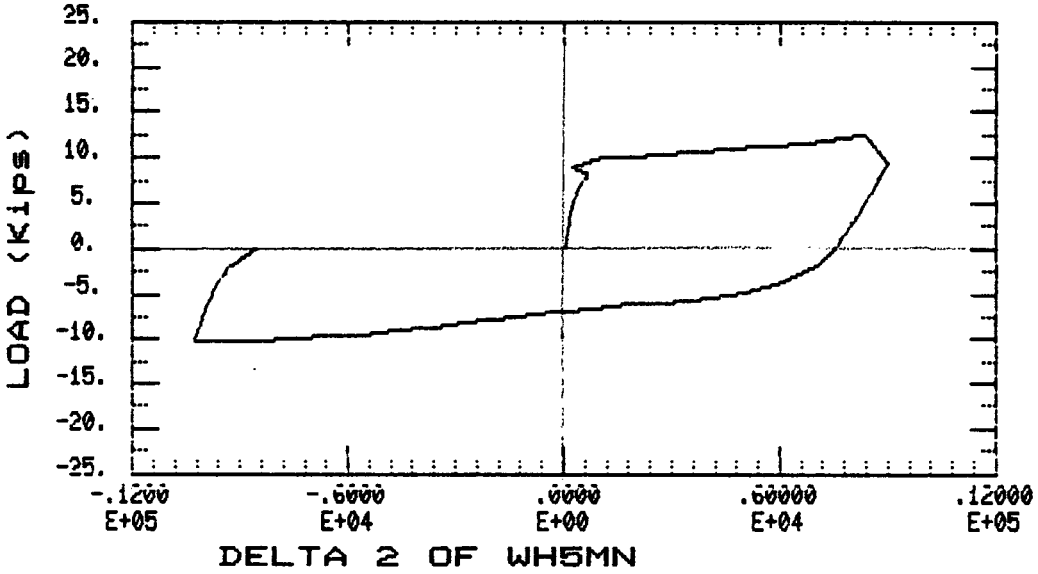
LOAD (Kips)
25.
20.
15.
10.
5.
0.
-5.
-10.
-15.
-20.
-25.
-.12000 E+05
-.60000 E+04
.00000 E+00
.60000 E+04
.12000 E+05
DELTA 2 OF WH5MN

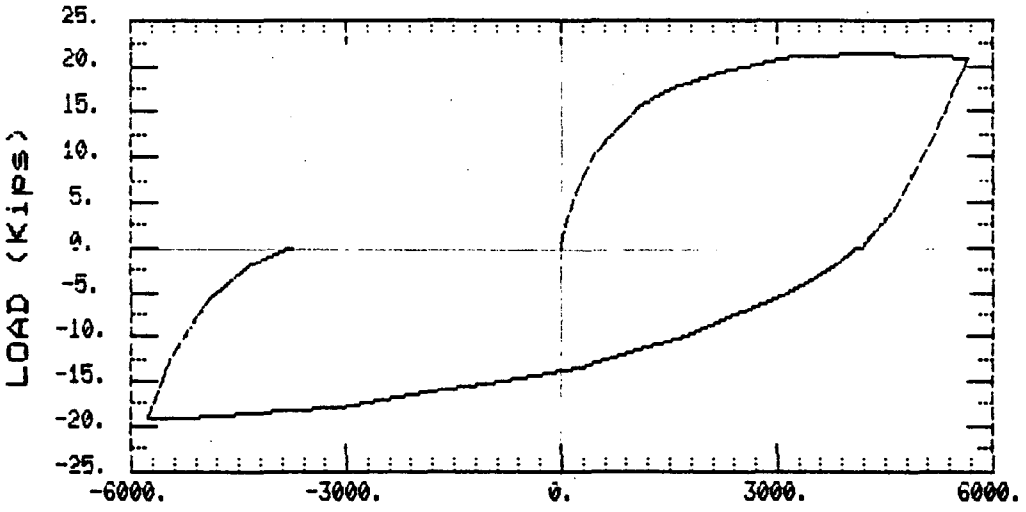

DELTA 1 OF WV2MN

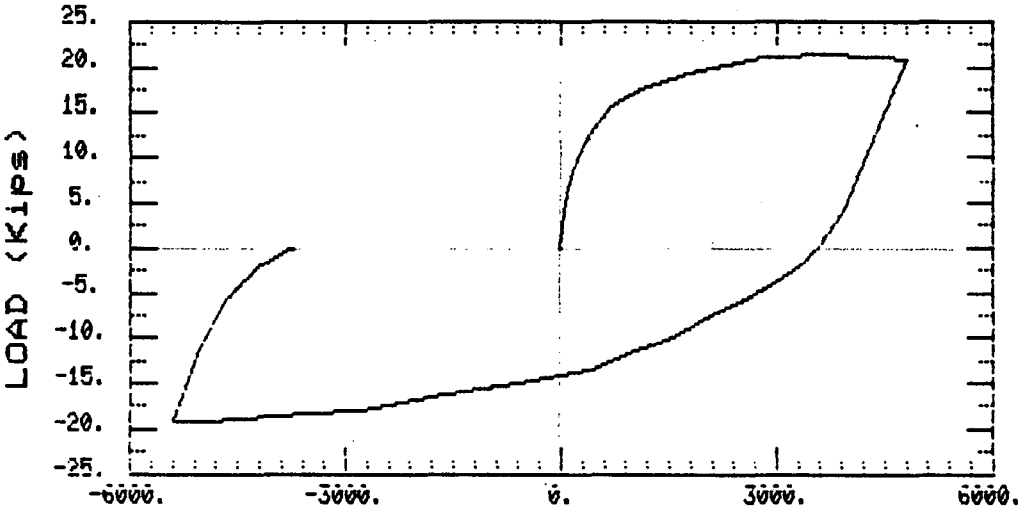

DELTA 2 OF WV2MN

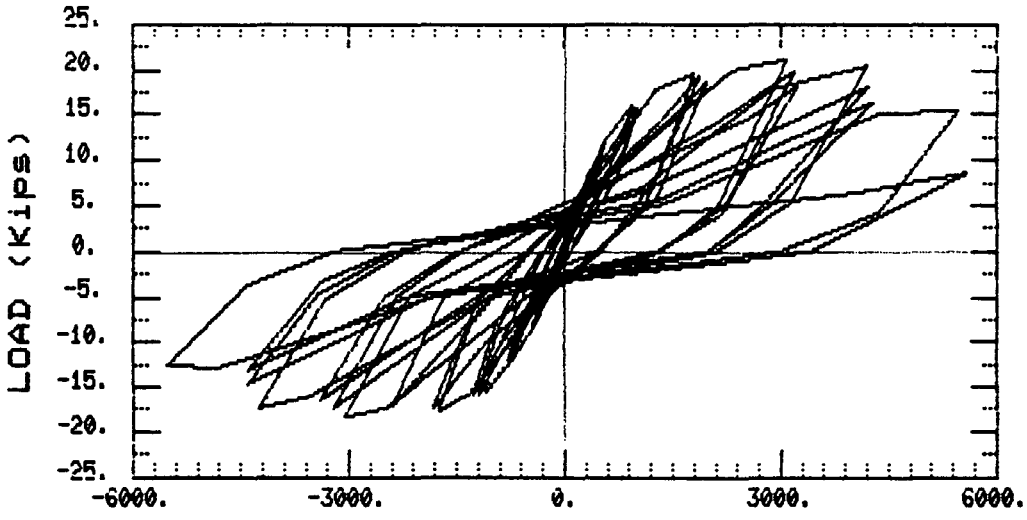

DELTA 1 OF WV1CY

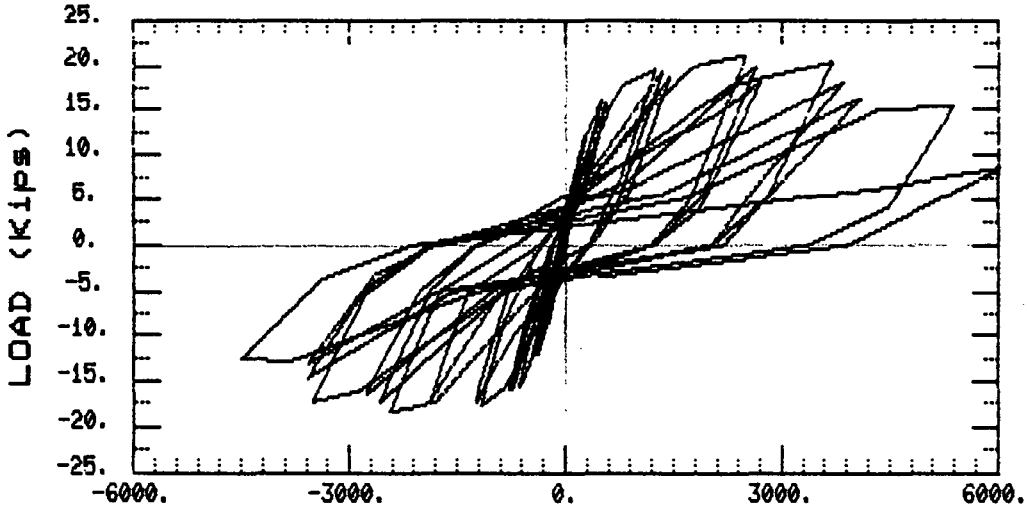

DELTA 2 OF WV1CY

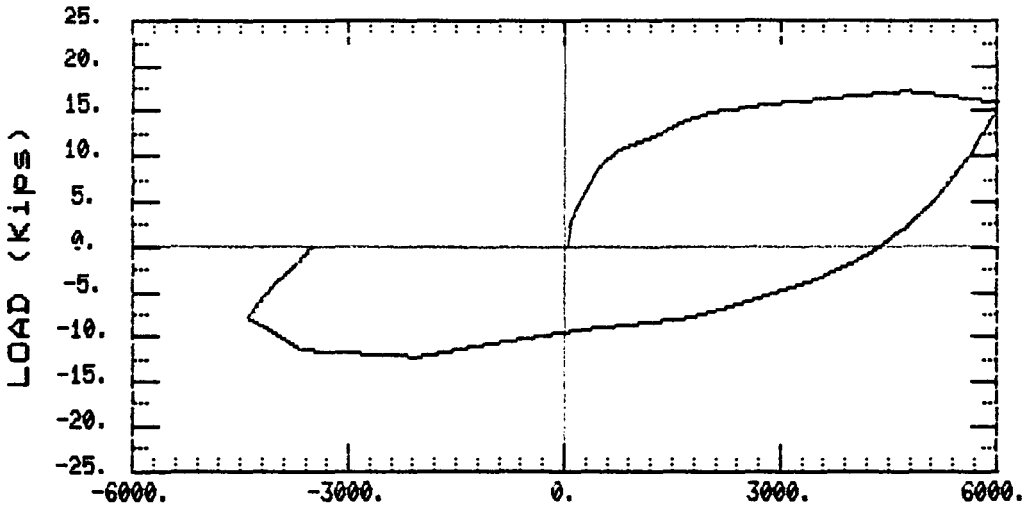

DELTA 1 OF FH5MN

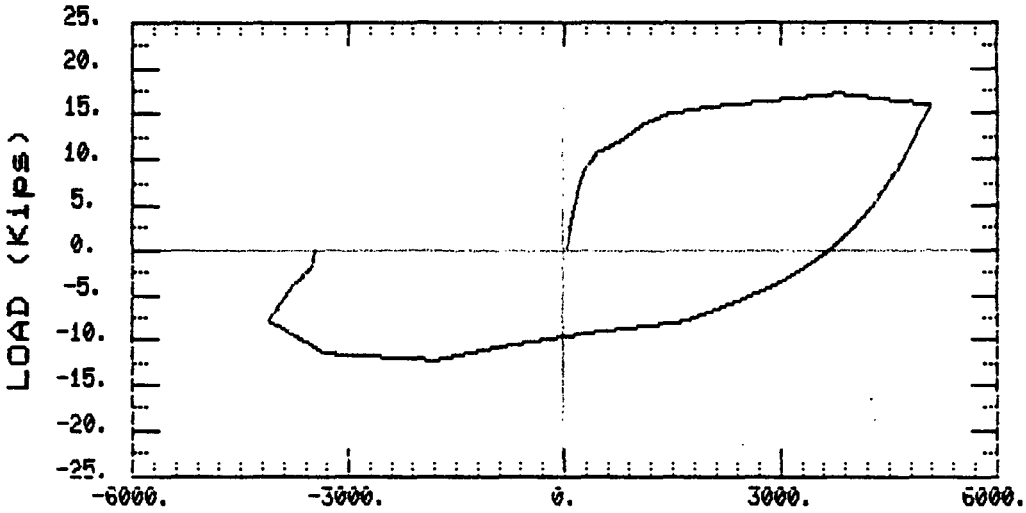

DELTA 2 OF FH5MN